ELECTROCHEMISTRY IN THIN LAYERS OF SOLUTION

Thesis by
Arthur Thornton Hubbard

In Partial Fulfillment of the Requirements
For the Degree of
Doctor of Philosophy

California Institute of Technology
Pasadena, California
1967
(Submitted November 22, 1966)

Acknowledgments

It is a pleasure to acknowledge that these studies were carried out under the direction of Professor F. C. Anson.

Financial support was provided in part by the National Science Foundation and the California Institute of Technology.

ABSTRACT

New electrodes for electrochemistry in thin layers of solution have been constructed which are easier to use and give more reproducible data than previous designs. The theory of voltammetry, chronopotentiometry and chronocoulometry in thin layers is derived and verified for simple systems using these electrodes. The particular advantages of the thin layer approach for study of systems in which adsorption of the reactants can occur and for elucidation of the stoichiometry of complicated reactions have been exploited in the present work.

The extent of adsorption of the I_2 - I^-, CoY^- - CoY^{-2} and FeY^- - FeY^{-2} couples (H_4Y = ethylenediaminetetraacetic acid) at platinum electrodes has been determined. About 2×10^{-9} mole/cm.^{2} of iodide ion or 2×10^{-9} mole/cm.^{2} iodine were shown to be adsorbed in a non-electroactive state. An additional 1×10^{-9} mole/cm.^{2} of iodine but no iodide was adsorbed in an electroactive state. About 3.1×10^{-10} mole/cm.^{2} of CoY^- or 4.7×10^{-10} mole/cm.^{2} of CoY^{-2} are adsorbed at bright platinum electrodes. No adsorption of FeY^- or FeY^{-2} was detected.

The stoichiometry of the electrochemical oxidation of $PtCl_4^{-2}$, $PtBr_4^{-2}$ and PtI_4^{-2}, and of the electrochemical reduction of $PtCl_6^{-2}$, $PtBr_6^{-2}$ and PtI_6^{-2} and their hydrolysis products has been examined. The effect of acidity and halide concentration on these reactions was investigated. The reduction of $PtCl_6^{-2}$ leads to $PtCl_4^{-2}$ in solutions containing sufficient acid or chloride, but proceeds directly to platinum metal in neutral, chloride-free solutions. The reduction of $PtBr_6^{-2}$ yields $PtBr_4^{-2}$ in 1 F bromide solutions, but proceeds to the metal in either acid or neutral bromide-free solutions. The oxidation of $PtCl_4^{-2}$ in 1 F chloride solutions appears to give a mixture of $PtCl_6^{-2}$ and $Pt(OH)_2Cl_4^{-2}$, whereas the oxidation of $PtBr_4^{-2}$ in 1 F bromide solutions gives simply $PtBr_6^{-2}$. The products of hydrolysis of $PtCl_6^{-2}$ and $PtBr_6^{-2}$ are more readily reduced than are the parent complexes.

CONTENTS

Part	Title	Page
I	Introduction	1
II	Theory	3
	1. Linear Potential Sweep Voltammetry in Thin Layers of Solution	3
	2. Chronocoulometry in Thin Layers of Solution	14
	3. Chronopotentiometry in Thin Layers of Solution	15
	Appendix 1. Conditions for Thin Layer Voltammetry	20
	Appendix 2. Conditions for Total Irreversibility in Thin Layer Voltammetry	26
	Appendix 3. Minimum Time Required for Q to Become Constant in Thin Layer Chronocoulometry	28
III	Apparatus	31
	1. Glass Capillary-Wire Electrode	31
	2. Micrometer Electrode	39
	3. Micrometer Mercury Electrode	44
	4. Circuitry	47

CONTENTS

Part	Title	Page
IV	Testing of Apparatus and Theory	48
	1. Testing of the Electrodes	48
	2. Thin Layer Voltammetry of the Fe(III)-Fe(II) Couple	53
	3. Thin Layer Chronocoulometry of the Fe(III)-Fe(II) Couple	57
	4. Ohmic Potential-Difference Effects	58
V	Examples	68
	1. Determination of Reactants Adsorbed on Platinum Electrodes	68
	(i) A Study of the I_2-I^- Couple at Platinum Thin Layer Electrodes	68
	(ii) A Study of the CoY^--CoY^{-2} and FeY^--FeY^{-2} Couples at Platinum Thin Layer Electrodes	95
	2. Elucidation of the Stoichiometry of Complicated Reactions--A Study of the Electrochemistry of the Chloride, Bromide and Iodide Complexes of Platinum (II) and (IV) by Means of Thin Layer Electrochemistry	109

CONTENTS

Part	Title	Page
(i)	Experimental	109
(ii)	$PtCl_4^{-2}$ and $PtCl_6^{-2}$	112
(iii)	Hydrolysis of $PtCl_6^{-2}$	115
(iv)	Supporting Electrolyte Effects	131
(v)	$PtBr_6^{-2}$ and $PtBr_4^{-2}$	131
(vi)	Hydrolysis of $PtBr_6^{-2}$	137
(vii)	PtI_6^{-2} and PtI_4^{-2}	142
(viii)	Conclusions	146
	Propositions	148

I. INTRODUCTION

The potential usefulness of thin layer electrochemical experiments in which diffusion limitation of mass transfer may be neglected was first recognized by Christensen and Anson (1). Equations for thin layer chronopotentiometry were derived by them and verified experimentally for the Fe(III)-Fe(II) couple in perchloric acid. Although Schmidt and Gygax constructed a "chamber electrode" which resembled one of the designs described in reference (1), it appears that diffusion-limited mass transfer prevailed in their experiments (2).

In the present work practical thin layer electrodes have been constructed which are much simpler to use than those previously employed; equations for thin layer voltammetry and chronocoulometry of reversible and irreversible systems have been derived; and the thin layer electrochemical approach has been exploited for the study of several chemical problems which are typical of the many to which it appears well suited.

The equations which govern the design and use of electrodes for chronopotentiometry, voltammetry and chronocoulometry in thin layers are developed in Part II.

---

[1] C. R. Christensen and F. C. Anson, Anal. Chem., 35, 205 (1963).

[2] G. Schmidt and H. R. Gygax, Chimia, 16, 165 (1962).

The details of construction and manipulation of the thin layer electrodes employed are given in Part III; in Part IV the results obtained with these electrodes for systems whose behavior is well known are compared with the theory. The suitability of thin layer electrochemistry for the study of systems where reactant adsorption occurs, and for the elucidation of the stoichiometry of complicated reactions is illustrated in Part V, where studies of the I_2-I^-, CoY^--CoY^{-2}, FeY^--FeY^{-2} (H_4Y = ethylenediaminetetra-acetic acid) and PtX_6^{-2} - PtX_4^{-2} (X = Cl, Br, I) couples are reported.

II. THEORY

The equations for linear potential sweep voltammetry, chronocoulometry and chronopotentiometry in thin layers of solution are derived here for reversible and totally irreversible reactions. The equations for reactions of intermediate reversibility, which are complicated by the presence of insoluble integrals, are of limited practical usefulness and will not be given here. In an attempt to make this section as readable as possible, consideration of convection, electrical migration, ohmic potential differences and the electrical double layer as possible sources of complicated behavior has been reserved for Part IV.

1. Linear Potential Sweep Voltammetry in Thin Layers of Solution

Case i: Reversible Reactions (3)

Consider a general reaction

$$Ox + ne^- \rightleftharpoons R$$

which obeys the Nernst equation. For linear potential sweep rates that are sufficiently small, the concentrations of Ox and R

---

[3] A. T. Hubbard and F. C. Anson, Anal. Chem., 38, 58 (1966).

in the thin layer cavity can be assumed uniform throughout the cavity (the conditions under which this is a good approximation are derived in Appendix 1). Using the Nernst equation, we have:

$$C_{ox} = C_{ox}^{0} \left[1 + \exp \frac{nF}{RT} (E^{0} - E)\right]^{-1}$$
$$C_{R} = C_{R}^{0} \left[1 + \exp \frac{nF}{RT} (E^{0} - E)\right]^{-1} \tag{1}$$

If Ox and R are soluble in the solution, the current flowing through the thin layer cell is given for a negative-going potential sweep by

$$i = -nF\, V \frac{dC_{ox}}{dt} \tag{2}$$

where V is the volume of the solution in the thin layer.

The rate of the potential sweep is

$$\frac{dE}{dt} = r. \tag{3}$$

Equations 1, 2, and 3 can be combined to give an equation for the current-potential curve

$$i = \frac{n^{2}F^{2}V(-r)\, C_{ox}^{0} \exp\left[\frac{nF}{RT} (E^{0} - E)\right]}{RT\left\{\exp\left[\frac{nF}{RT} (E^{0} - E)\right] + 1\right\}^{2}} \tag{4}$$

A plot of Equation 4 is given in Figure 1. The peak current i_p occurs at E^0 and is given by

$$i_p = \frac{n^2 F^2 (-r) V C^0_{ox}}{4RT} \tag{5}$$

As would be expected, Equations 4 and 5 are identical to those derived by Scott for voltammetry with linear voltage sweep using a conventional coulometric cell and assuming infinitely good stirring (4).

Comparison of Equation 4 with the Randles-Ševčik´ equation (5, 6) points out at once the greater simplicity inherent in thin layer potential sweep voltammetry owing to the absence of diffusion limited mass transfer. The peak-current expression for thin layers does not contain the diffusion coefficient and applies without change to stepwise reactions or mixed reactants provided that the standard potentials of the reactants differ by $\frac{0.2}{n}$ volt (otherwise the current components are additive). Two peaks can be distinguished qualitatively when the standard potentials differ by about 0.05 volt. Multiple-sweep experiments

---

[4] F. A. Scott, et. al., Anal. Chem., 33, 1024 (1961).

[5] J. E. B. Randles, Trans. Farad. Soc., 44, 327 (1948).

[6] A. Ševčík, Coll. Czech. Chem. Commun., 13, 349 (1948).

Figure 1

Theoretical current-potential curve for a reversible reaction:

$$\frac{\exp\left[\frac{F}{RT}\ (E - E^0)\right]}{\left\{\exp\left[\frac{F}{RT}\ (E - E^0)\right] + 1\right\}^2} \quad \text{plotted against E.}$$

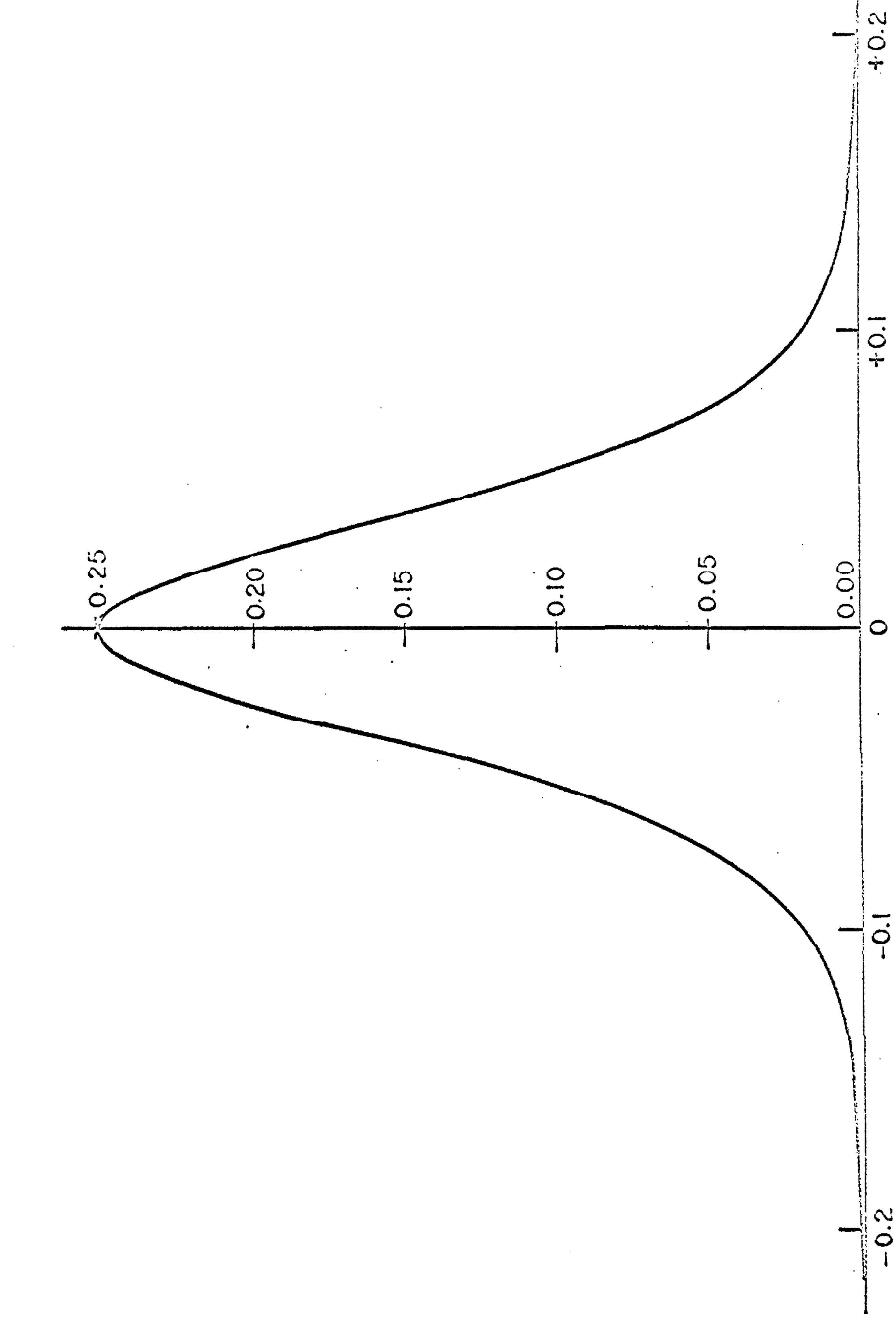
0.25
0.20
0.15
0.10
0.05
0.00
-0.2
-0.1
0
+0.1
+0.2
E°

in thin layers of solution involve no additional complications. The peak current expression is identical for the anodic and cathodic sweeps for any number of cycles.

More than an order of magnitude smaller current densities are necessary than in ordinary linear sweep voltammetry, which allows the otherwise impossible study of irreversible systems that react quite close to the supporting electrolyte. This can be seen from the following calculation: the expression for i_p in ordinary voltammetry is

$$i_p = \frac{0.452\, n^{\frac{3}{2}}\, F^{\frac{3}{2}}\, A\, C^0_{ox}\, D^{\frac{1}{2}}\, r^{\frac{1}{2}}}{R^{\frac{1}{2}}\, T^{\frac{1}{2}}} \tag{6}$$

Thus, making all the corresponding parameters equal, we have the ratio of current densities

$$\frac{i_p}{i_p\ (\text{thin layer})} = \left[\frac{RTD}{nF}\right]^{\frac{1}{2}} \frac{3.616}{r^{\frac{1}{2}}\, \ell} = \frac{0.579\, D^{\frac{1}{2}}}{r^{\frac{1}{2}}\, \ell}$$

For instance if $r = 10^{-3}\ \frac{\text{volt}}{\text{sec.}}$, $\ell = 10^{-3}$ cm. and $D = 6 \times 10^{-6}\ \frac{\text{cm.}^2}{\text{second}}$, we have

$$\frac{i_p}{i_p\ (\text{thin layer})} = 45.$$

Case ii. Irreversible Reactions

In the event that the reaction does not obey the Nernst equation, the preceeding equations do not apply. Instead, for sufficiently small sweep rates (Appendix 1), the current will be given for a cathodic sweep by

$$i = -nFV \frac{dC_{ox}}{dt} = nFA\,(k_f C_{ox} - k_b C_R) \tag{7}$$

If the anodic component of the current can be neglected (the conditions under which this is a good approximation are derived in Appendix 2), Equation 7 becomes

$$\frac{dC_{ox}}{dt} = \frac{-A}{V} k_f C_{ox}$$

which after integration yields

$$C_{ox} = C^0_{ox} \exp \frac{A}{V} \frac{RT}{n_0 F} \frac{1}{\alpha r}\; k_f \tag{8}$$

k_f is related to E by

$$k_f = k^0 \exp \frac{-\alpha n_0 F}{RT} (E - E^0) \tag{9}$$

n_0 is the number of electrons involved in the rate-determining step and α is the charge-transfer coefficient of the electrode process. Equations 7, 8, and 9 can be combined to give the equation for the current-potential curve

$$i = nFAk^0 C^0_{ox} \exp \left\{ \frac{-\alpha n_0 F}{RT} (E - E^0) + \frac{A}{V} \frac{RT}{\alpha n_0 F} \frac{k^0}{r} \exp \left[\frac{-\alpha n_0 F}{RT} (E - E^0) \right] \right\} \qquad (10)$$

A plot of Equation 10 for several values of k^0 appears in Figure 2.

The shape of the curves is not affected by k^0 in the range for which Equation 10 applies; the curves are merely shifted along the axis of potentials. However, the breadth of the current-potential curve increases substantially with decreasing values of αn_0. The peak potential is

$$E_{p(\text{cathodic})} = E^0 + \frac{2.303\ RT}{\alpha n_0\ F} \log \left[\frac{ART\ k^0}{\alpha n_0 F(-r)V} \right] \qquad (11)$$

The peak current is

$$i_p = \frac{\alpha n n_0\ F^2 V\ (-r)\ C^0_{ox}}{e\ RT} \qquad (12)$$

where e = 2.718. Dividing Equation 12 with Equation 5, we have the ratio

$$\frac{i_p \text{ (thin layer, irreversible)}}{i_p \text{ (thin layer, reversible)}} = 1.470 \frac{n_0 \alpha}{n}$$

Figure 2

Theoretical (cathodic) current-potential curves for irreversible reactions

A. Reversible reaction (shown for comparison)

B. $k^0 = 10^{-6}\ \frac{\text{cm.}}{\text{second}}$

C. $k^0 = 10^{-8}\ \frac{\text{cm.}}{\text{second}}$

D. $k^0 = 10^{-10}\ \frac{\text{cm.}}{\text{second}}$

The following values have been assumed in making the plots:

$r = 2.0\ \frac{\text{millivolt}}{\text{second}}$

$n = 1$

$A = 0.5\ \text{cm.}^2$

$C^0_{ox} = 1.0$ milliFormal

$\alpha = 1/2$

$n_0 = 1$

$V = 2.0$ microliter

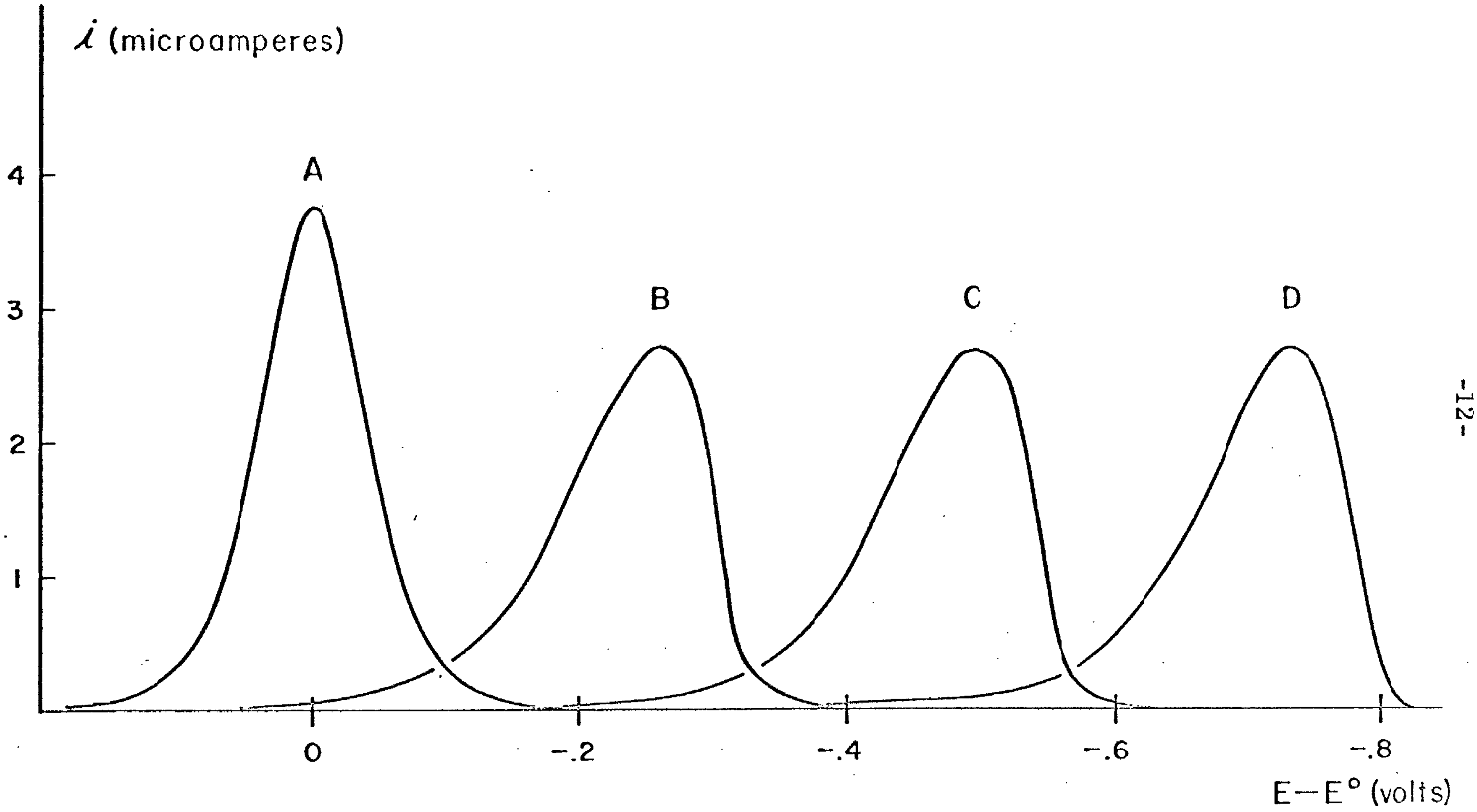
i (microamperes)
4
3
2
1
A
B
C
D
0
-.2
-.4
-.6
-.8
E—E° (volts)

Thus, since $n_0 \leqq n$, the peak current expected for irreversible cases will be smaller than for the reversible except when α is greater than about 0.7.

Equations 10, 11, and 12 apply to anodic processes after the following changes are made:
α is replaced by $(1 - \alpha)$, C^0_{ox} by C^0_R, and n_0 (cathodic) by n_0 (anodic).

By combining Equations 11 and 12 and solving for k^0 we obtain

$$k^0 = \frac{i_p e}{nFAC^0_{ox}} \exp\left[\frac{i_p e(E_p - E^0)}{nFV(-r)C^0_{ox}}\right] \tag{13}$$

Equation 13 allows the calculation of the rate constant k^0 from the measured values of the peak current and potential whenever the standard potential E^0 of the reaction is known.

2. Chronocoulometry in Thin Layers of Solution (7)

In a typical chronocoulometric experiment the electrode potential is varied instantaneously from a potential E_1 at which no current flows to a potential E_2 at which the electrochemical reaction can occur, and the current integrated electronically. In thin layers of solution the charge Q required for complete consumption of the reactant is given by Faraday's law

$$Q = nFVC^0 \qquad (14)$$

Equation 14 is applicable whether or not the reaction is reversible so long as it is allowed to proceed to completion. The time required for Q to become constant is about 0.1 second for reversible systems, but is somewhat longer (depending on the values of k^0 and E_2) for irreversible ones (see Appendix 3).

---

[7] A. T. Hubbard, F. C. Anson, and R. A. Osteryoung, Anal. Chem., 38, 692 (1966).

3. Chronopotentiometry in Thin Layers of Solution

Although the chronopotentiometric measuring technique can usually be abandoned in favor of voltammetry and chronocoulometry, there are instances in which its constant current density or uncomplicated circuitry make it the best approach. The theory of thin layer chronopotentiometry was derived by Christensen and Anson (1) for reversible reactions; a summary of their results is included in what follows.

Case i. Reversible Reactions (1)

Consider the general reaction

$$Ox + ne^- \rightleftharpoons R$$

which obeys the Nernst equation

$$E = E^0 + \frac{RT}{nF} \ln \frac{C_{ox}(O,t)}{C_R\,(O,t)} \tag{15}$$

If Ox is reduced at constant current and $\frac{\ell^2}{3D\tau}$ is made sufficiently small, we have

$$C_R\,(O,t) = C^0_{ox} - C_{ox}\,(O,t) = \frac{it}{nFV} \tag{16}$$

Combining Equations 16 and 17 gives

$$E = E^0 + \frac{RT}{nF} \ln \left(\frac{C^0_{ox}\, nFV}{it} - 1 \right). \qquad (17)$$

A plot of Equation 17 appears in Figure 3. The transition time τ, at which $C_{ox}(O, t)$ becomes zero, is given by

$$\tau = \frac{nFVC^0}{i} \qquad (18)$$

within a relative error less than ϵ, provided that $\frac{\ell^2}{3D\tau} < \epsilon$. For instance, if $\ell = 10^{-3}$ cm, $D = 10^{-5}\ \frac{\text{cm.}^2}{\text{second}}$, and we require $\epsilon < 10^{-2}$ (1% relative error), then the experimental conditions must be adjusted to give τ values in the range $\tau > 3.3$ second.

Case ii. Irreversible Reactions

In the event that the Nernst equation is not obeyed, the transition time τ is given by Equation 19 as for a reversible reaction; however, Equation 18 for the current-time curve is no longer applicable. It is easy to show that for $k_f < \frac{i}{AC^0F}$ the back reaction can be neglected so that

$$i = nFAk^0 C_{ox} \exp \left[\frac{-\alpha n_a F}{RT} (E - E^0) \right] \qquad (19)$$

Figure 3

Theoretical chronopotentiometric potential-time curves

A. reversible reaction

B. irreversible reaction

The following values have been assumed in making the plot:

E^0 = 0.00

T = 298°k

$n = n_0 = 1$

C^0_{ox} = 1.0 milliFormal

V = 1.0 microliter

i = 10 microampere

A = 0.5 cm.^2

$k^0 = 10^{-6} \frac{\text{cm.}}{\text{sec.}}$

α = 0.5

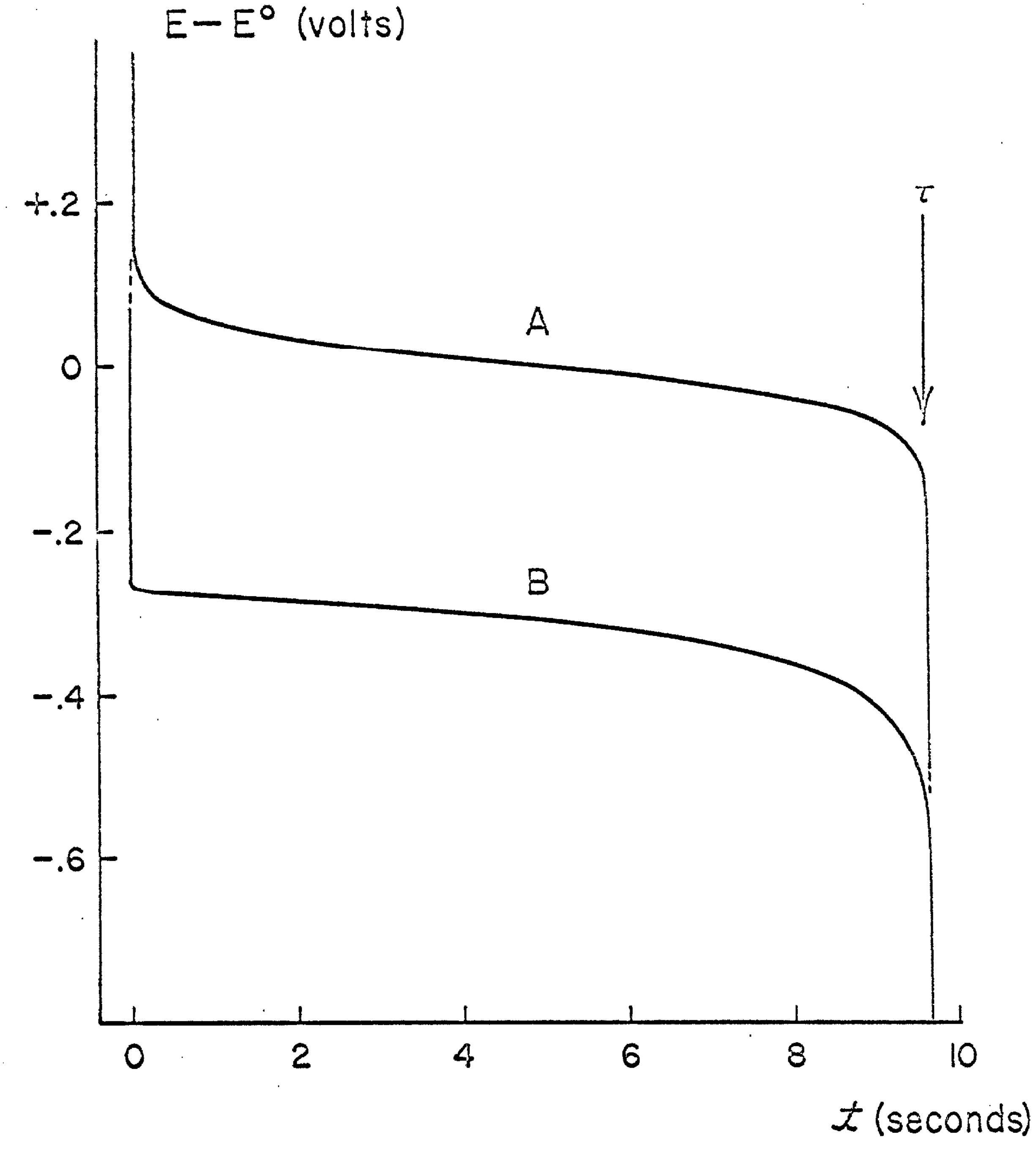
E − E° (volts)
+.2
0
−.2
−.4
−.6
A
B
τ
0
2
4
6
8
10
t (seconds)

Equation 19 can be written

$$i = nFAk^{\circ}(C^{0} - \frac{it}{nFV}) \exp \frac{-\alpha n_0 F}{RT} (E - E^{0}) \qquad (20)$$

Solving for E we have

$$E = E^{0} + \frac{RT}{\alpha n_0 F} \ln (C^{0} - \frac{it}{nFV}) (\frac{nFAk^{0}}{i}) \qquad (21)$$

A plot of Equation 21 appears in Figure 3.

A theoretical basis for obtaining the transition time from the chronopotentiometric curve of sufficient generality to allow its use in practical situations (where currents of uncertain magnitude are required by double-layer-charging and by background reactions) has not been deduced. In the present work a graphical method has been employed which appears to give consistent results (Part IV).

Appendix 1

Conditions for Thin Layer Voltammetry

In order to estimate the maximum sweep rate for which Equations 1, 4, and 5 hold, it is necessary to solve the problem taking diffusion effects into account, and to determine the conditions under which this exact solution becomes identical with the simple theory. We seek a solution of the diffusion equation in the form

$$\frac{\partial C_{ox}(x,t)}{\partial t} = D_{ox} \frac{\partial^2 C_{ox}(x,t)}{\partial x^2}$$

subject to the boundary conditions that C_{ox} and C_R be given by the Nernst equation at the electrode surface. The analogous problem in heat diffusion has been solved by Carslaw and Jaeger (8). If the thin layer cavity is composed of parallel planar electrode surfaces, the solution is

$$C_{ox} = C^0_{ox} \sum_{k=0}^{\infty} \exp\left(\frac{-(2k+1)^2\pi^2 Dt}{\ell^2}\right) \sin \frac{(2k+1)\pi x}{\ell} \times$$

$$\left[\frac{4}{\pi(2k+1)} + \frac{4D\pi}{\ell^2}(2k+1)\int_0^t \frac{\exp\left(\frac{(2k+1)^2\pi^2 Dy}{\ell^2}\right)}{1+\exp\left(\frac{nF}{RT}[E - E(0)] - ry\right)} dy\right] \qquad \text{(i)}$$

---

[8] H. S. Carslaw and J. C. Jaeger, Conduction of Heat in Solids, 2nd ed., Section 3.5, Oxford: Clarendon Press, 1959.

ℓ is the thickness of the thin layer cavity and D is the diffusion coefficient of Ox.

For values of r sufficiently small the integral appearing in Equation (i) can be approximated according to Equation (ii):

$$I \equiv \int_0^t \frac{\exp\left(\frac{(2k+1)^2\pi^2 Dy}{\ell^2}\right)}{1 + \exp\left(\frac{nF}{RT}\left[E^0 - E(0)\right] - ry\right)}\, dy \approx \frac{\ell^2 \exp\left(\frac{(2k+1)^2\pi^2 Dt}{\ell^2}\right)}{\pi^2 D(2k+1)^2\left[1 + \exp\left(\frac{nF}{RT}\left[E^0 - E(0)\right] - rt\right)\right]} \qquad \text{(ii)}$$

so that Equation (i) becomes

$$C_{ox} = C^0_{ox}\left[\frac{1}{\exp\left(\frac{nF}{RT}\left[E^0 - E(0)\right] - rt\right) + 1}\right] = C^0_{ox}\frac{1}{\exp\left[\frac{nF}{RT}\left(E^0 - E\right)\right] + 1} \qquad \text{(iii)}$$

That is, for sufficiently small values of r, Equation (i) reduces to the Nernst equation.

The values of r for which Equation (ii) applies can be determined as follows: decompose the range of integration (0, t) into N equal parts (where $N \approx t$)

$$I = \sum_{\lambda = 1}^{N} \int_{\frac{(\lambda-1)t}{N}}^{\frac{\lambda t}{N}} \frac{\exp\left(\frac{(2\kappa + 1)^2 \pi^2 Dy}{\ell^2}\right)}{1 + \exp\left(\frac{nF}{RT}\left[E^0 - E(0)\right] - ry\right)} \, dy \qquad \text{(iv)}$$

For typical values of the experimental parameters ($\ell^2 = 10^{-6}$ sq. cm., $D = 10^{-5}$ sq. cm./sec., $E^0 - E(0) = -0.2$ volt, and $T = 298°$ K.), the numerator of the integrand increases very rapidly with y for all values of k while the denominator changes much more slowly; thus, for suitable values of r, we have

$$I \approx \sum_{\lambda = 1}^{N} \frac{1}{1 + \exp\left(\frac{nF}{RT}\left[E^0 - E(0)\right] - \frac{r\lambda t}{N}\right)} \times \int_{\frac{(\lambda - 1)t}{N}}^{\frac{\lambda t}{N}} \exp\left(\frac{(2\kappa + 1)^2 \pi^2 Dy}{\ell^2}\right) dy \qquad \text{(v)}$$

which after integration yields

$$1 \approx \sum_{\lambda = 1}^{N} \frac{\ell^2\left[\exp\left(\frac{(2k + 1)^2 \pi^2 D\lambda t}{\ell^2 N}\right) - \exp\left(\frac{(2k + 1)^2 \pi^2 D(\lambda - 1)t}{\ell^2 N}\right)\right]}{\pi^2 D(2k + 1)^2 \left\{1 + \exp\left(\frac{nF}{RT}\left[E^0 - E(0) - \frac{r\lambda t}{N}\right]\right)\right\}} \qquad \text{(vi)}$$

The summation (vi) is clearly dominated by its $\lambda = N$ term;

keeping only this term we obtain

$$I \approx \ell^2 \frac{\left[\exp\left(\frac{(2k+1)^2\pi^2 Dt}{\ell^2}\right) - \exp\left(\frac{(2k+1)^2\pi^2 D(N-1)t}{N}\right)\right]}{\pi^2 D(2k+1)^2\left[1+\exp\left(\frac{nF}{RT}\left[E^0 - E(0) - rt\right]\right)\right]} \qquad \text{(vii)}$$

$\frac{N-1}{N}$ can be chosen so that $\exp\left(\frac{(2k+1)^2\pi^2 Dt}{\ell^2}\right)$ is always larger than $\exp\left(\frac{(2k+1)^2\pi^2 D(N-1)t}{N\ell^2}\right)$ by some factor M in which case case Equation (vii)takes the simpler form of Equation (ii)

$$I \approx \frac{1}{\pi^2 D(2k+1)^2} \times$$

$$\frac{\ell^2 \exp\left(\frac{(2k+1)^2\pi^2 Dt}{\ell^2}\right)}{\left[1+\exp\left(\frac{nF}{RT}\left[E^0 - E(0)\right] - rt\right)\right]}$$

the relative error incurred in this approximation being 1/M; the required values of N are:

$$N \leqq \frac{(2k+1)^2\pi^2 Dt}{(2.3\log M)\ell^2} \qquad \text{(viii)}$$

It remains to find the range of r for which the approximations (v) through (vii) included in the derivation of (ii) lead to a relative error of less than ϵ. Since the error in the approximation leading to (ii) arises from the departure of the denominator of the integrand from its assumed constancy, we have the relation

$$\frac{1 + \exp\left(\frac{nF}{RT}\,[E^0 + E(0) - rt]\right)}{1 + \exp\left(\frac{nF}{RT}\,[E^0 - E(0)] - r\,\frac{(N-1)}{N}\,t\right)} - 1 < \epsilon \qquad \text{(ix)}$$

where $\frac{N-1}{N}$ is to be calculated from (viii). Since the accuracy of the approximations improves sharply with increasing k, it is sufficient to consider only the case for which k = 0. For convenience in manipulation of (ix) assume that

$$t = \frac{E^0 - E(0)}{r}$$

Thus, from (viii) and (ix) we obtain an expression giving the maximum sweep rate for which C_{ox} will be given by the Nernst equation with a relative error less than ϵ:

$$|r| \leqq \frac{RT}{nF}\,\frac{\pi^2 D}{\ell^2 \ln M}\,\log_e\left(\frac{2}{\epsilon + 1} - 1\right) \qquad \text{(x)}$$

It is easily seen that the relative error in i is twice that in C_{ox}; to assure that the relative error in i will be less than ϵ we must have

$$|r| \leq \left| \frac{RT}{nF} \frac{\pi^2 D}{\ell^2 \log_e M} \log \left(\frac{4}{\epsilon + 2} - 1 \right) \right| \qquad \text{(xi)}$$

As examples, if $\ell^2 = 10^{-6}$ sq. cm., $D = 10^{-5}$ sq. cm./sec., $E^0 - E(0) = -0.2$ volt, $M = 10^3$, and $T = 298°$ K., Equation (xi) becomes

$$|r| \leqq \left| \log \left[\frac{2}{1 + \frac{1}{2}\epsilon} - 1 \right] \right|$$

and if $\epsilon = 0.05$ we must have

$$|r| \leqq 22 \text{ mv./sec.}$$

or if $\epsilon = 0.01$ we must have

$$|r| \leqq 5 \text{ mv./sec.}$$

Equation (xi) is useful in the construction and use of thin layer electrodes, since it relates the thin layer cavity thickness ℓ to the relative error ϵ incurred in the use of the simplified theory for a given set of experimental conditions.

Appendix 2

Conditions for Total Irreversibility in Thin Layer Voltammetry

The conditions under which Equation 7 applies can be obtained from the following calculation: The back reaction, which is most rapid near the beginning of the sweep, leads to a larger reactant concentration at a given potential than would be observed in the absence of a back reaction. Thus, the relative error entailed in neglecting the back reaction will be less than ϵ provided that

$$\frac{C_R}{C^0_{ox}} = \frac{C^0_{ox} - C_{ox}}{C^0_{ox}} \leqq \epsilon \qquad \text{(i)}$$

whenever

$$\frac{k_b}{k_f} \geqq \epsilon \qquad \text{(ii)}$$

Thus, we have

$$C^0_{ox} - C_{ox} = \frac{1}{nFV} \int_0^t idt \leqq \epsilon\, C^0_{ox} \qquad \text{(iii)}$$

Calculation of (iii) is simplified by employing the relation $i \leq nFA\, C^0_{ox} kf$. Combining Equations (i), (ii) and (iii) and solving for k^0, we have

$$k^0 \leqq \frac{\epsilon \alpha n_0 VF(-r)}{ART} \left\{ \epsilon^{-\alpha} - \exp\left[\frac{-\alpha n_0 F}{RT} \left(E(0) - E^0 \right) \right] \right\}^{-1} \quad \text{(iv)}$$

The exponential term is vanishingly small and

$$k^0 \leqq \frac{\alpha n_0 VF(-r)}{ART} \quad \epsilon^{1 + \alpha}$$

Thus, for a typical set of experimental conditions ($E^0 = 0$, $r = 2$ mv/second, $C^0_{ox} = 10^{-3}$M, $A = 0.5$ cm.^{2}, $V = 1 \times 10^{-3}$ cm.^{3}, $\alpha = 1/2$, $n_0 = 1$, $T = 298°$ K), we must have $k^0 \leqq 10^{-6} \frac{\text{cm.}}{\text{sec.}}$ in order that $\epsilon \leqq 0.05$.

Appendix 3

Minimum Time Required for Q to Become Constant in Thin Layer Chronocoulometry.

Consider a general reaction

$$Ox + ne^- \rightleftharpoons R$$

which obeys the Nernst equation. Before the start of the experiment the potential is adjusted to E_1, where virtually all of the reactant should be present in the oxidized form; at t = 0 the potential is changed instantaneously to E_2 where virtually complete reduction to R can occur. If the rate of reduction at E_2 is controlled solely by the rate of diffusion of Ox to the surface of the thin layer electrode, and the thin layer cavity is composed of parallel planar electrode surfaces, the concentration of Ox in the cavity will be given (8) by

$$C(x, t) = \frac{4C^0}{\pi} \sum_{m=1}^{\infty} \frac{1}{2m - 1} \exp\left[\frac{-(2m - 1)^2 \pi^2 Dt}{\ell^2}\right] \sin \frac{(2m - 1)\pi x}{\ell} \tag{i}$$

The current-time equation is

$$i(t) = nFAD\left(\frac{\partial C(x, t)}{\partial x}\right)_{x=0} = \frac{4nFADC^0}{\ell} \sum_{m=1}^{\infty} \exp\left[\frac{-(2m - 1)^2 \pi^2 Dt}{\ell^2}\right] \tag{ii}$$

which after integration yields

$$Q(t) = nFVC^0 \left\{1 - \frac{8}{\pi^2} \sum_{m=1}^{\infty} \left(\frac{1}{2m - 1}\right)^2 \exp\left[\frac{-(2m - 1)^2 \pi^2 Dt}{\ell^2}\right]\right\} \tag{iii}$$

The summation on the right of Equation (iii) tends rapidly to zero as t increases, so that Q(t) is given simply by Faraday's law for t sufficiently large. If $\ell^2 < 10^{-5}$ cm^2 and $t > 0.02$ second, (iii) takes the simpler form

$$Q(t) = nFVC^0 \left\{1 - \exp\left[\frac{-\pi^2 Dt}{\ell^2}\right]\right\} \tag{iv}$$

From Equation (iv) we obtain

$$\tau_{\text{min}} = \frac{-\ell^2}{\pi^2 D} \ln \epsilon \tag{v}$$

which gives the minimum time τ_{min} required to complete a thin layer chronocoulometric measurement. For instance, if $D = 10^{-5} \frac{\text{cm}^2}{\text{sec.}}$, and $\epsilon = 0.01$ (1% relative error), τ_{min} will be 0.046 and 0.46 second for ℓ^2 equal to 10^{-5} and 10^{-6} cm^2, respectively.

In case the Nernst equation is not obeyed, Equations (i)-(iv) are not applicable. Instead, if the reaction is totally irreversible (that is, if $k_f(E_2) = k^0 \exp\left[\frac{-\alpha n_0 F}{RT}(E_2 - E^0)\right] < 10^{-4} \frac{\text{cm.}}{\text{sec.}}$ -- see Appendix 2) the current density will always be sufficiently small that the reactant concentration can be assumed relatively uniform throughout the cavity, and we have

$$\frac{dC(t)}{dt} = \frac{Ak_f(E_2)C(t)}{V}, \qquad \text{(vi)}$$

which leads to

$$C(t) = C^0 \exp\left[\frac{-Ak_f(E_2)t}{V}\right]. \qquad \text{(vii)}$$

The current is

$$i = nFV\frac{dC}{dt} = nFVAk_f C^0 \exp\left[\frac{-Ak_f(E_2)t}{V}\right] \qquad \text{(viii)}$$

and after integration we have

$$Q(t) = nFVC^0\left\{1 - \exp\left[\frac{-Ak_f(E_2)t}{V}\right]\right\} \qquad \text{(ix)}$$

Putting $Q(t) = (1 - \epsilon)nFVC^0$ in Equation (ix) we obtain τ_{min} (irreversible) $= \frac{-V}{Ak_f(E_2)} \ln \epsilon$. For instance, if $V = 1 \times 10^{-3}$ cm.^{3}, $A = \frac{1}{2}$ cm.^{2}, and $k_f = 10^{-4} \frac{\text{cm.}}{\text{sec.}}$, then τ_{min} (irreversible) = 92 seconds as compared with ca. 0.1 second for a reversible reaction.

III. Apparatus

Although the thin layer electrodes employed prior to this study (1) served to demonstrate the potential usefulness of the thin layer approach, they were unnecessarily difficult to use. In this study (9), three new electrodes were devised which were simple to construct and could be rapidly filled and cleaned.

The first electrode imprisoned the thin layer of solution between the inner wall of a short section of precision-bore glass capillary tubing and a close-fitting platinum wire inserted into the tubing (Figure 4). The second electrode was constructed from a micrometer to which platinum faces had been attached; the thin layer of solution was confined between the faces of the micrometer which were equipotential (Figure 6). A more difficult task, construction of a thin layer electrode having a mercury surface, was also accomplished (Figure 8).

1. The Glass Capillary-Wire Electrode

The glass capillary-wire electrode (Figure 4)

---

[9] A. T. Hubbard and F. C. Anson, Anal. Chem., 36, 723 (1966).

Figure 4

Glass capillary-wire electrode

A. Unit constructed with standard-taper glass supporting members.

B. Unit constructed with Teflon supporting members.

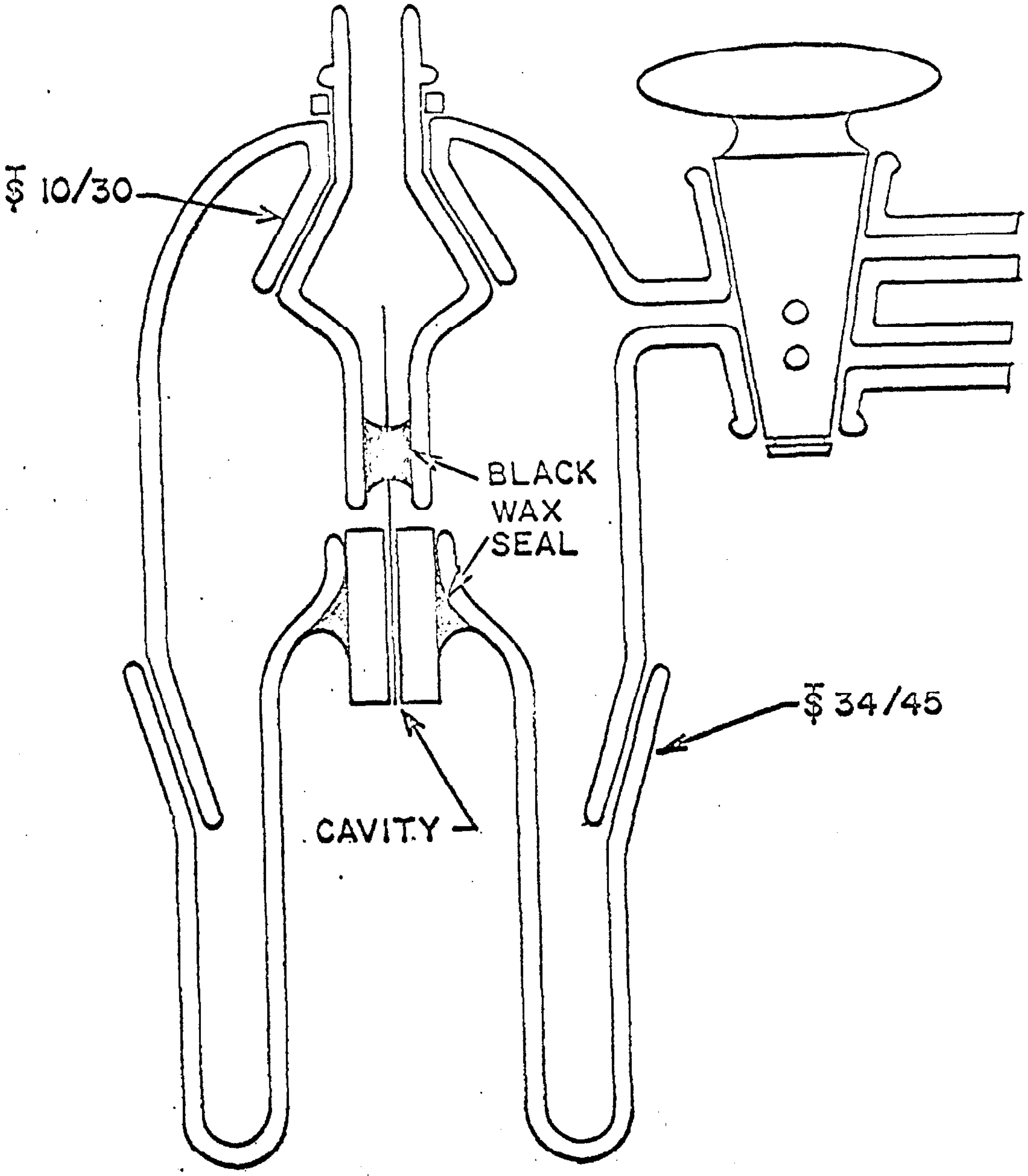
$ 10/30
BLACK
WAX
SEAL
$ 34/45
CAVITY

4-A

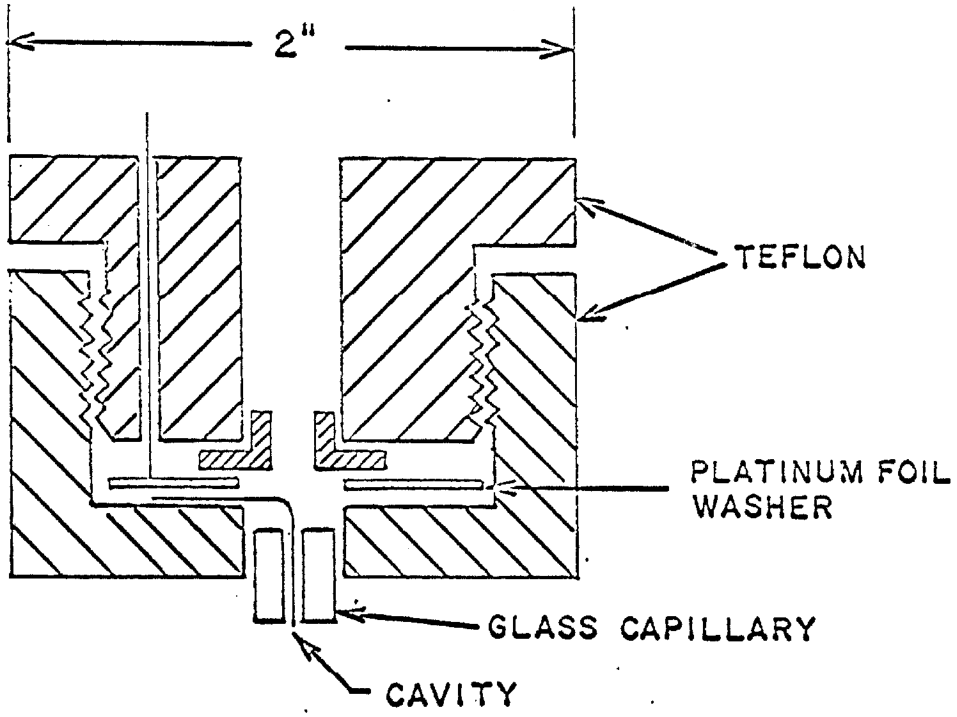
2"
TEFLON
PLATINUM FOIL WASHER
GLASS CAPILLARY
CAVITY

4-B

was made from readily available standard glass pieces. Precision-bore capillary tubing, having inside diameters of from 0.003 ± 0.0002 inch to 0.031 ± 0.0002 inch, was obtained from the Wilmad Glass Co., Buena, N. J. The capillary tubing was cut to approximately the desired length on a glass saw and polished to exact tolerances on a glass-grinding wheel; capillary lengths of 0.500, 1.000, and 1.500 cm. were used. Each capillary length was fitted with a platinum wire having a diameter exactly 0.001 inch smaller than the inside diameter of the capillary. Although the tolerance of the tube diameters specified in the guarantee, ± 0.0002 inch, would introduce an uncertainty of about 20% into the geometry of the electrodes, the present set of electrodes, when calibrated against a standard iron(III) solution, agreed with the prescribed dimensions within a few per cent.

The function of the glassware shown in Figure 4-A was to hold the capillary and wire in position and to allow removal of solution by a flow of nitrogen. The three-way stopcock allowed convenient application and release of nitrogen pressure; during the electrolysis it was positioned with the cell arm blocked. Use of the glass capillary electrode was simplified by construction of a modified H-cell of the type shown in Figure 5. Supporting electrolyte was deaerated in the solution reservoir, R, and allowed to flow into the contact arm; the protruding tip of the

Figure 5

H-cell for glass capillary-wire electrode

R. Supporting electrolyte reservoir

D. Sintered glass disk

C. Compartment for auxilliary and reference electrodes.

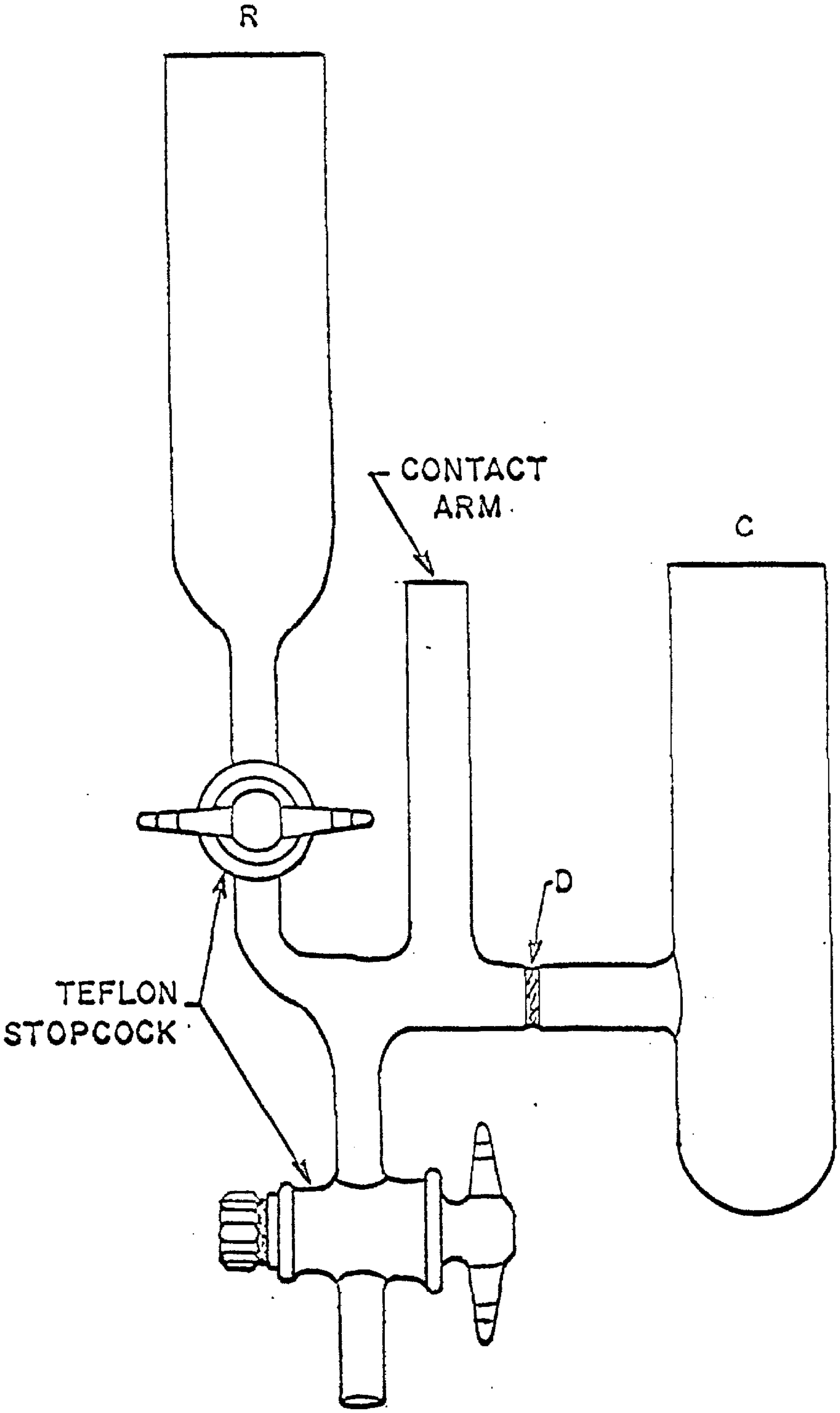
R
CONTACT ARM
C
D
TEFLON STOPCOCK

capillary tube was placed in contact with the liquid in the contact arm of the H-cell. Both the auxilliary electrode and the reference electrode were placed in compartment C.

The glass-capillary electrode had a slight disadvantage in that it was difficult to position the capillary tip precisely in the H-cell because visibility was restricted by the lower standard-taper glass member. To overcome this drawback a second type of glass-capillary electrode was designed in which some of the glass members were replaced by ones made from Teflon. The design is shown in Figure 4-B. With this electrode it was much easier to position the capillary tip precisely. All of the glass-capillary wire electrode data reported in this paper were obtained with the electrode in Figure 4-A.

2. The Micrometer Electrode

In construction of the micrometer electrode, the faces of a metric micrometer caliper with removable anvil (L. S. Starrett Co., Athol, Mass., Model No. 2MARL) were replaced by a pair of pure platinum cylinders which were connected to the original faces by a pair of Teflon adapters (Figure 6). The platinum pieces were carefully machined and polished to have a geometry and finish as nearly as possible like those of the original micrometer.

The micrometer electrode was used with a modified H-cell of the type shown in Figure 7. The micrometer was mounted in a horizontal position and the contact arm of the H-cell brought to within 1 mm. of the cavity; a slight flow of liquid in the contact arm was permitted until the liquid at the tip of the arm extended into contact with the electrode cavity; the unit was then ready for use. The deaerated electrolyte was stored in the upper solution reservoir and the auxiliary and reference electrodes were contained in the solution compartments.

Figure 6

Micrometer electrode

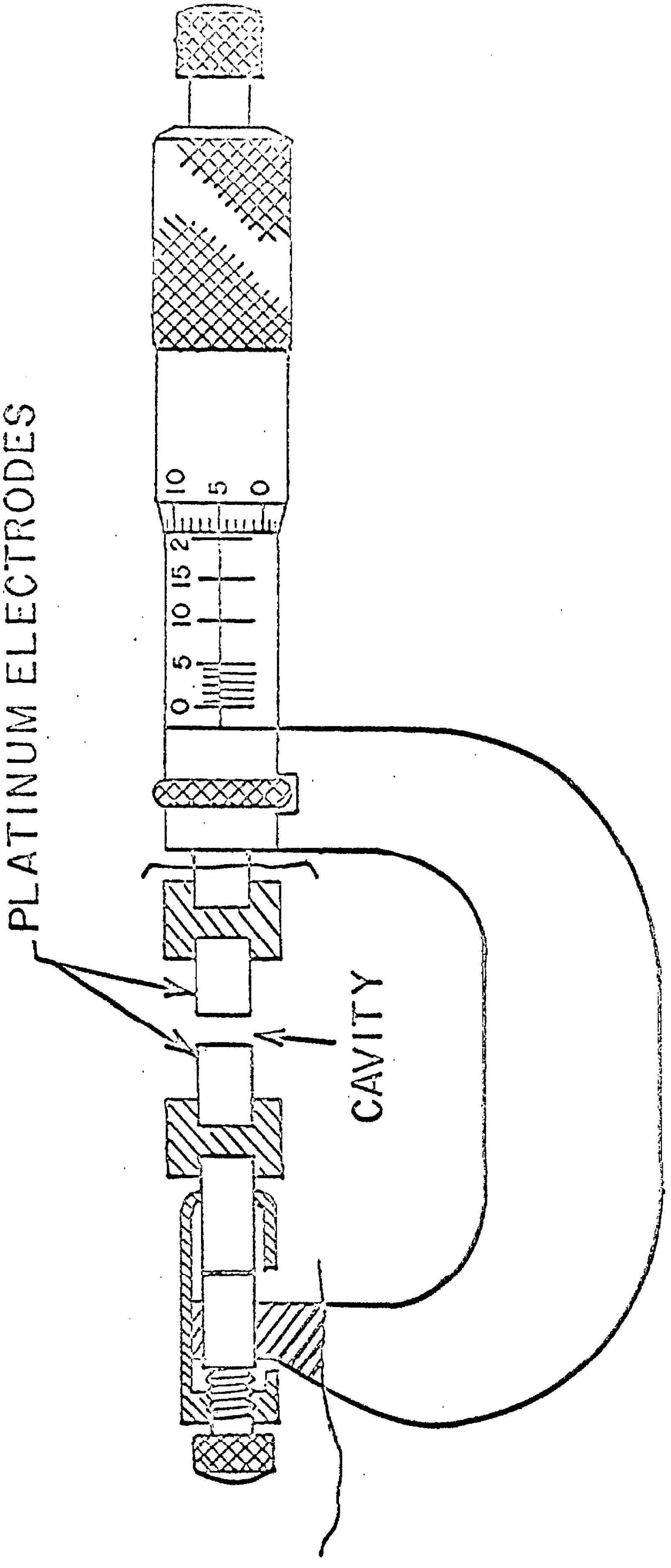
PLATINUM ELECTRODES
CAVITY

Figure 7

H-cell for micrometer electrode

Right-hand compartment contained auxiliary and left-hand compartment contained reference electrode.

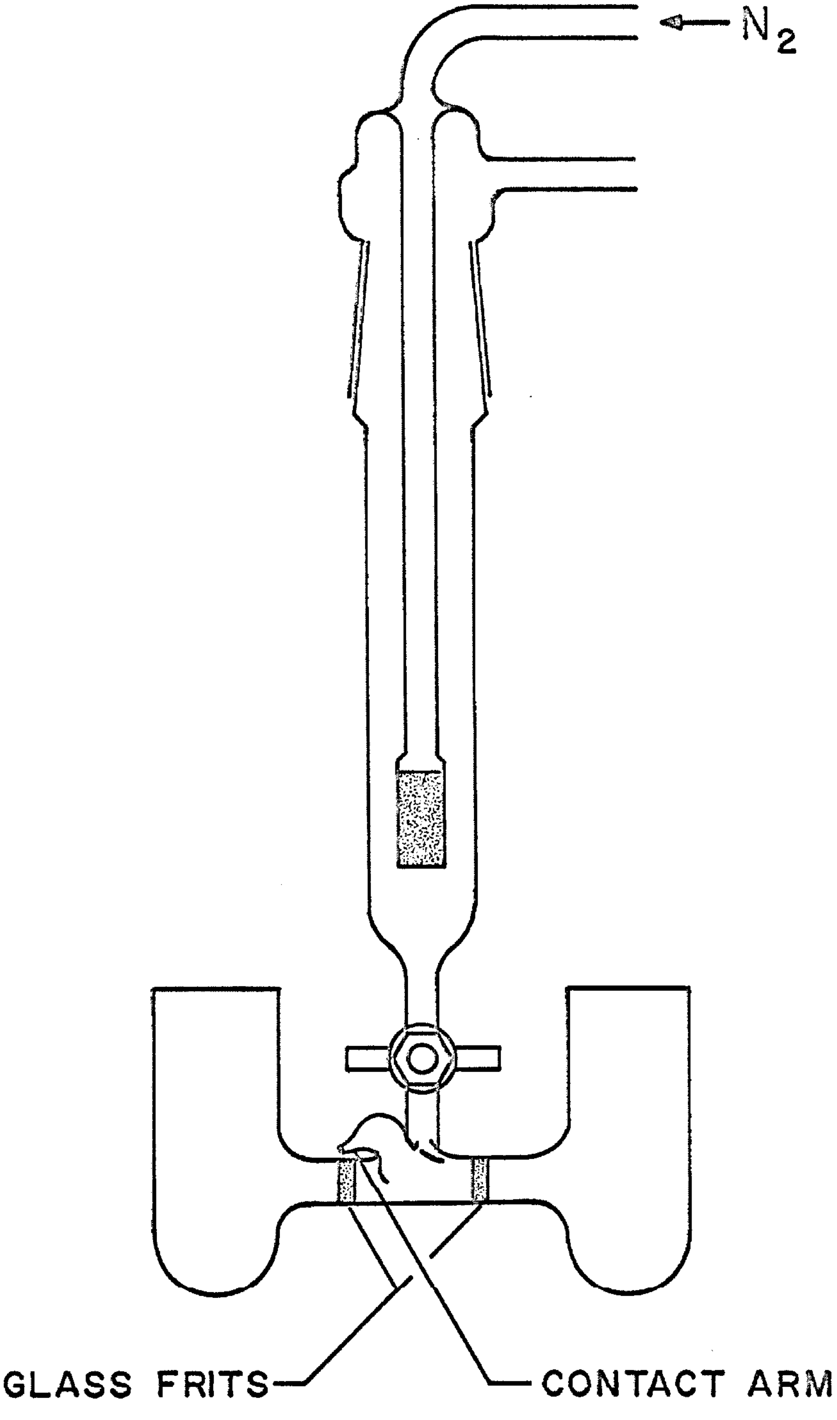
N₂
GLASS FRITS
CONTACT ARM

3. The Micrometer Mercury Electrode

The construction and use of the thin layer electrode having a mercury surface were similar to that of the micrometer electrode. The thin layer of solution was contained between a mercury-coated platinum rod which had a convex hemispherical end and a matching glass piece which had a concave hemispherical end of 20 micron larger radius (Figure 8). The platinum piece was wetted with a film of mercury. Wetting was achieved by treating the platinum surface with sodium amalgam, followed by thorough rinsing, first with water, and then with pure mercury. The micrometer was mounted vertically with the mercury-wetted platinum piece at the bottom. The H-cell shown in Figure 7 was employed. The thickness of the mercury film was reproducible; the extent of its variation was, in fact, too small to be observed in the present measurements. The total thickness of the mercury film at the center of the hemisphere was *ca.* 4×10^{-4} cm.

Figure 8

Micrometer mercury electrode

Micrometer is shown in Figure 6.

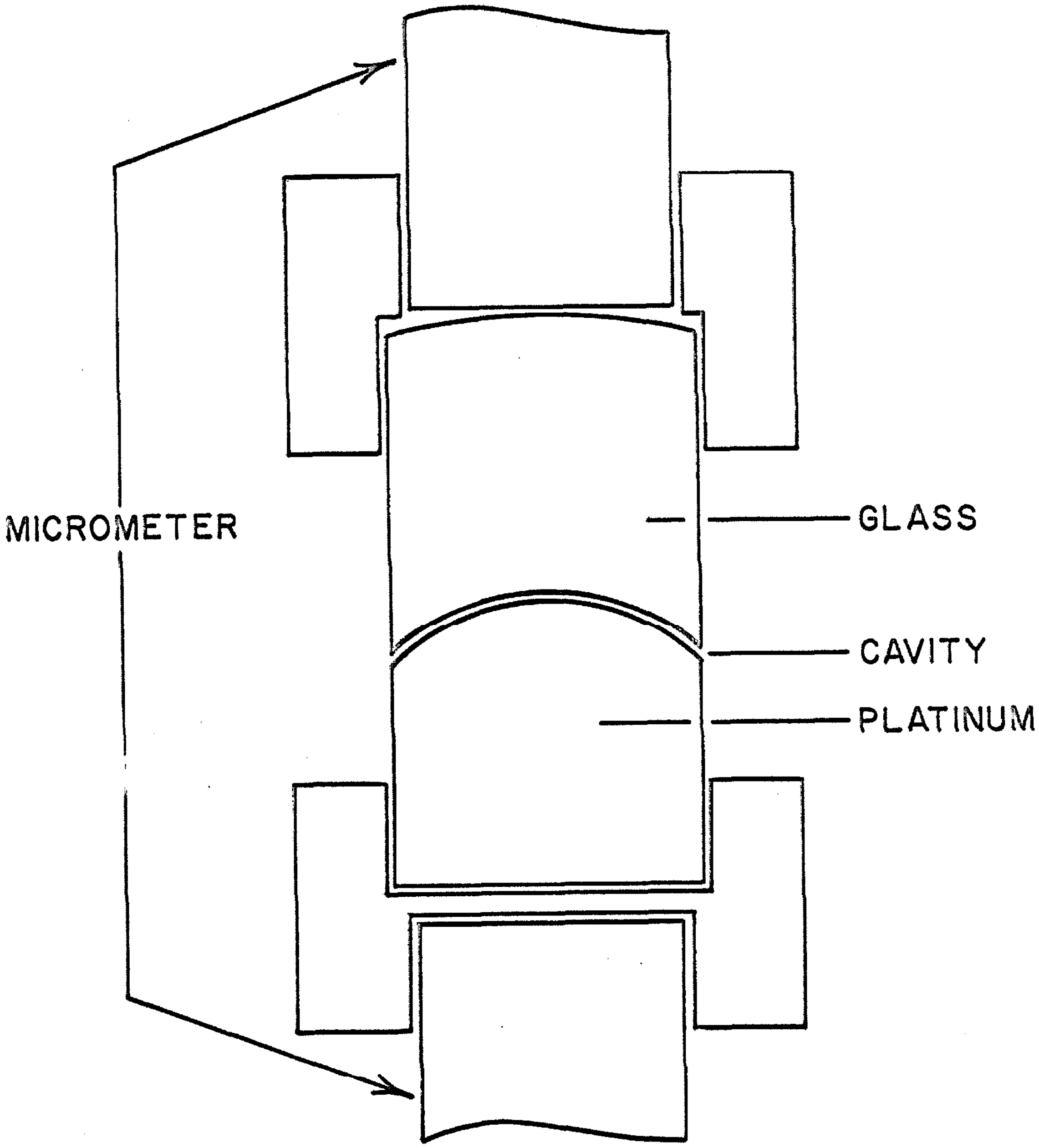
MICROMETER
GLASS
CAVITY
PLATINUM

4. Circuitry

The circuitry employed was conventional (10). Measurement of electrode potentials, current and current-integrals was achieved with the use of operational amplifiers (George Philbrick Researches, Inc., Type P 65 and P 75). All potentials were measured *vs.* the saturated calomel electrode (S. C. E.) and are reported as such.

---

[10] G. Lauer, *et. al.*, *Anal. Chem.*, *35*, 1789 (1963).

IV. Testing of the Apparatus and Theory

The accuracy and reproducibility of the electrodes described in Section III were tested for chronopotentiometric reduction of Fe(III) in 1 F $HClO_4$. The equations for thin layer voltammetry and chronocoulometry of reversible systems were verified experimentally for the Fe(III) - Fe(II) couple using electrodes of the micrometer type.

1. Testing of the Electrodes

To prepare the electrodes for use, they were subjected to alternate anodic and cathodic polarization in 1 F H_2SO_4; the final cycle was cathodic and the electrodes were held at ca. 0.4 volt S. C. E. for several minutes before each trial.

The glass-capillary electrodes were filled before each trial by thorough rinsing with the solution to be used in the experiment. Rinsing and filling were accomplished in about 5 minutes. A drop of solution was placed at the tip of the capillary and the cavity filled itself by capillary attraction. The liquid was removed from the cavity by a flow of nitrogen introduced into the cavity through the stopcock. After several rinsings, the electroactive material was introduced into the cleaned cavity in the same manner and the chronopotentiogram was recorded.

Filling of the micrometer electrode was extremely simple and was accomplished by placing a drop of solution containing the electroactive material on one face of the micrometer and adjusting the micrometer to give the desired distance setting (from 1 to 5×10^{-3} cm.). The solution that was squeezed from the crevice during the adjustment flowed down the side of the lower electrode face and away from the crevice. The crevice height (*ca.* 0.001 cm.) was small in comparison with electrode diameter (*ca.* 0.7 cm.) and irregularities in the shape of the exposed portion of the body of solution contained in the crevice had no appreciable effect on the volume contained by the crevice.

Typical data demonstrating the accuracy and reproducibility obtainable with the capillary-wire and micrometer electrodes appear in Tables I and II.

The graphical method suggested by Reinmuth (11) was employed to obtain the transition time from the chronopotentiometric curves.

The precision of the micrometer electrode was limited primarily by the precision of the caliper movement which had as its smallest scale division 0.001 cm. The cavity thickness of the electrode could be varied from 1 to 10×10^{-3} cm. without noticeable effect on the performance of the electrode except for an accurately predictable change in the cavity volume and in

---

[11] W. H. Reinmuth, *Anal. Chem.*, *33*, 485 (1961).

Table 1. Calibration and Reproducibility Data for Thin Layer Electrodes

Capillary-Wire electrode		Micrometer electrode	
Trial	Transition time, sec.	Trial	Transition time, sec.
1	68.0	1	54.0
2	68.6	2	54.3
3	67.0	3	54.0
4	68.0	4	53.6
5	67.6	5	53.6
		6	54.7
Av.	67.8	Av.	54.0
Calcd. from geometrical volume and Faraday's law: 68.6 sec.		Calcd. from geometrical volume and Faraday's law: 54.0 sec.	

Experimental Conditions: Each trial represents a separate filling of the electrode. Capillary-wire electrode: Capillary diameter = 0.004 inch; wire diameter = 0.003 inch; cavity height = 1.0 cm.; current = 5.0 μa. Micrometer electrode: Cavity thickness = 3.60×10^{-3} cm.; electrode area (both faces) = 0.618 cm.^{2}: current = 200 micro ampere.

Table II. Current-Transition Time Data for Micrometer Electrode

0.139F Fe(III) in 1 F $HClO_4$

Cavity thickness = 2.6×10^{-3} cm.

Current, μa.	Observed transition time, seconds	Theoretical transition time, seconds
50	215	216
100	106	108
200	53	54
400	28.0	27
1000	a	10.8

Cavity thickness = 1.6×10^{-3} cm.

Current, μa.	Observed transition time, seconds	Theoretical transition time, seconds
50	140	130.4
100	64.5	65.2
200	34.8	32.6
400	16.0	16.3
600	a	10

[a] Chronopotentiogram too ill-defined to measure τ, but approximate τ much too short.

the transition time for the trial.

The rates of loss of Fe(III) from the electrode cavities resulting from diffusion into the iron-free supporting electrolyte were measured and found to be quite small. For example, the capillary-wire electrode used to obtain the data of Table I showed diffusive losses of less than 1% in 20 minutes with the electrode dipping in iron-free 1 F $HClO_4$ and the micrometer electrode showed no detectable diffusive loss in 60 minutes with a cavity thickness of 2.6×10^{-3} cm. and the H-cell in place.

As indicated in connection with Table II, the shape of the chronopotentiograms deteriorates for large current densities. This is apparently due to inclusion within the measured potential of part of the ohmic potential difference between the working and auxiliary electrodes. This effect is discussed in greater detail in IV-4.

2. Thin Layer Voltammetry of the Fe(III) - Fe(II) Couple

Typical current-potential curves and peak current-sweep rate data for the Fe(III) - Fe(II) couple in 1 F HCl are given in Figure 9 and Table III. The agreement between observed and calculated peak currents, which is quite good, demonstrates the potential usefulness of this technique for estimating the n-values of reversible reactions. This application is particularly attractive because of the second-order dependence of the peak current on n.

From Table III it can be seen that the anodic and cathodic peak potentials are in good agreement only for the slowest sweep rates. This trend,which is apparently due to inclusion of an ohmic potential difference within the measured potential, will be discussed further in IV-4.

Figure 9

Single-cycle current-potential curves for
Fe(II) and Fe(III) in 1 F HCl

A. Oxidation of Fe(II)

B. Reduction of Fe(III)

Experimental conditions: Solution was 1.0×10^{-3} F Fe(II) in 1 F HCl; thin layer volume was 1.4 microliter (ℓ = 44.2 microns); sweep rate was 4.0 $\frac{\text{millivolt.}}{\text{second}}$

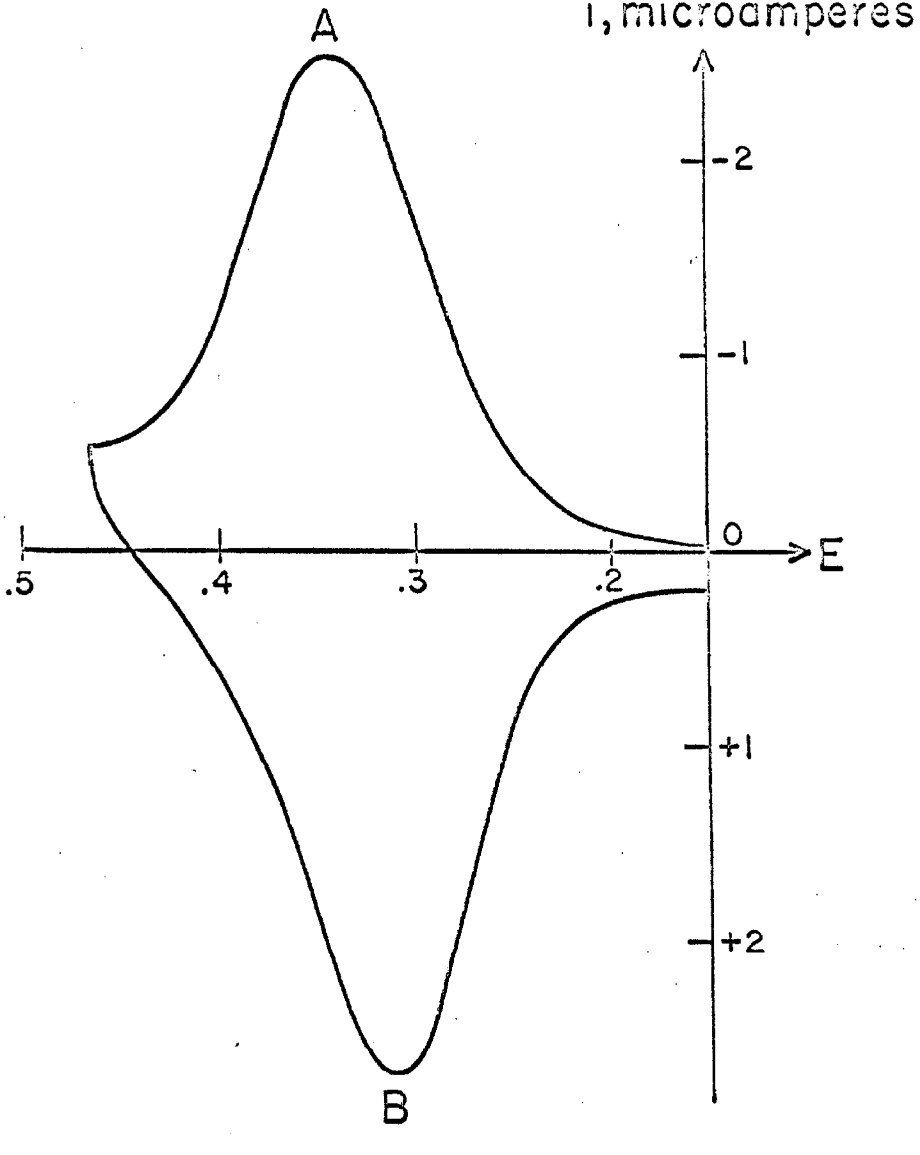
A
i, microamperes
-2
-1
0
E
.5
.4
.3
.2
+1
+2
B

Table III. Thin-Layer Voltammetry of Fe(III) and Fe(II) in 1 F HCl[a]

Sweep rate, mv./sec.	Peak current, μa.			Peak potential volt vs. SCE	
	Observed		Calculated		
	Anodic	Cathodic		Anodic	Cathodic
1.0	0.6	0.6	0.594	0.33	0.33
2.1	1.3	1.3	1.25	0.33	0.34
4.0	2.5	2.6	2.37	0.34	0.31
8.0	5.5	5.6	4.74	0.35	0.30
16.0	10.0	10.8	9.50	0.37	0.28[b]
32.0	22.0	24.0	19.0	0.46	0.28[b]
64.0	37.0	40.0	38.0	0.50	0.26[b]

[a] The test solution was 1.00×10^{-3} F Fe(II) in 1 F HCl. Thin layer volume = 0.628 μl.

[b] The larger differences in peak potentials at the higher sweep rates result from ohmic potential differences and less uniform current distribution.

3. Thin Layer Chronocoulometry of the Fe(III) - Fe(II) Couple

The current integrals Q obtained for reduction of Fe(III) in 1 F $HClO_4$ using the chronocoulometric measuring technique were in agreement with those calculated from Equation 14, as expected. However, the comparatively large potentiostatic currents required for chronocoulometric experiments resulted in the inclusion of comparatively large ohmic potential differences in the potential-control circuit, with the result that the time τ_{min} required for Q to become constant was lengthened by an amount which increased with the bulk concentration of the reactant.

4. Ohmic Potential-Difference Effects

Ohmic potential differences were unavoidably included in the measuring circuit as the result of two closely related causes. First, as is clear from Figures 5 and 6, at least part of the ohmic potential difference between the working and auxiliary electrodes was included in the measured electrode potential. This effect was minimized by employing H-cells with separate compartments for the reference and auxiliary electrodes (Figure 7.) A second source of ohmic potential difference in the measuring circuit was non-uniformity of the current density. The way in which non-uniform current density originated can be pictured as follows (Figure 10): the solution in the cavity acted as a resistor R(y, z, t) toward charge flowing from the point of entry into the thin layer cavity to points elsewhere in the cavity; charge flowing from the point of entry 0 to a point A near 0 encountered less resistance than charge flowing to some point B more distant from 0; thus, the current density at A was greater than at B.

In potentiostatic experiments (for instance, voltammetry and chronocoulometry) the potential E experienced by the reactant at the electrode surface was not uniformly equal to E (applied) along the surface but instead varied according to

$$E = E\text{ (applied)} + i\,[\,R(y,z,t) + R\,]$$

In chronopotentiometric experiments the measured potential

Figure 10

Schematic diagram of the micrometer electrode cavity (not to scale)

Points 0, A and B are described in the text.

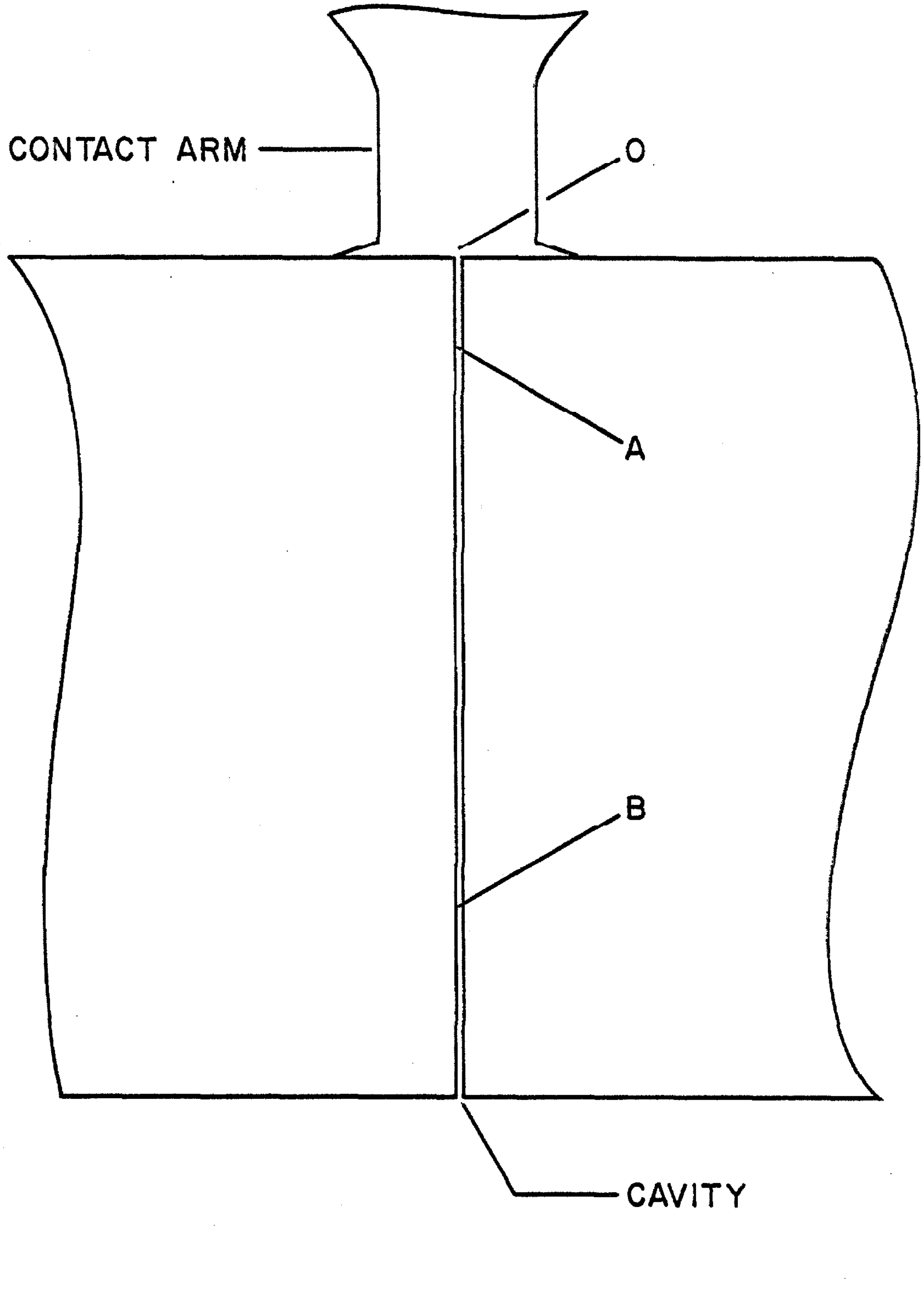
CONTACT ARM
O
A
B
CAVITY

E (meas.) was not equal to E(cell) but instead

$$E\ (\text{meas.}) = E\ (\text{cell}) - i\,[\,R(y, z, t) + R]$$

The departure from ideal behavior observed for large current densities is illustrated for the reduction of Fe(III) in Figures 11, 12, and 13. In linear potential sweep voltammetry ohmic potential differences decreased the peak current below its expected value and caused it to occur at potentials different from E^0 (Figure 11). In chronocoulometry, the effect was to lengthen the time required for the current integral to become constant (Figure 12). As Figure 13 shows, when $i\,R(y, z, t)$ was sufficiently large the galvanostatic reduction of Fe(III) was interrupted by an interfering reaction (solvent reduction) with the result that the transition time could not be determined from the chronopotentiometric curve.

In experimental applications of thin layer techniques, such as those described in Part V, it is generally possible to make the ohmic potential differences included within the measuring circuit very small by placing reasonable limits on the magnitude of the applied current.

Figure 11

Single-cycle thin layer current-potential curves for the Fe(III) - Fe(II) couple in 1 F $HClO_4$.

A. 10.0 milliFormal Fe(II)

x = 5 microampere

B. 100.0 milliFormal Fe(II)

x = 50 microampere

The electrode employed was of the micrometer type ($\ell = 20.8$ micron).

The volume of the Fe(II) was 0.78 microliter.

The sweep rate was 2.0 $\frac{\text{millivolt}}{\text{second}}$.

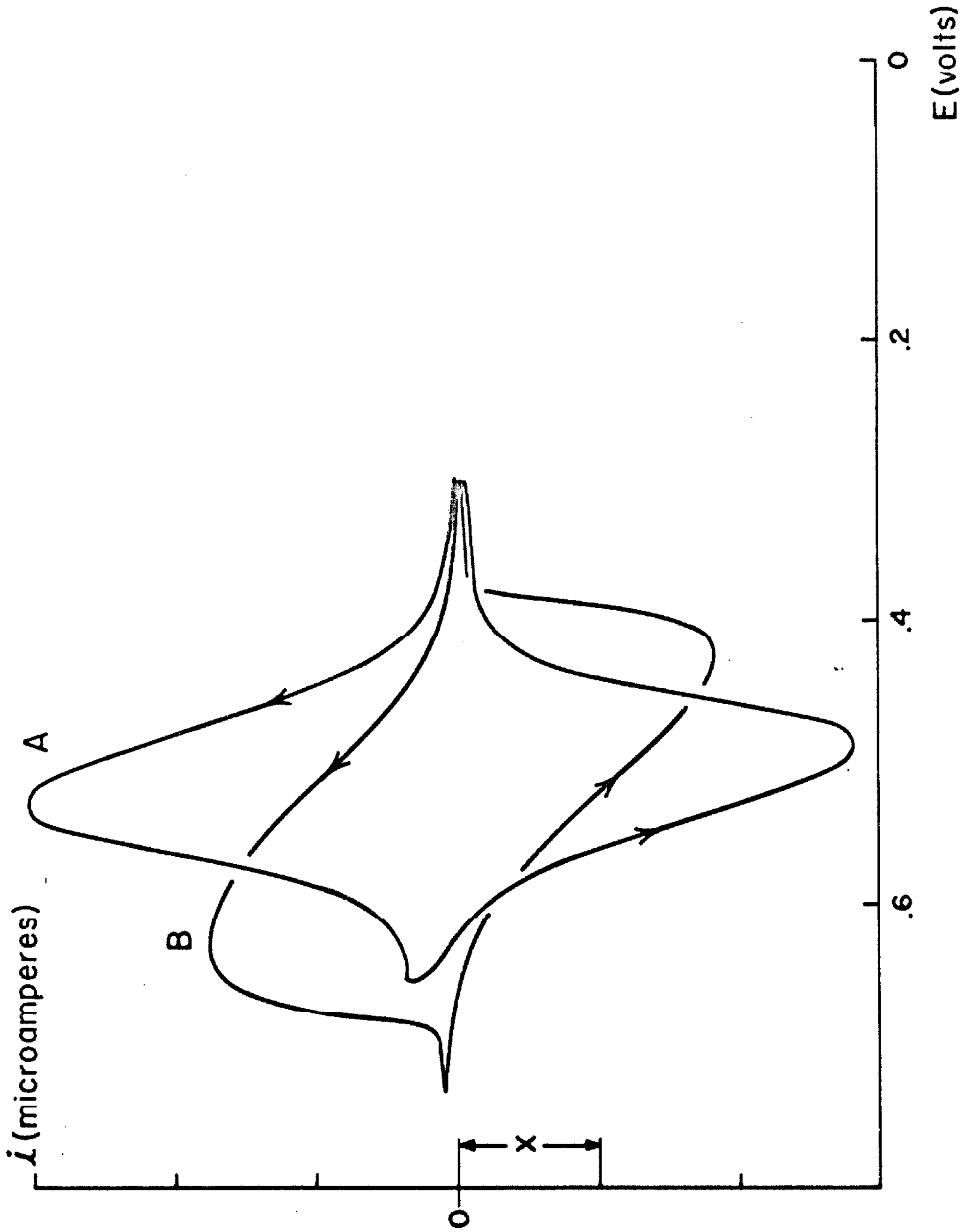
i (microamperes)
0
x
A
B
E (volts)
0
.2
.4
.6

Figure 12

Thin layer chronocoulometric charge-time curves for oxidation of Fe(II) in 1 F $HClO_4$.

A. 10.0 milliFormal Fe(II)
   x = 200 microcoulomb
B. 100.0 milliFormal Fe(II)
   x = 2.0 millicoulomb

The electrode employed was of the micrometer type (ℓ = 20.8 micron).

The volume of Fe(II) was 0.78 microliter.

The potential-step was from 0.65 to 0.30 volt S. C. E.

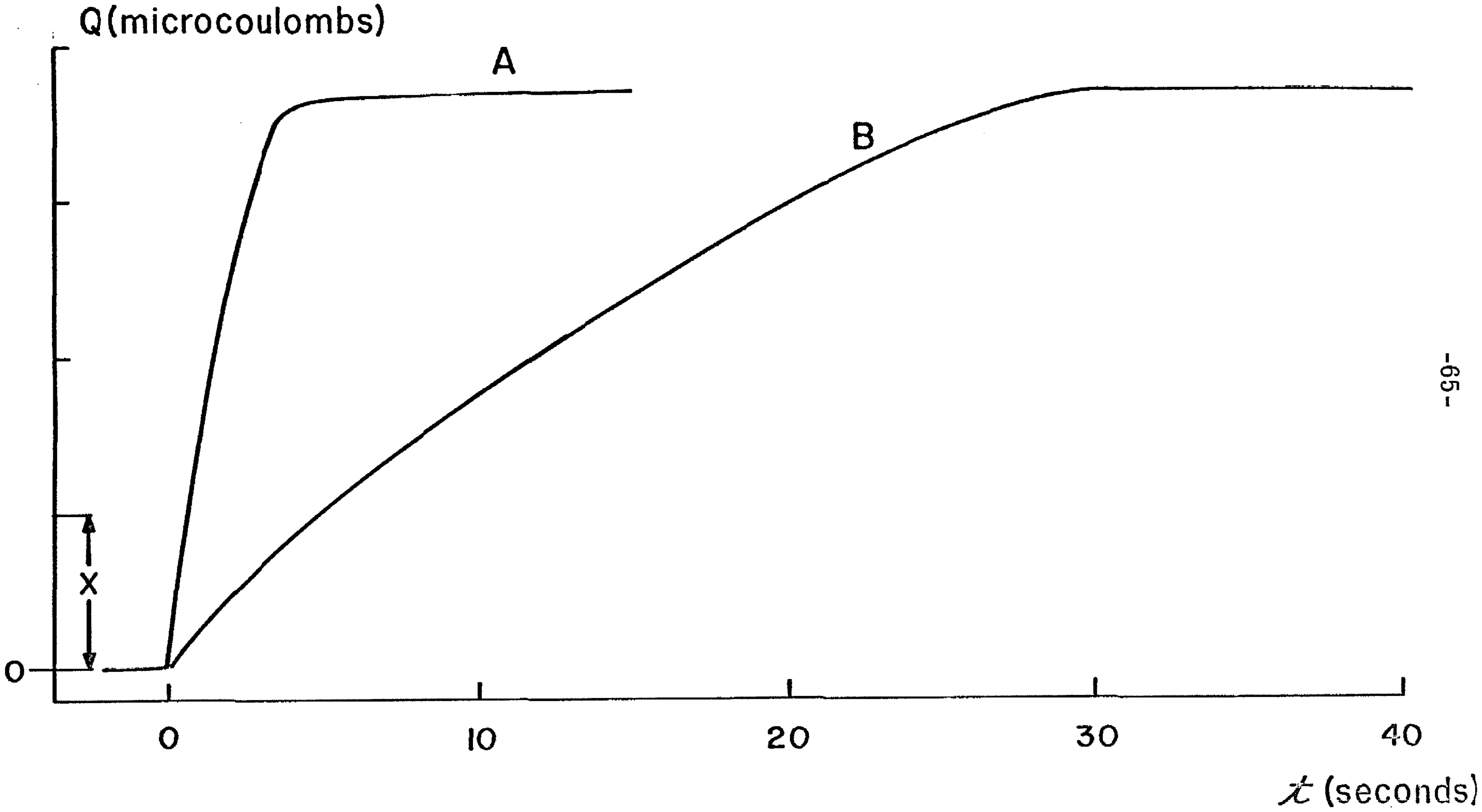
Q(microcoulombs)
A
B
X
0
0
10
20
30
40
t (seconds)

Figure 13

Thin layer chronopotentiometric potential-time curve for oxidation of Fe(II) in 1 F $HClO_4$.

A. 10.0 milliFormal Fe(II).

The current was 100 microampere.

B. 100.0 milliFormal Fe(II).

The current was 1.0 milliampere.

The electrode employed was of the micrometer type (ℓ = 20.8 micron).

The volume of Fe(II) was 0.78 microliter.

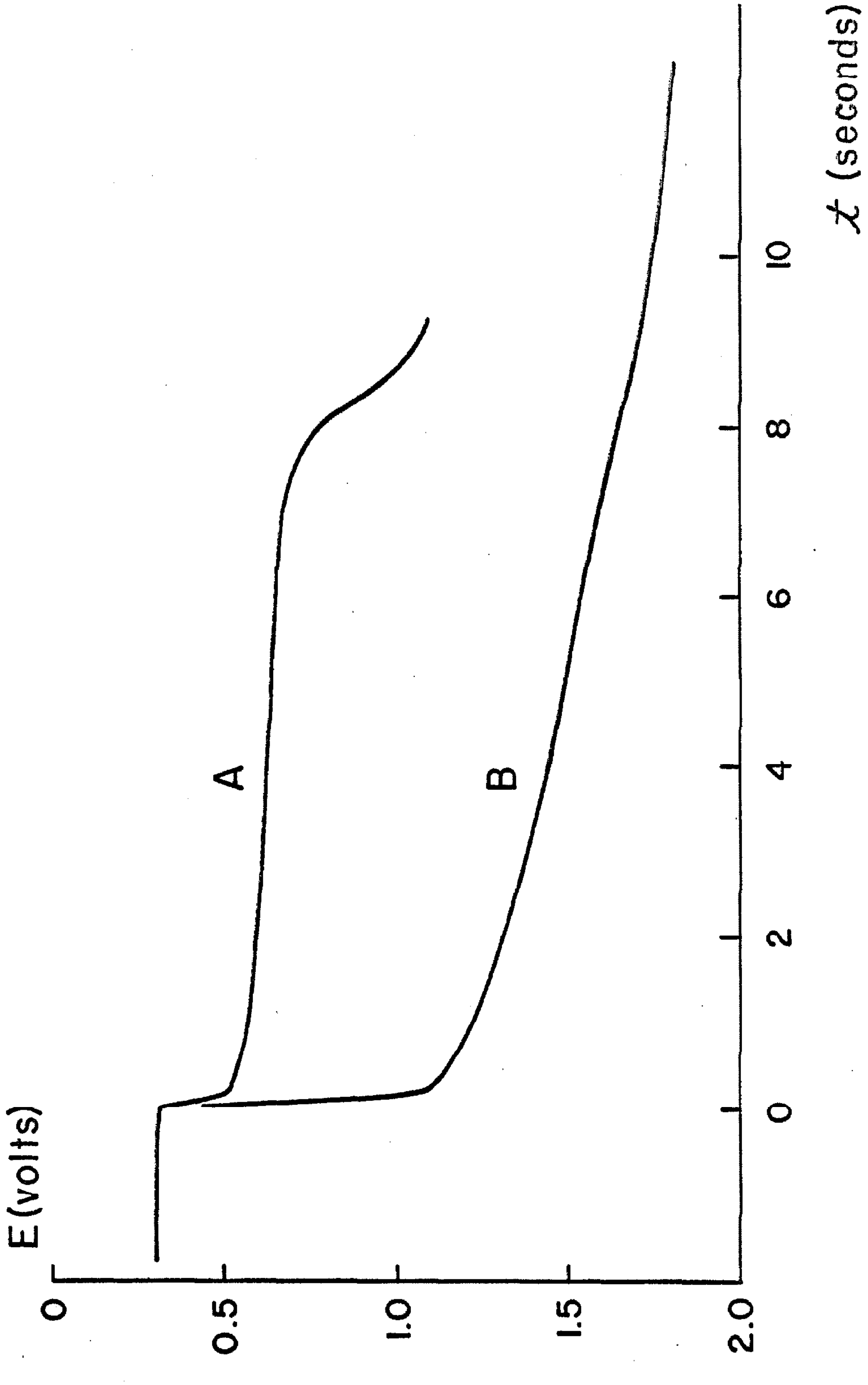
E (volts)
0
0.5
1.0
1.5
2.0
A
B
0
2
4
6
8
10
𝜏 (seconds)

V. Examples

Experiments which demonstrate the suitability of the thin layer approach for study of systems where reactant adsorption can occur, and for elucidation of the stoichiometry of complicated reactions are reported in this section.

1. Determination of Reactants Adsorbed on Platinum Electrodes.

(i) A Study of the Iodide-Iodine Couple at Platinum Electrodes (12, 13)

The electrochemical behavior of iodine and iodide ion at platinum electrodes has been treated in some detail in a number of recent papers (14, 15, 16). Extensive adsorption of both iodide and iodine was shown to occur and it was demonstrated

---

[12] A. T. Hubbard and F. C. Anson, J. Electroanal. Chem. 9, 163 (1965).

[13] A. T. Hubbard, R. A. Osteryoung, and F. C. Anson, Anal. Chem., 38, 692 (1966).

[14] R. A. Osteryoung, Anal. Chem., 35, 1100 (1963).

[15] R. A. Osteryoung, G. Lauer, and F. C. Anson, J. Electrochem. Soc., 110, 926 (1963).

[16] R. A. Osteryoung and F. C. Anson, Anal. Chem., 36 975 (1964).

that although the adsorbed iodine was electroactive--i. e., could be reduced near the reversible iodide-iodine potential--the adsorbed iodide ion was not. Among the data presented (16) was a brief set of experiments involving the technique of chronopotentiometry in thin layers of solution. The apparently contradictory results of these earlier experiments, coupled with the particular suitability of thin layer techniques for studies involving adsorbed reactants, prompted the additional experiments described in this paper.

Experimental

The electrode used was of the micrometer type. Ten- to fifty-micron layers of solution were confined between the faces of the micrometer which were equipotential. The diameter of each electrode face was 0. 250 inches, giving an area of each face of 0. 3175 $cm.^2$

Solutions were prepared from reagent-grade chemicals. Iodine solutions were prepared as follows: Solid iodine was added to deaerated 1 F H_2SO_4 and saturation allowed to occur; the resulting solutions were electrolyzed with a large platinum gauze electrode controlled at +0. 55 volt to remove possible traces of iodide and then diluted with deaerated 1 F H_2SO_4 to approximately the desired concentrations and their titer determined immediately before use by titration with standard thiosulfate solution. Standard iodide solutions were prepared determinately in air-free 1 F H_2SO_4.

1 F H_2SO_4 was used as the rinse solution and supporting electrolyte. All solutions were air-free and the experiments were performed with the thin layer cell mounted in a polyethylene tent which was continuously being flushed with prepurified nitrogen.

At various points in the experiments it was necessary to pipet microliter quantities of standard solutions into the thin layer cell. An example of the special pipets that were constructed for this purpose is shown in Figure 14. The solution to be pipeted was contained inside a length of glass tubing having an inside diameter of about 0.02 cm. Calibration of the pipets was achieved by weighing the water delivered by the pipets, by recording thin layer chronopotentiograms on standard solutions delivered by the pipets, and by measuring the volume delivered by the pipets into a micrometer electrode whose geometry was already accurately known. Calibrations made by these three independent methods agreed within 1%.

The contents of the pipets were delivered by expelling the solution with nitrogen pressure onto one electrode face with the micrometer opened to provide a gap of several millimeters. The micrometer was then closed to leave a layer thickness calculated to provide a gap volume corresponding exactly to the volume of liquid added. Visual inspection of the crevice was used to confirm that the liquid just filled the gap. In cases

Figure 14.

Micropipet used for precise additions of solutions to the thin layer electrode.

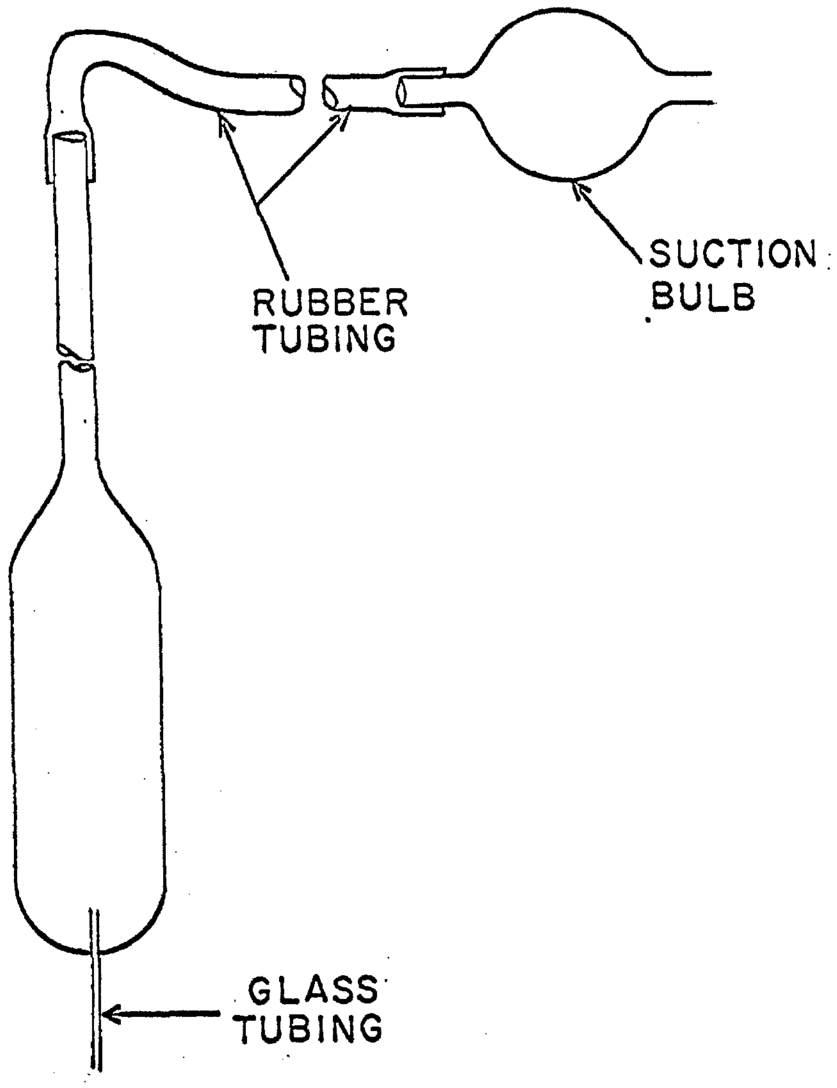
RUBBER TUBING
SUCTION BULB
GLASS TUBING

where some of the liquid had been squeezed out (due, possibly, to insufficient drying of the electrode faces before addition of the test solution aliquot), or if the crevice was not completely full of solution, the run was discontinued and the electrode recleaned, rewashed, and refilled.

Electrode Pretreatment

It has been shown (15) that the iodide and iodine adsorbed on platinum electrodes can be removed by oxidation of the electrode in 1 F H_2SO_4. The cleaning procedure used in the present experiments consisted of the following steps: The micrometer was opened to a gap of a few millimeters and the electrodes were oxidized potentiostatically at a potential of 1.2 volts. During this electrolysis pure, deaerated 1 F H_2SO_4 was continuously flowing through the gap between the electrodes. The electrodes were reduced by imposing a potential of 0.4 volt with a potentiostat for several minutes. The cycle was repeated several times.

Careful inspection of anodic chronopotentiograms obtained with electrodes that had been treated with iodide or iodine confirmed that the procedure described was effective in removing adsorbed iodide and iodine. Figure 15 shows chronopotentiograms for the oxidation of an electrode cleaned as described and for oxidation of a cleaned electrode in 1 F H_2SO_4 after it had been bathed in 2mM iodide solution and washed free of unadsorbed iodide. With the clean electrode, the first indication of a potential halt occurred at about +0.7 volt, whereas the corresponding potential for the iodide-coated electrode was about +1.06 volts; that is, the presence of adsorbed iodide (or of iodine, which behaved similarly) caused a 360 millivolt suppression of the potential at which chronopotentiometric oxidation of the electrode occurred.

A second feature to be noted is the sharp potential inflection which occurred at about 1.25 volts when the electrode had been iodide- (or iodine-) coated but not when the electrode had been previously freed of iodide (or iodine). This potential inflection was quite sensitive to the presence of iodide or iodine on the electrode and was useful in these experiments as a convenient verification of the absence of these species on the electrode after cleaning: The inflection was observed with all electrodes known to contain adsorbed iodide or iodine and disappeared only after the electrode was subjected to the cleaning procedure described.

The cleaning procedure led to some increase in the roughness of the electrode surface as it was repeatedly oxidized and reduced. The amounts of measured adsorbed iodide and iodine are reported on the basis of the apparent geometric electrode area and will, therefore, depend somewhat on the electrode history. It was observed that the adsorption values decreased by about 20% if the cleaned electrode surfaces were bathed briefly with aqua regia (which would tend to dissolve finely divided platinum) and reduced just before an experiment.

Figure 15

Chronopotentiograms for oxidation of the platinum electrodes in 1 F H_2SO_4.

(a) Freshly cleaned electrode

(b) Electrode cleaned and prebathed in 2mM iodide

The current was 10 μa.

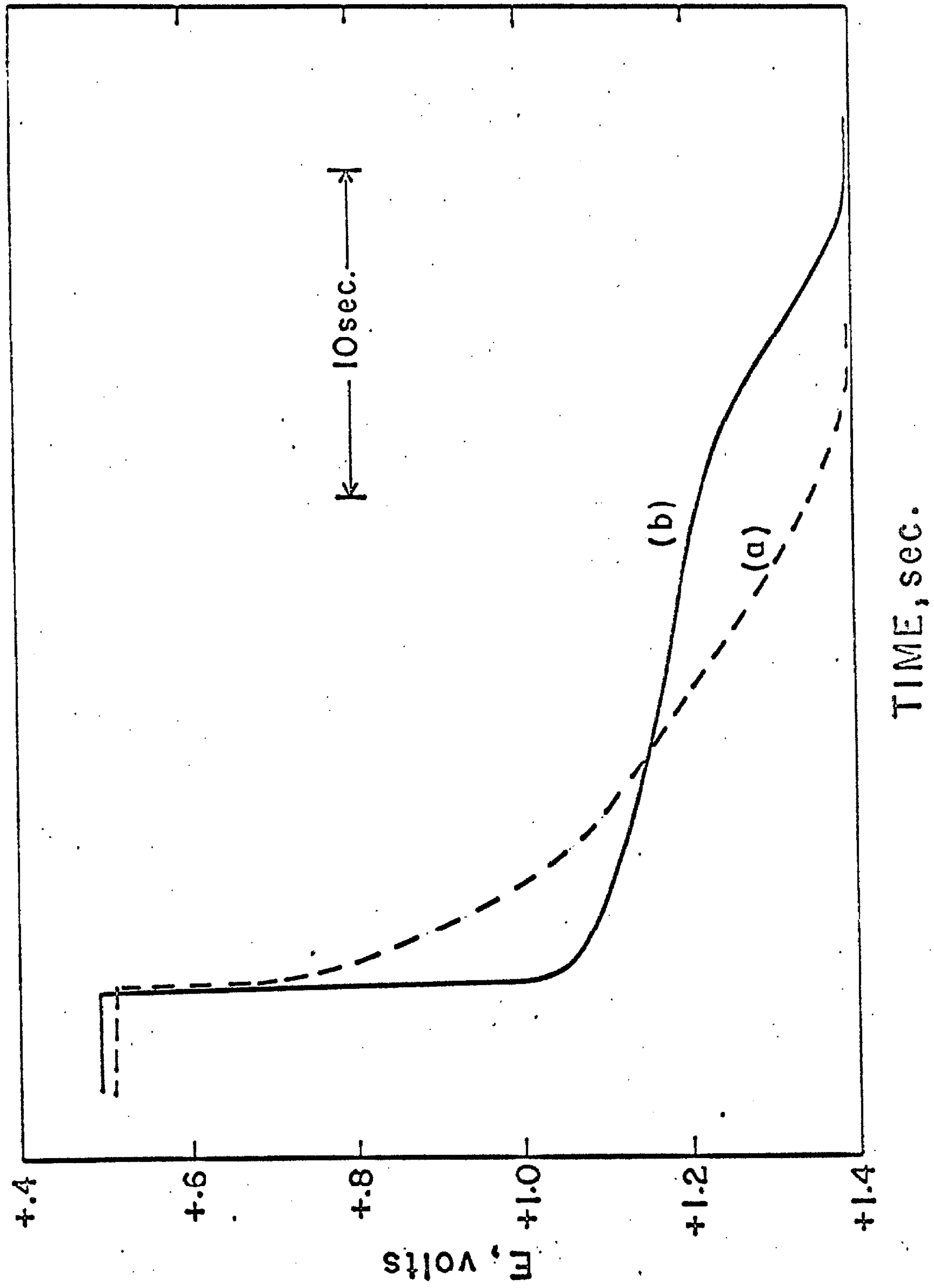
+.4
+.6
+.8
+1.0
+1.2
+1.4
E, volts
TIME, sec.
10sec.
(a)
(b)

Results

Determination of Electroactive Adsorbed Iodine.

When a reactant is adsorbed in an electroactive state on platinum and the micrometer electrode surfaces are bathed in an excess of the reactant solution before the micrometer gap is closed to squeeze out all of the solution except for that contained in the thin layer volume, the equations for the transition time and potentiostatic current integral will not be those that are obeyed in the absence of adsorption (Equations 14 and 18). Instead, the following equations will apply

$$\tau = \frac{nF}{i} \; (VC^0 + A\Gamma) \tag{22}$$

$$Q = nF \; (VC^0 + A\Gamma) \tag{23}$$

Γ is the amount of adsorbed reactant in moles/cm.^{2} Thus the charge in excess of that calculated from Faraday's Law (Equations 14 and 18) that is obtained in a thin layer experiment corresponds to the quantity of electroactive adsorbed reactant.

The data in Table IV were obtained by thin layer chronopotentiometry and demonstrate the adsorption of 9.4×10^{-10} moles/cm.^{2} of electroactive iodine from a 1.14×10^{-3} M iodine solution.

Nonelectroactive Adsorbed Iodide

Experiment 2 in Table IV demonstrates the absence of any electroactive adsorbed iodide from a 1.0×10^{-3} M iodide solution. Inasmuch as there is ample independent evidence that iodide ion is adsorbed on platinum (15, 17, 18, 19) the behavior of iodide in Experiment 2 must be ascribed to the fact that adsorbed iodide is not electroactive.

Determination of Nonelectroactive Adsorbed Iodide.

If a small volume of a standard solution of a reactant that is adsorbed only in a nonelectroactive state is pipeted into the thin layer cell with cleaned platinum electrodes, the total charge obtained will be smaller than that calculated from Faraday's law by an amount corresponding to the adsorbed nonelectroactive reactant. The transition time or charge

---

[17] N. Balashova, Zh. Fiz. Khim. 32, 2266 (1958).

[18] N. Balashova, Z. Physik Chem. (Leipzig), 207, 340 (1957).

[19] N. Balashova, N. S. Merkulova, Proc. 4th Soviet Conf. Electrochem., 1956, p. 48.

Table IV. Search for Adsorption of Electroactive Iodide and Iodine on Platinum

Expt. no.	Solution	$i\tau$, calcd. from Equation 18 μcoulombs	$i\tau$ observed, μcoulombs	$\Gamma \times 10^{10}$ Calcd. from Equation 22, moles/cm.^{2}
1	1.14mM I_2	304	422	9.4
2	1.0mM I^-	135	134	0

$i\tau$ observed represents the average of several trials with a standard deviation of about 2%. Current was 10 μa. Electrodes were bathed in excesses of the test solution before the micrometer gap was set at 44.2 microns and excess solution removed.

will be given by

$$\tau = \frac{nF}{i} (VC^{\circ} - A\Gamma) \tag{24}$$

$$Q = nF (VC^{0} - A\Gamma) \tag{25}$$

where Γ is the amount of reactant adsorbed in moles/cm.^{2}

Such pipet experiments were carried out with iodide solutions. A typical set of data is presented in Table V. The values of Γ in Table V were calculated from Equation 25 and indicate that $14\text{-}18 \times 10^{-10}$ moles per cm.^{2} of iodide ion were removed from the solution by adsorption on the platinum electrode surfaces and that the adsorbed iodide was not oxidizable at the potential where the unadsorbed iodide was rapidly oxidized. Note that Experiments 5 and 6 demonstrate that Equation 14 was obeyed with electrodes that had been presaturated with iodide or iodine.

Experiment 5 in Table V also shows that the adsorbed iodide was not removed by copious washing with iodide-free 1 F H_2SO_4 because such washing was performed as part of this experiment.

Oxidation of Adsorbed Iodide.

Experiments confirming the presence of about 2×10^{-9} moles per cm.^{2} of non-electroactive adsorbed iodide ion on platinum electrodes were performed by taking advantage of the following facts:

Table V. Nonelectroactive Adsorption of Iodide on Platinum

Expt. no.	KI concn., mM (all solutions were 1 F in H_2SO_4)	Number of Trials	Q observed, μ coulomb	Q blank, μ coulomb	Q observed-Q blank, μ coulomb	Q calc. from Equation 14, μ coulomb	Γ_{I^-}, calcd. from Equation 25, $\times 10^{10}$ moles/cm^2
1	1	4	25.3 ± 0.6	22 ± 0.6	3.3 ± 1	96.5	15.3 ± 1
2	2	4	113 ± 6	10 ± 0.4	104 ± 6	193.0	14.5 ± 2
3	3	5	201 ± 12	10 ± 0.4	191 ± 12	289.5	14.5 ± 2
4	5	3	384 ± 14	10 ± 0.4	374 ± 14	482.5	17.7 ± 2
5[a]	1	5	104 ± 2	10 ± 0.4	97 ± 2	96.5	0
6[b]	1	5	110 ± 1	11 ± 0.8	99 ± 2	96.5	0

Experimental conditions: 1.00 liters of the solutions were pipeted into the cell for each experiment. The micrometer was then set to give a gap of 31.5 microns which just contained the 1.00 $\mu\ell$. of solution. The potential was stepped from +1.3 to +0.7, where the current was integrated. Q blank was determined with electrodes which had been treated with 1 $\mu\ell$. of iodide solution (Expt. 1-5) or iodine solution (Expt. 6) of the same concentration and then thoroughly rinsed with H_2SO_4 and filled with 1.0 microliter of 1 F H_2SO_4.

a The electrodes were rinsed with 1.00 mM KI and then with 1 F H_2SO_4 before filling.

b The electrodes were rinsed with 1.00 mM I_2 and then with 1 F H_2SO_4 for at least 1 minute before filling.

Previous experiments (16) have demonstrated that adsorbed iodide can be oxidatively desorbed from platinum electrodes by adjusting the electrode potential to +1.2 volts in 1 F H_2SO_4. At this potential the iodide was oxidized to iodate and extensive oxidation of the electrode occurred. The reduction of iodate to iodine at the oxidized thin layer electrode in 1 F H_2SO_4 occurred at about 0.80 volt as is shown in the linear-potential sweep current-potential curve in Figure 16. The iodate reduction occurred before much reduction of platinum oxide (or oxygen) commenced.

Accordingly, if the thin layer electrode surfaces were saturated with respect to iodide adsorption, washed free of unadsorbed iodide, the cell filled with 1 F H_2SO_4 and the electrodes potentiostated briefly at 1.2 volts, the resulting solution in the cavity should have contained an amount of dissolved iodate ion equivalent to the initially adsorbed nonelectroactive iodide. This iodate could be determined with fair accuracy by constant-potential coulometry at 0.7 volt as shown in Figure 17 and Table VI.

The cathodic charge corresponding to iodate reduction will be given by

$$Q = nFA\Gamma_{I^-} \tag{26}$$

Figure 16

Thin layer linear-potential sweep current-voltage curves for iodate reduction at oxidized platinum electrodes

1. 1.00 μliter of 1 F H_2SO_4 was pipeted onto one electrode, the gap set at 31.5 microns, the electrode oxidized at 1.2 volts for 60 seconds, the potential adjusted to 1.0 volts, where potential was swept cathodic at 1.8 mv. per second
2. 1.00 μliter of 1.00 mM KI in 1 F H_2SO_4 pipeted onto one electrode, thereafter as in 1
3. 1.00 μliter of 1.00 mM KIO_3 in 1 F H_2SO_4 pipeted onto one electrode, thereafter as in 1

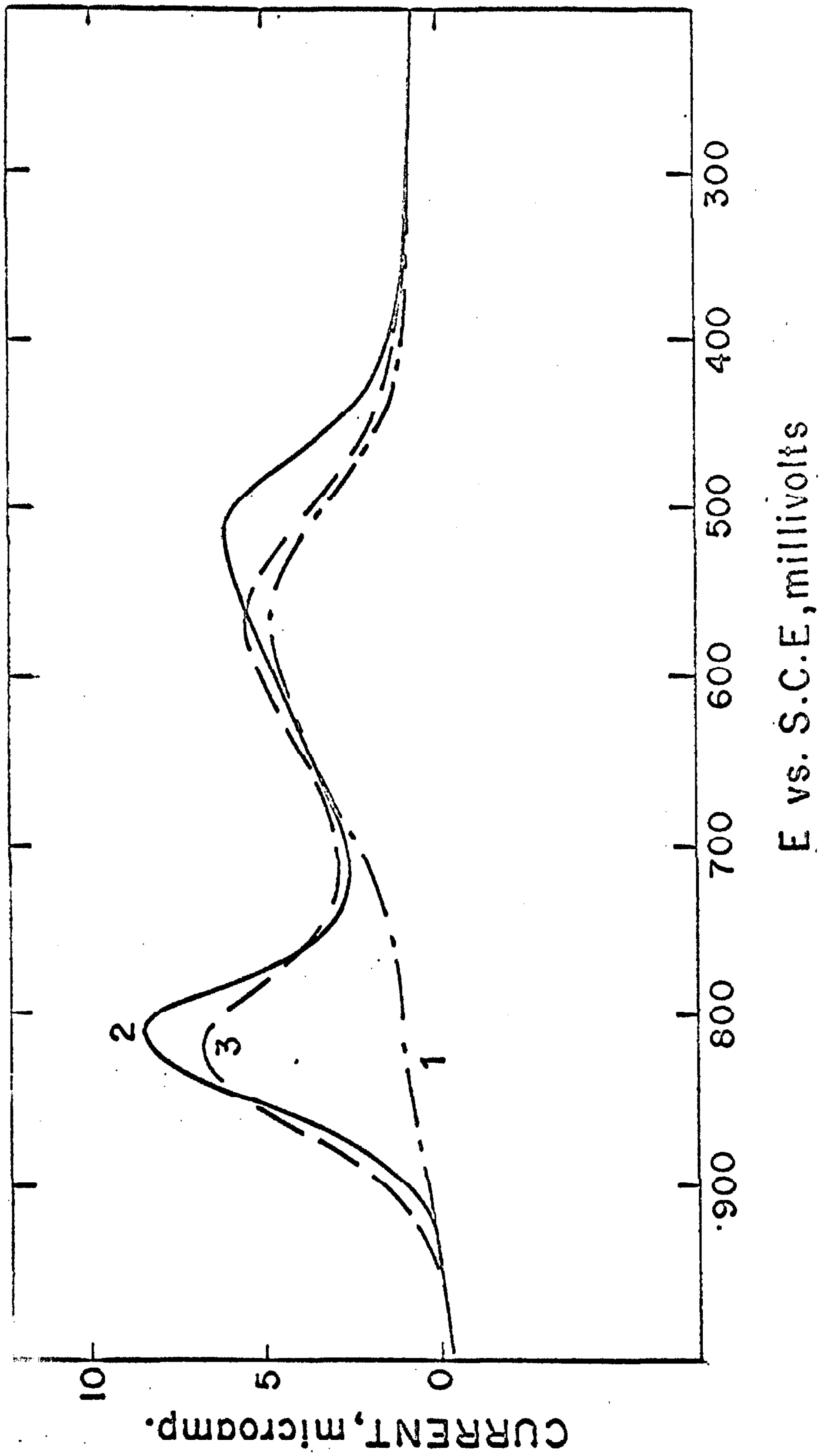
CURRENT, microamp.
10
5
0
E vs. S.C.E, millivolts
300
400
500
600
700
800
900
1
2
3

Figure 17

Thin layer charge-time curve for iodate reduction at oxidized electrode in 1 F H_2SO_4

1. 1.00 μliter in 1 F H_2SO_4 was pipeted onto one electrode, the gap was set at 31.5 microns, the electrode was oxidized at 1.2 volts for 60 seconds, the potential was adjusted to 0.9 volt and then stepped to 0.7 volt where the resulting current was integrated
2. 1.00 μliter of 1.00 mM KI in 1 F H_2SO_4 was pipeted onto one electrode, thereafter as in 1

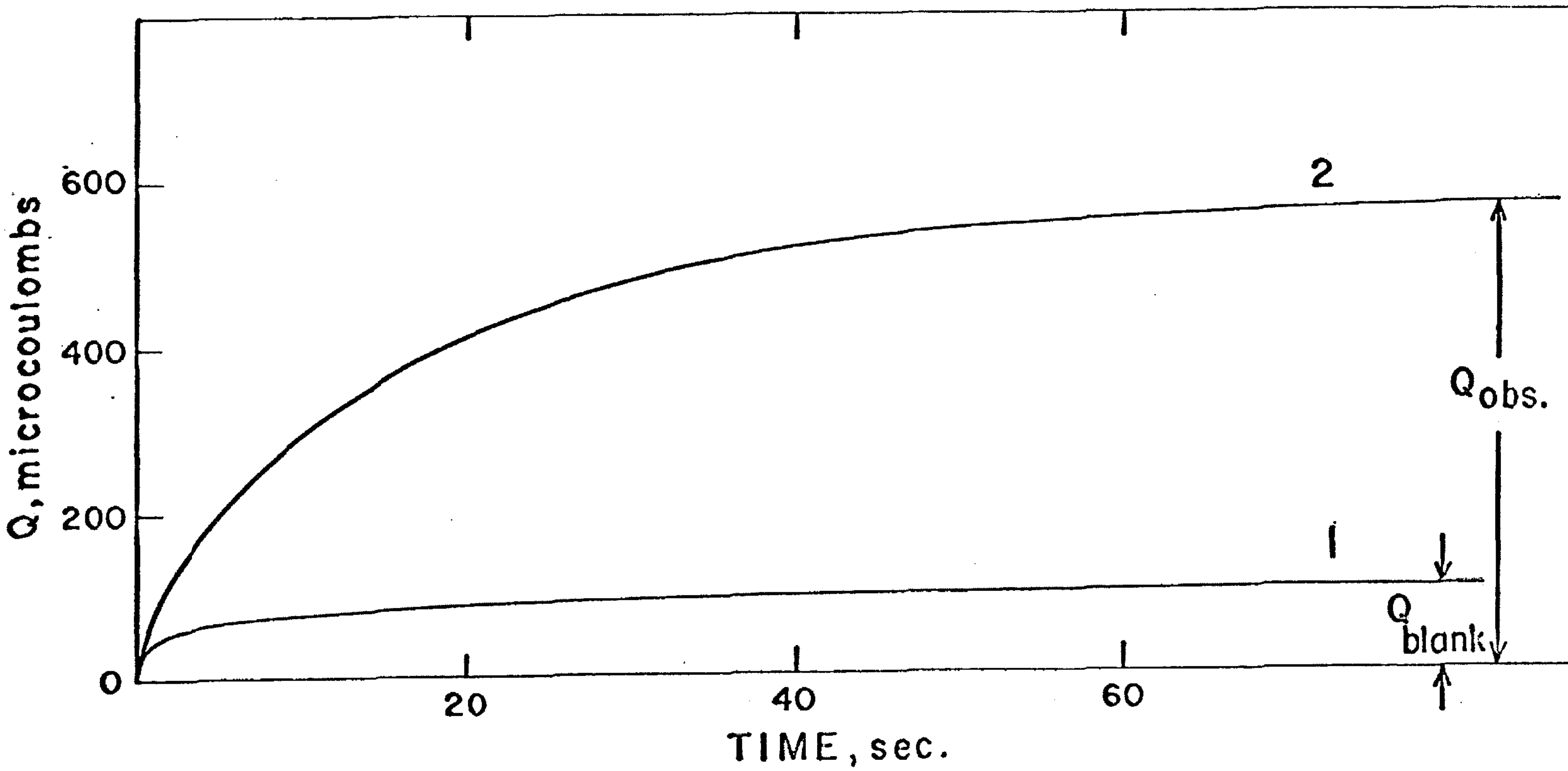
Q, microcoulombs
600
400
200
0
20
40
60
TIME, sec.
2
1
Q obs.
Q blank

Table VI. Determination of Iodate with Oxidized Electrodes

Expt. no.	Starting reagent	Q observed, μ coulomb	Q blank, μ coulomb	Qobs-Q bl = Q iodate, μ coulomb	Q iodate, calcd. from Equation 14, μ coulomb
1	Iodide	570	105 ± 6	484 ± 25	482.5
		575			
		600			
		610			
		av. $\overline{589}$ ± 19			
2	Iodate	605	105 ± 6	461 ± 54	482.5
		605			
		580			
		540			
		500			
		av. $\overline{566}$ ± 49			

Experimental conditions: 1.00 μliter of 1.00 mM KI (Expt. 1) or 1.00 mM KIO_3 (Expt. 2) were pipeted onto the cleaned electrode. The micrometer was set to give a gap of 31.5 microns (which just contained the solution) and the electrodes were oxidized potentiostatically at 1.2 volts for 60 seconds. The potential was adjusted to +0.9 volt and then stepped from +0.9 to +0.7 volt where the current was integrated. Q_{blank} was obtained by oxidizing cleaned electrodes in 1 F H_2SO_4 at 1.2 volts, adjusting the potential to 0.9 volt, and stepping the potential to 0.7 volt where the current was integrated.

where n = 5 and Γ_{I^-} is the amount of iodide initially adsorbed. The values of Γ_{I}^{-} calculated from Equation 26 are shown in Table VII and are close to the values obtained from the direct micropipet experiments with iodine (Table V). The presence of nonelectroactive adsorbed iodide is thus clearly established.

Determination of Nonelectroactive Adsorbed Iodine.

Although the titer of iodide-free solutions of iodine was difficult to maintain because of the volatility of the iodine, it was possible to repeat the micropipet experiments (as summarized in Table V for iodide) with iodine solutions by titrating the solution with thiosulfate just before it was used. These experiments were performed chronopotentiometrically and the results, summarized in Table VIII, show that extensive adsorption of iodine in a nonelectroactive form took place, just as was true of iodide ion. This nonelectroactive iodine was not previously detected because the techniques employed (14, 15, 16) measured only the electroactive adsorbed iodine which was present (Table IV) if the electrode was exposed to sufficient iodine to saturate its surface with both nonelectroactive and electroactive iodine.

The presence of nonelectroactive adsorbed iodine could be confirmed in the same way that was used for iodide: oxidative desorption and determination as iodate. Table IX contains the results of these experiments.

Table VII. Determination of Nonelectroactive Adsorbed Iodide as Iodate

Expt. no.	Q observed μcoulomb	Q blank, μcoulomb	Q observed⁻ Q blank, μcoulomb	$\frac{\text{Q observed}^- \text{Q blank}}{5}$ = Q adsorbed, μcoulomb	$\Gamma_{I^-} \times 10^{10}$ moles/cm^2
1	760	105 ± 6	619 ± 50	124 ± 10	20 ± 1.8
2	700				
3	780				
4	660				
5	720				
	724 ± 44				

Experimental conditions: the electrodes were rinsed with excess 1.00mM KI, washed with excess 1 F H_2SO_4, and the micrometer set to give a gap of 44.2 microns. The electrode was then potentiostatically oxidized at 1.2 volts for 60 seconds, the potential was adjusted to 0.9 volt and then stepped to 0.7 volt where the current was integrated. Q blank was obtained by oxidizing cleaned electrodes in 1 F H_2SO_4 at 1.2 volts, adjusting the potential to 0.9 volt, and stepping the potential to 0.7 volt where the current was integrated.

Table VIII. Nonelectroactive Adsorption of Iodine on Platinum

Expt. no.	Iodine concn. mM	Vol. pipeted into crevice, μl.	Layer thickness, microns	i_τ calcd. from Equation 1, μcoulombs	i_τ observed, μcoulombs	Γ_{I_2}, calcd. from Equation 3, moles/cm.^{2} × 10^{10}
1	0.2	1.40	44	54	0	>2.8
2	0.2	7.76	245	298	50 ± 50	20[a]
3[b]	0.2	1.40	44	54	48 ± 10	<0.5
4[b]	0.2	3.88	122	148	135 ± 29	<0.5

Each entry represents the average of several trials with the reproducibility shown. The electrode was freshly cleaned before each trial. Current was 10 μa. throughout.

[a] A small amount of iodine is unavoidably lost due to volatilization from the solution during the pipeting step. The difference between the measured and observed i_τ values with the iodine-bathed electrodes (Expt. 3 and 4), at which no further I_2 adsorption should occur, gives an estimate of the extent of the systematic loss of I_2 as around 10%. Accordingly a better approximation for Γ_{I_2} obtained in Experiment 2 is about 18 × 10^{-10} moles/cm.^{2}.

[b] The electrode was bathed in the iodine solution, thoroughly rinsed with 1 F H_2SO_4 and dried before Experiments 3 and 4.

Table IX. Determination of Nonelectroactive Adsorbed Iodine

Expt. no.	Q observed, μcoulomb	Q blank, μcoulomb	Q observed − Q blank, μcoulomb	$\frac{\text{Q observed} - \text{Q blank}}{5}$ = Q adsorbed, μcoulomb	$\Gamma \times 10^{10}$ moles/cm^2
1	1040	105 ± 6	971 ± 86	194 ± 18	16 ± 1.6
2	1060				
3	1000				
4	1060				
5	1020				
	1076 ± 80				

Experimental conditions: the electrodes were rinsed with excess of a saturated iodine solution in 1 F H_2SO_4, washed with excess 1 F H_2SO_4 and the micrometer set to give a gap of 44.2 microns. The electrode was then potentiostatically oxidized at 1.2 volts for 60 seconds, the potential was adjusted to 0.9 volt, and then stepped to 0.7 volt where the current was integrated. Q blank was obtained by oxidizing cleaned electrodes in 1 F H_2SO_4 at 1.2 volts, adjusting the potential to 0.9 volt, and stepping the potential to 0.7 volt where the current was integrated.

Error in a Recent Paper.

In a recent paper (16), in which some preliminary thin layer chronopotentiometric experiments with iodide-free iodine solutions were described, the amount of iodine to which the electrode surfaces were actually exposed was not known because the addition of solutions to the cell was not performed with micropipets. However, the fact that a cathodic transition time was observed after the electrode was filled makes it clear that the electrode surfaces must have been saturated with nonelectroactive iodine. In those experiments it was observed that if some iodine was reduced and then the direction of the current was reversed the anodic transition time was shorter than the cathodic electrolysis time unless the electrodes were bathed in an iodide solution and rinsed prior to the addition of the iodine solution. It has been possible to reproduce that result in the present experiments only with incompletely reduced electrodes. So long as the cleaned electrodes were very thoroughly reduced (potentiostating at 0.35 volt for 3-4 minutes) prior to being filled with the iodine solution, the cathodic electrolysis time and anodic transition time were equal. It seems likely that the behavior reported in the earlier paper (16) was the result of incomplete reduction of the electrode inasmuch as potentiostatically controlled reduction was not employed. The present experiments simply demonstrate that iodide is not adsorbed on an electrode which has already been saturated with adsorbed iodine.

Conclusions

Several new conclusions result from the data presented in this study. First is the fact that at saturation ca. 2×10^{-9} mole/cm^2. of iodine is adsorbed in a nonelectroactive state on platinum electrodes. An additional 1×10^{-9} mole/cm^2. of iodine is also adsorbed in an electroactive state. Inasmuch as the sum of the two forms of adsorbed iodine is considerably greater than the amount of iodine adsorption measured in the previous radiotracer experiments in which an electrode was immersed in a radio-iodine solution, washed and counted (9, 16, 17, 18), it seems highly probable that only the electroinactive iodine remains on an electrode that is extensively washed with 1 F H_2SO_4. The radiotracer experiments were thus not measuring the same iodine as were the electrochemical experiments (thin layer experiments excepted) and the rough correspondence between the amount of adsorbed iodine found by the two techniques (14, 15) was accidental. This point of view makes it easier to understand the fact that extensive iodine adsorption can be demonstrated with radio-iodine on a platinum electrode which gives no cathodic transition time when used in an ordinary chronopotentiometric experiment in 1 F H_2SO_4. (16).

The present thin layer experiments provide the first direct electrochemical estimate of the extent of iodide adsorption on platinum electrodes--ca. 1.2×10^{-9} mole/cm^2. at saturation (Table V). This value corresponds to the approximate value reported previously on the basis of radio-iodine experiments (17). The electroinactivity of the adsorbed iodide is confirmed by all of the experiments presented here. The data in Tables IV, V, and VI show that the adsorption of iodide on the electrode eliminates the further adsorption of nonelectroactive iodine and iodide. The adsorption of nonelectroactive iodine is also shown to eliminate further adsorption of iodide (Table V). Electroactive iodine adsorption, however, continues to occur on both iodide-and iodine-coated electrode surfaces.

The common practice of activating platinum electrodes toward adsorption of reactants--e. g., by platinization--in an attempt to increase the rate of an electrode reaction may be precisely the wrong approach for reactants which mimic the behavior of the iodide-iodine couple.

Conversations with Dr. R. A. Osteryoung assisted with the progress of this study.

(ii). A Study of the CoY^- - CoY^{-2} and FeY^- - FeY^{-2} Couples At Platinum Electrodes (20)

Previous studies in these laboratories in which diffusion chronopotentiometry was employed as the measuring technique (21, 22) produced evidence that both CoY^- and CoY^{-2}(H_4Y = ethylenediaminetetracetic acid) are extensively adsorbed on bright platinum electrodes. Quantitative measurement of the amount of each complex adsorbed was not attempted because of the poor definition of the waves and the possibility that the data contained some contribution from oxide film formation or supporting electrolyte reduction. When bromide or iodide ion was added to the solutions the adsorption of the cobalt complexes appeared to be prevented, presumably because of the preferential adsorption of the halides.

The thin layer electrochemical technique has been applied to the CoY^- - CoY^{-2} couple to check the earlier results and to provide a quantitative measure of the extent of the adsorption. The iron complexes FeY^- and FeY^{-2} were also examined for possible adsorption.

---

[20] A. T. Hubbard and F. C. Anson, Anal. Chem., 38, 1601 (1966).

[21] F. C. Anson, Anal. Chem., 36, 521 (1964).

[22] F. C. Anson, J. Electrochem. Soc., 110, 436 (1963).

Experimental

A micrometer thin layer electrode was employed. The total geometric area of the electrode cavity was 0.635 cm^2. The electrode was cleaned by alternate potentiostatic oxidation (1.2 volts vs. SCE) and reduction (0.0 volts vs. SCE) while a stream of oxygen-free 1 F H_2SO_4 was flowing across the electrode faces. After the cleaning cycle the electrode was maintained at 0.4 volt vs. SCE for several minutes until any residual current decayed to less than one microampere.

Both linear potential sweep and chronocoulometric (potential-step with current integration) techniques were employed. All solutions were deaerated with prepurified nitrogen and the electrode was enclosed in a nitrogen-filled polyethylene tent during measurements.

Reagents.

A 0.1 F solution of CoY^{-2} was prepared by mixing equimolar quantities of $CoSO_4 \cdot 7H_2O$ and $Na_2H_2Y \cdot 2H_2O$ in a 1 F pH 7 phosphate buffer solution.

Crystalline $NaCoY \cdot 4H_2O$ (23) was prepared as follows:

An aqueous solution of $Ba(CoY)_2 \, . \, 4H_2O$, prepared according

---

[23] J. L. Hoard and H. A. Weakliem, J. Am. Chem. Soc., 81, 549 (1959).

to the published procedure (24), was treated with a slight excess of Na_2SO_4, the resulting $BaSO_4$ removed by filtration, and the filtrate added to a large volume of anhydrous ethanol. The resulting precipitate was recrystallized from an aqueous solution to give large violet crystals which were dried for 24 hours at 50° C. Purity of the crystals was confirmed by thin layer electrochemical analysis of weighed portions.

Attempts to prepare pure $NH_4FeY \cdot H_2O$ by the published procedure (25) were unsuccessful. However, $NaFeY \cdot 3H_2O$ was successfully obtained by the following modified procedure: A fresh precipitate of $Fe(OH)_3$ was prepared by adding excess aqueous ammonia to a solution of ferric sulfate. The precipitate was thoroughly washed by decantation and then treated with slightly less than the stoichiometric quantity of ethylene-diaminetetraacetic acid, H_4Y, and the pH of the mixture adjusted to about 8.5 with NaOH. The remaining $Fe(OH_3)$ was removed by filtration and the filtrate adjusted to pH 5 by addition of perchloric acid; the volume was reduced slowly on the steam bath until crystals began to form. Such solutions yielded large brown-colored crystals of $NaFeY \cdot 3H_2O$ which were

---

[24] T. Moeller, (ed.), Inorganic Syntheses, 5, 186 McGraw-Hill Book Co., N.Y., 1957.

[25] H. Brintzinger, et. al., Z. An. Chem., 251, 285 (1943).

collected by filtration, washed with ethanol and ether, and air dried. Purity of the crystals was confirmed by thin layer electrochemical analysis of weighed portions.

Solutions of FeY^{-2} were prepared by potentiostatic reduction of FeY^{-} at a large platinum gauze electrode in the absence of oxygen.

Other chemicals were reagent grade and were used without further purification. The water was triply distilled; the second distillation was from alkaline permanganate.

The special micropipets employed have been previously described.

Results and Discussion

CoY^{-} and CoY^{-2}.

The single-cycle thin layer current-potential curve for reduction of CoY^{-} and subsequent oxidation of CoY^{-2} in 1 F $NaClO_4$ supporting electrolyte is shown in Figure 18, Curve A. The great irreversibility of this couple observed in the earlier studies (21, 22) persists even under thin layer conditions.

Addition of iodide ion to the solution causes the electrode reactions to become more nearly reversible, as shown in curve B in Figure 18. This effect is believed to result from the preferential adsorption of iodide ion on the electrode which causes desorption of the cobalt complexes which, when adsorbed, interfere with the electrode reactions (21, 22). This ability of iodide ion both to desorb

Figure 18

Thin Layer Current Potential Curves for Reduction of Cobalt(III)-EDTA.

A - No iodide--1.77 μ liters of 1.00 mF CoY^- in 1 F (pH 7) phosphate buffer.

B - With iodide--1.40 μ liters of 1.00 mF CoY^- in 1 F $NaClO_4$ (pH 5) plus 1.00 μ liter of 2.00 mF KI.

Sweep rate was 2 mv./sec. Potentials are volts *vs.* SCE.

Cathodic current is negative current.

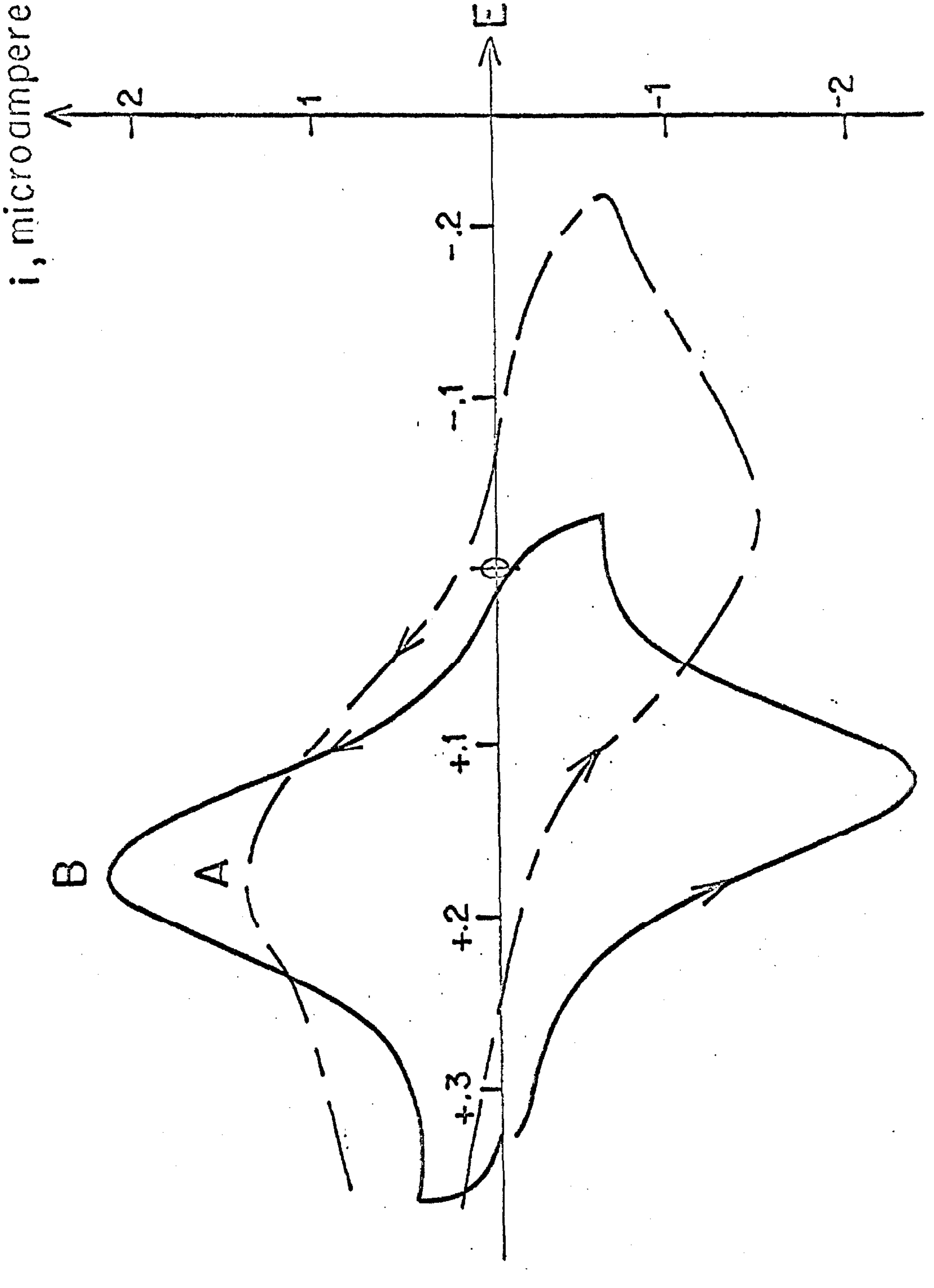
i, microampere
E
2
1
-1
-2
-.2
-.1
0
+.1
+.2
+.3
B
A

the cobalt complexes and to render the electrode reactions more reversible was exploited to measure the extent of adsorption of the cobalt complexes. To do this the following procedure was employed: The cleaned electrode was rinsed and filled with an exact volume of a solution containing 1 F phosphate buffer (pH = 7) and millimolar CoY^- or CoY^{-2}. The gap was then opened to a width of 2-3 millimeters (the cobalt solution adhered, without loss, to one of the electrode faces at this point) and an exact amount of a 2 milliformal KI solution was pipeted onto the face of one electrode where it adhered. The gap was then set to contain the total volume of solution added. Connection was made to the capillary-tipped salt bridge and the total amount of CoY^- or CoY^{-2} in the crevice was determined by the chronocoulometric technique.

The amount of adsorbed CoY^- or CoY^{-2} was calculated from Equation 23

$$Q = nFVC^0 + nFA\Gamma$$

The experimental results are summarized in Table X. Substantial adsorption of both CoY^- and CoY^{-2} was found (Experiment numbers 1 and 3) in agreement with the previous chronopotentiometric evidence (21, 22). Because both the adsorbed CoY^- and CoY^{-2} had to be desorbed by iodide in order to be measured in these experiments, it was necessary to show that iodide, in the concentration range used, desorbed the cobalt complexes completely. That this was the case was demonstrated by Experiment

Table X. Adsorption of CoY^- and CoY^{-2} on Platinum CoY^- Reduction

Exp. No.	No. of Trials	Q (total), μc	Q (blank), μc	Q(total) - Q(blank) μc	Q (theory, for no adsorption, μc	Γ from Equation 1, moles/cm^2 × 10^{10}
1	4	208 ± 3	18 ± 1	190 ± 4	171	3.1 ± 0.4
2	4	189 ± 5	18 ± 1	171 ± 6	171	0 ± 1
3	6	106 ± 3	14 ± 2	92 ± 5	91	-----------
				CoY^{-2} Reduction		
4	4	230 ± 3	30 ± 3	200 ± 6	171	4.7 ± 0.9
5	4	202 ± 5	30 ± 3	172 ± 8	171	0 ± 1
6	5	115 ± 6	24 ± 2	91 ± 8	91	-----------

Experimental Conditions: In experiments 1 and 4 the electrode faces were rinsed with reactant solution (1.00mM CoY^- or CoY^{-2} in 1 F phosphate buffer, pH = 7) and then filled with 1.77 microliter of reactant solution and 1.00 microliter of KI solution, as described in the text. In experiments 2 and 5 the electrode faces were first rinsed with 2.00 mM KI solution, next with excess of the reactant solution, and then were treated by the same procedure. In experiments 3 and 6, 0.94 microliter of reactant solution was added to the clean cell from a micropipet followed by addition of 0.94 microliter of KI solution, as described in the text.

The potential step was: 0.25 to -0.05 volt in experiments 1, 2, and 3; 0.00 to 0.30 in experiments 4, 5, and 6. The values of Q blank were obtained by repeating the appropriate procedure except that the phosphate supporting electrolyte solution was substituted for the reactant solution in each case.

numbers 3 and 6 in Table X. In these experiments an exactly measured volume of the cobalt complex was pipeted into the cleaned cell, the gap closed to this volume to allow the cobalt complex to be adsorbed, the gap opened and an exactly measured aliquot of iodide was added, and the amount of cobalt complex in the cell determined in the usual way. The fact that all of the cobalt complex initially added was recovered in this process demonstrates that the iodide left none adsorbed and unreactive.

The values of Γ reported here are, however, somewhat smaller than the previous chronopotentiometric data suggest. No values for Γ were calculated in the previous study, but if any of the usual approximate models (26) are applied to the data, values of $25\text{-}90 \times 10^{-10}$ moles/cm.^{2} for Γ result, and it seems likely that the chronopotentiometric transition times were seriously lengthened by the overlap of CoY^- reduction with supporting electrolyte reduction in the iodide-free solutions. We regard the thin layer values for Γ as the most reliable because they could be obtained in iodide-containing solutions in which the reduction and oxidation of CoY^- and CoY^{-2} are well separated from the background reactions.

---

[26] S. V. Tatwawadi, and A. J. Bard, Anal. Chem. 36, 2 (1964).

FeY^- and FeY^{-2}.

In contrast with the corresponding cobalt complexes, FeY^- and FeY^{-2} behaved reversibly at platinum electrodes in the absence of any added iodide ion. A typical thin layer current-potential curve for this couple is shown in Figures 19. The peak currents (3.39 microamperes-cathodic and 3.37 microamperes-anodic) agree well with each other and with the theoretical values of 3.33 microampere (Equation 5).

The possibility of adsorption of FeY^- or FeY^{-2} was examined with the chronocoulometric technique in thin layers, and the results are summarized in Table XI. The data show that neither FeY^- nor FeY^{-2} are adsorbed on the platinum electrodes. Similar experiments in which the electrodes were maintained at potentials between +0.6 and +0.1 volt vs. SCE during the washing and filling steps gave identical behavior. There is thus a clear difference in behavior between the cobalt and the iron chelates of EDTA.

Conclusions.

The ability of the thin layer technique to provide quantitative adsorption data for systems which thwart most other electrochemical techniques is clearly demonstrated by the CoY^- - CoY^{-2} couple. The idea of trapping an adsorbate within the thin layer by prewashing and then desorbing it by addition of a preferentially adsorbed substance (for example, iodide ion) may prove of general utility

Figure 19

Thin Layer Current Potential Curve for Fe(III)-EDTA.

1.77 μ liters of 1.00 mF FeY^- in 1 F Na_2SO_4 (pH 5).

Sweep rate was 2 mv./sec. Potentials are volts *vs.* SCE.
Cathodic current is negative current. The dashed line is for an iron-free solution.

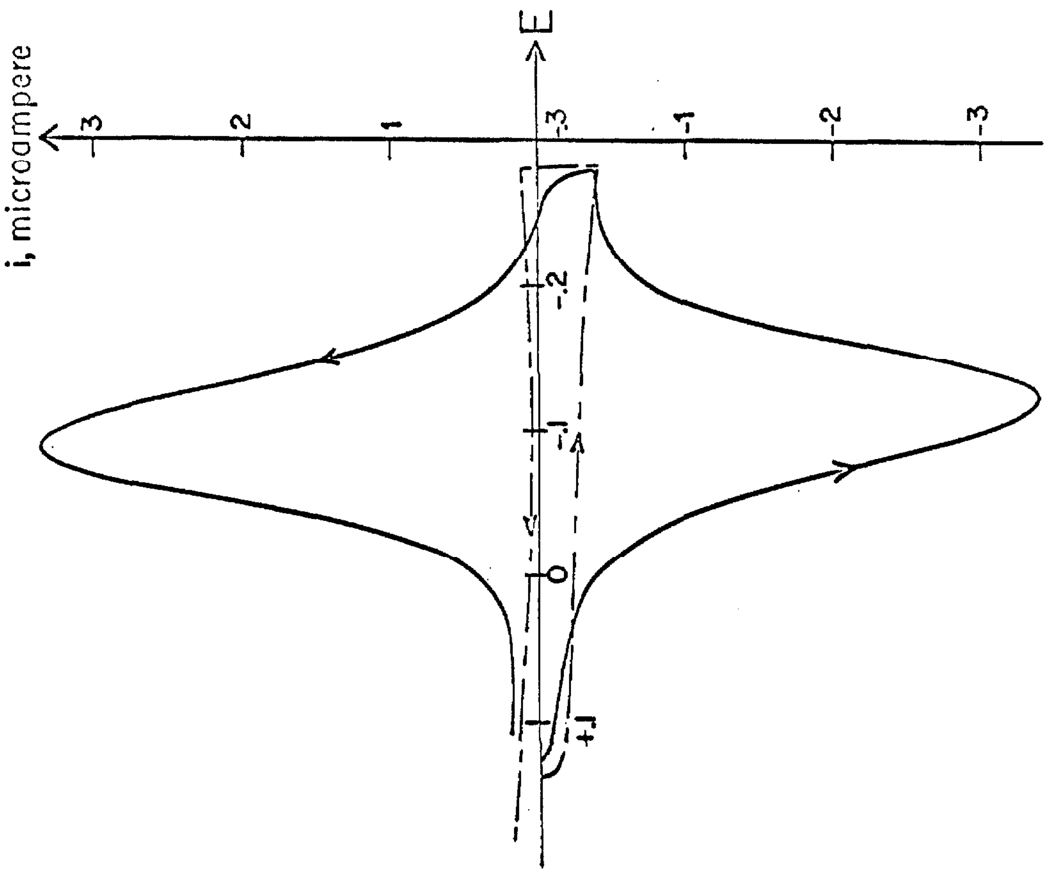
i, microampere
E
3
2
1
-1
-2
-3
+.1
0
-.1
-.2
-.3

Table XI Search for Adsorption of FeY^{-} and FeY^{-2} on Platinum

Exp. No.	Reactant Solution	Number of Trials	Q(total) μc	Q(blank) μc	Q(total) - Q(blank), μc	Q theory (for no adsorption), μc
1	1mM FeY^{-} in 1 F pH 5 acetate buffer	6	190 ± 4	20 ± 1	170 ± 5	171
2	1mM FeY^{-2} in 1 F pH 5 acetate buffer	6	184 ± 9	21 ± 1	163 ± 10	171
3	1mM FeY^{-} in 1 F Na_2SO_4 - $NaHSO_4$, pH 5	4	187 ± 3	15 ± 0.5	172 ± 3	171
4	1mM FeY^{-} in 1 F $NaClO_4$ - $HClO_4$, pH 5	7	189 ± 8	16 ± 1	173 ± 9	171

Experimental conditions: Thin-layer volume was 1.77 microliter. Potential step was 0.05 to -0.25 volt *vs.* SCE in experiments 1, 3, 4, and -0.25 to 0.05 volt *vs.* SCE in experiment 2. Q blank was obtained in the corresponding chelate-free supporting electrolyte with the same potential steps.

in studies of systems in which the adsorbed reactant interferes with, or completely prevents, the reaction of unadsorbed reactant.

2. Elucidation of the Stoichiometry of Complicated Reactions - A Study of the Electrochemistry of the Chloride, Bromide and Iodide Complexes of Platinum(II) and (IV) by Means of Thin Layer Electrochemistry (27).

Although the electrochemistry of the platinum halides has not escaped previous study (28, 29, 30), it cannot be considered to be well understood.

In the present study, the stoichiometry of the electrochemical oxidation of $PtCl_4^{-2}$, $PtBr_4^{-2}$ and PtI_4^{-2} and of the electrochemical reduction of $PtCl_6^{-2}$, $PtBr_6^{-2}$, PtI_6^{-2} and their hydrolysis products has been examined by means of thin layer electrochemical techniques. The effect of acidity and halide concentration on these reactions has been investigated. The particular advantages of the thin layer approach for the study of irreversible redox couples have been pointed out in the above discussion, and these advantages have been exploited in the present study.

(i). Experimental

The micrometer thin layer electrode and associated circuitry

---

[27] A. T. Hubbard and F. C. Anson, Anal. Chem. 38, in press (1966).

[28] A. N. Frumkin, Trans. Faraday Soc., 54, 156 (1958).

[29] V. I. Kravtsov, and B. V. Sinakov, Vestn. Leningr. Univ., 19, Ser. Fiz. i Khim. No. 2, 90 (1964).

[30] J. J. Lingane, J. Electroanal. Chem., 7, 94 (1964).

have been described above. The measurements of total charge consumed by particular electrode reactions were carried out in two different ways: When the electrode potential was potentiostatically stepped from one value (where no current flowed) to another, the resulting current was integrated by means of operational amplifiers and the integral was recorded. For the experiments in which the electrode potential was swept linearly but very slowly, the area under the resulting individual current potential peaks was evaluated graphically. When more than one current peak occurred, the areas were divided at the current minima.

Because the electrode reactions exhibited considerable irreversibility, even at the low current densities prevailing in the thin layer experiments, it was necessary to match the potential sweep rates to the reactant concentrations in order to keep the peak currents constant and small. In this way the observed peak potentials remained constant even though the concentrations of the individual components varied.

The very slow potential sweep rates (0.125 - 0.5 millivolts/second) were obtained by means of a synchronous motor-driven potentiometer instead of the operational amplifier sweep generator previously described (Part III). All potentials were measured *versus* the saturated calomel electrode.

The platinum thin layer electrodes were cleaned before each experiment by alternate, anodic (1.5 volts) and cathodic (0 volt), polarization in 1 F H_2SO_4; after several such cycles the electrode was potentiostated at 0.4 volt for several minutes until any residual current decayed to less than one microampere and was then used immediately.

Reagents

K_2PtCl_6 was prepared by mixing excesses of 1 F KCl solution with an 0.1 F solution of H_2PtCl_6 in 3 F HCl. The precipitated K_2PtCl_6 was washed with ice water, ethanol and anhydrous ether.

Hydrolyzed solutions of K_2PtCl_6 and K_2PtBr_6 were prepared by either of the following two methods (solutions prepared by either method behaved identically): (1) Solutions of K_2PtCl_6 or K_2PtBr_6 in water were irradiated for two hours at room temperature with a mercury arc lamp (General Electric Co. No. H4AB, 100 watts) located 10 cm. from the solution and then allowed to stand 48 hours before use. (2) Solutions of K_2PtCl_6 or K_2PtBr_6 in water were allowed to stand under nitrogen for several weeks at room temperature under ordinary laboratory illumination.

K_2PtCl_4 was prepared according to a published procedure (31) K_2PtBr_6 was prepared as follows: Several grams of $H_2PtCl_6 \cdot 6H_2O$ were treated with 10 ml. per gram of 48% HBr and the mixture kept near 90° C for two hours. A slight excess of KBr was added and the resulting precipitate of K_2PtBr_6 was recrystallized several times from 1 F HBr.

---

[31] J. Kleinberg (ed.), Inorganic Syntheses, 7, 240, McGraw-Hill Book Co., N.Y., 1963.

Other chemicals were of reagent grade and were used without further purification.

All solutions were stored and used under an atmosphere of prepurified nitrogen. The thin layer electrode was contained in a small polyethylene tent that was continuously flushed with nitrogen.

It should be pointed out that the use of the thin layer electrode was essential in these experiments for two reasons: The electrode reactions are irreversible so that poorly defined waves are obtained at the usual current densities required in macro-electrochemical cells. In addition, platinum metal is deposited during many of the reductions. In the thin layer cell the amount of deposition during the course of each experiment is manageably small. In macro-cells, however, so much more platinum is deposited that the effective electrode area does not remain constant during an individual experiment.

(ii). $PtCl_4^{-2}$ and $PtCl_6^{-2}$

Figure 20, curve A shows the thin layer current-potential curve that resulted when a slow linear potential sweep was applied to a solution of $PtCl_6^{-2}$ in 1 F HCl. The difference between the observed peak potential (0.1 volt) and the accepted standard potential --0.43 volt S.C.E. (32)--illustrates the irreversibility of the reaction. The current potential curve does not show a distinct

---

[32] W. L. Latimer, Oxidation Potentials, 2nd ed., p. 207, N.Y.: Prentice Hall, 1952.

Figure 20

A. Thin layer current-potential curve for reduction of 1.00 mF K_2PtCl_6 in 1 F HCl.

B. As in A except that the direction of the potential scan was reversed at + 0.05 volt.

C. Current-potential curve in 1 F HCl alone. Thin layer volume was 1.25 μ liters. Scan rate was 2 millivolts/sec.

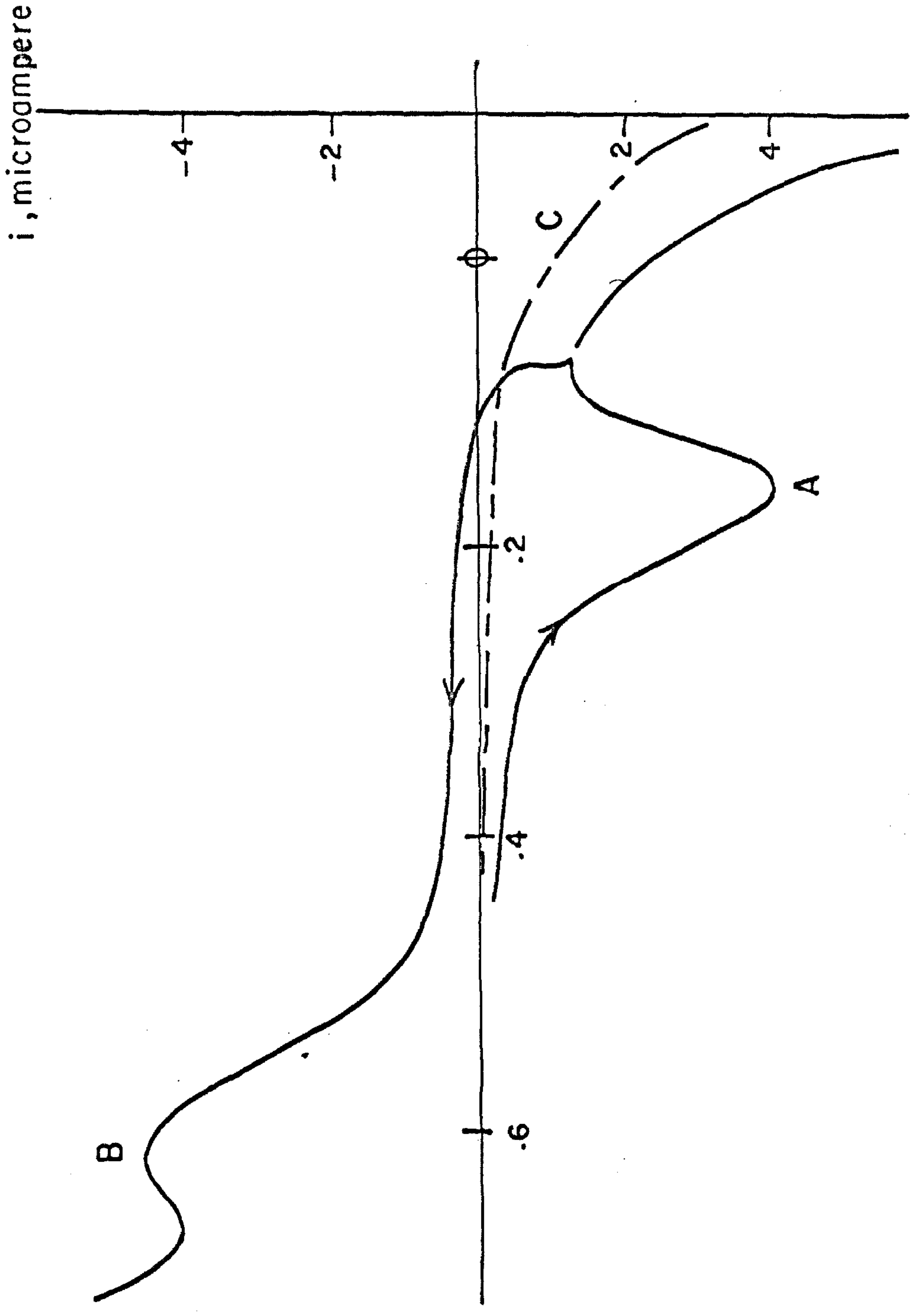
i, microampere
-4
-2
2
4
C
A
B
.2
.4
.6

second peak for the reduction of $PtCl_4^{-2}$ because of the extreme irreversibility of this reaction. However, it is certain that $PtCl_4^{-2}$ is formed from the reduction of $PtCl_6^{-2}$ because reversal of the potential scan direction immediately after the $PtCl_6^{-2}$ reduction wave leads to an anodic current peak (Figure 20, curve B) which is identical to the peak obtained with a separate solution of pure $PtCl_4^{-2}$ (Figure 21-A).

The results of potential-step current integration experiments with $PtCl_6^{-2}$ solutions are given in Table XII. It is clear that in 1 F HCl electrolyte under the conditions prevailing in the thin layer experiments the n-values are 2 for both the reduction of $PtCl_6^{-2}$ and the oxidation of $PtCl_4^{-2}$. This result is in disagreement with the proposal of Lingane (30) that Pt(III) is a stable intermediate in the reduction of $PtCl_6^{-2}$.

Figure 21b shows the thin layer current-potential curve that results when the oxidation of $PtCl_4^{-2}$ is followed by reversal of the potential scan direction. The product of the oxidation of $PtCl_4^{-2}$ is not simply $PtCl_6^{-2}$ but a mixture of at least two species. The "new" platinum (IV) complex is surely of the general type $Pt(OH)_mCl_{6-m}^{-2}$, there being no ligands other than Cl^- and OH^- (or H_2O) present in the solution. The exact identity of the species present is discussed in the following sections.

(iii). Hydrolysis of $PtCl_6^{-2}$

The hydrolysis of $PtCl_6^{-2}$ has been studied in some detail by

Figure 21

A. Thin layer current-potential curve for oxidation of 1.00 mF $K_2PtCl_4^{-2}$ in 1 F HCl followed by

B. Reduction of the oxidation products.

C. Background current. Conditions as in Figure 20.

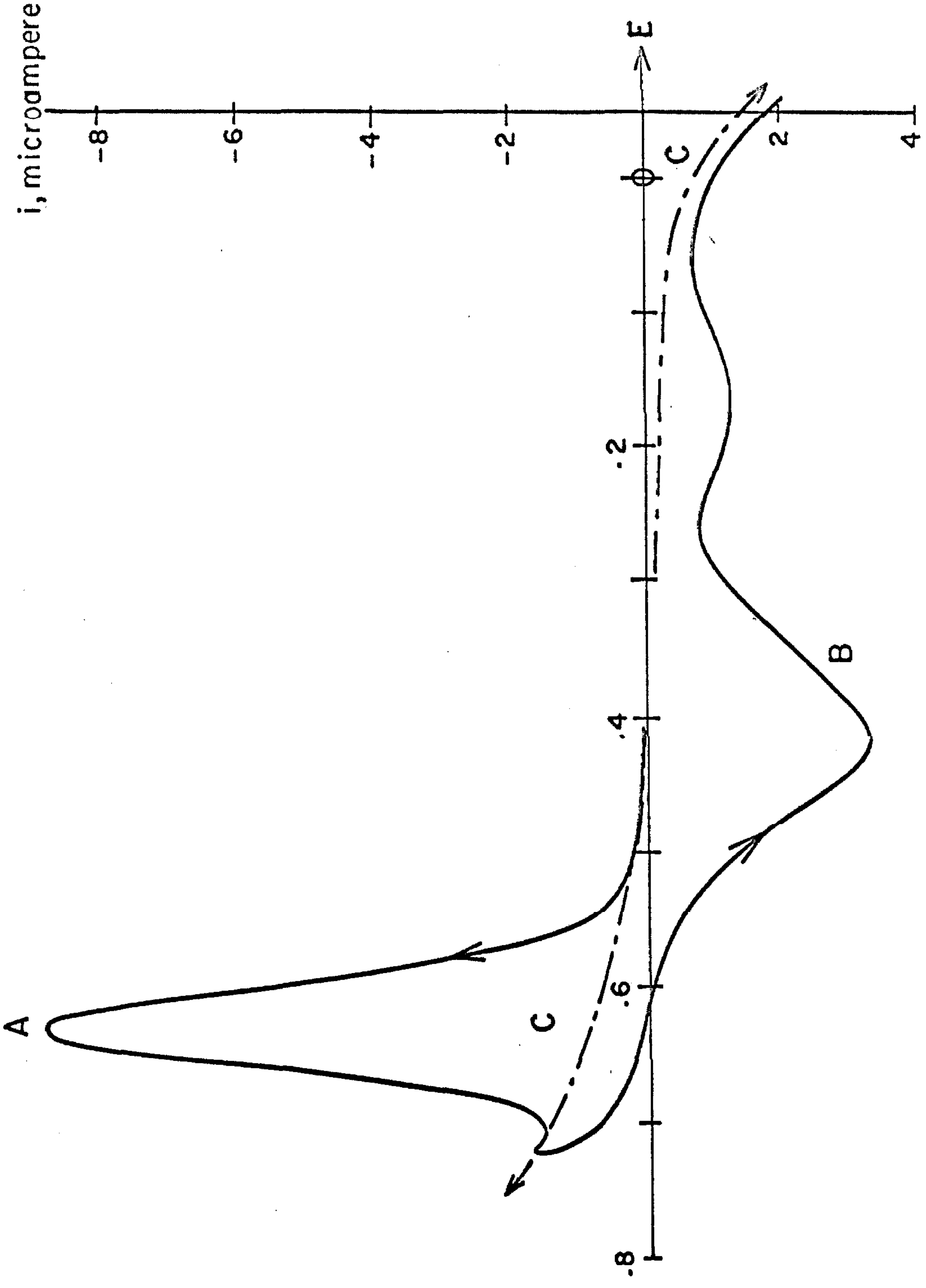
i, microampere
-8
-6
-4
-2
0
2
4
E
.2
.4
.6
.8
A
B
C
C

Table XII Determination of the n-values for $PtCl_6^{-2}$ reduction and $PtCl_4^{-2}$ oxidation in 1 F HCl by potential step with current integration in thin layers of solution (a)

Exp. No.	Solution Employed	Number of Trials	$E_1^{(b)}$	E_2	Q observed,(c) μc	Q blank,(d) μc	Q obs - Q blank, μc	$n = \frac{Q\ obs - Q\ blank}{FVC^o}$
1	1.00 mF K_2PtCl_6 in 1 F HCl	4	+0.4	0.0	325 ± 2	80 ± 4	245 ± 6	2.02 ± 0.04
2	1.00 mF K_2PtCl_4 in 1 F HCl	5	+0.4	0.75	417 ± 15	166 ± 11	251 ± 26	2.08 ± 0.2

Experimental Conditions

(a) The thin layer volume was 1.25 microliter.

(b) E_1 is the initial electrode potential; E_2, the potential to which it was stepped in volts vs. S.C.E.

(c) About 5 seconds were required for the integral to become constant.

(d) The blank solution was 1.0×10^{-3} F K_2PtCl_4 in 1 F HCl in exp. No. 1 and 1 F HCl alone in exp. No. 2.

The large values of Q blank result from slow reduction of $PtCl_4^{-2}$ to platinum metal at 0.0 volt in exp. No. 1 and from slow but appreciable oxidation of the platinum electrode at 0.75 volt in exp. No. 2.

Dreyer (33) who showed that aqueous $K_2PtCl_6^{-2}$ solutions slowly hydrolyze according to the generalized reaction

$$PtCl_6^{-2} + \overline{m}\,H_2O \rightarrow \sum_{m=1}^{6} a_m Pt(OH)_m Cl_{6-m}^{-2} + \overline{m}\,H^{+} \tag{27}$$

The average extent of hydrolysis $\overline{m}$, is defined according to

$$\overline{m} = \frac{1}{C^{\circ}} \sum_{m=0}^{6} m\,C_m = \frac{\text{moles } OH^{-} \text{ required in titration of hydrolyzed sol'n.}}{\text{moles Pt(IV) in sample}} \tag{28}$$

where C° is the total Pt concentration and C_m is the concentration of the mth hydrolyzed form, $Pt(OH)_m Cl_{6-m}^{-2}$. The value of $\overline{m}$ for any solution can be determined conveniently by titration of the partially hydrolyzed solution with standard NaOH, taking advantage of the fact that the rate of reaction between OH^{-} and the unhydrolyzed platinum complex is rather slow in the absence of Pt(II) compounds or intense irradiation.

In the present work hydrolyzed $PtCl_6^{-2}$ solutions of several different total Pt concentrations were titrated with standard NaOH solution to a phenolphthalein end point. The results are

---

[33] R. Dreyer, et. al., Z. phys. Chem., 224, 199 (1963).

summarized in Table XIII and Figure 22. The observed dependence of $\overline{m}$ on the initial concentration of $PtCl_6^{-2}$ is in agreement with the experiments of Dreyer (33). This concentration dependence and the fact that the hydrolysis appears to cease could be explained either by the reaction having achieved equilibrium or by an acid and/or chloride inhibition of the kinetically controlled hydrolysis reaction. Neither Dreyer's experiments nor our own permitted a choice to be made between these two alternatives.

To study the electrochemical behavior of the hydrolyzed $PtCl_6^{-2}$ solutions aliquots were made 1 F in $NaClO_4$ and subjected to slow linear potential sweep experiments in the thin layer electrode. The current-potential curves in Figure 23 resulted. The area under each peak in these current-potential curves was determined graphically.

The total area under each current-potential curve is given by Equation 14.

n equals 4 in Equation 14 for the reduction of $PtCl_6^{-2}$ in $NaClO_4$ solutions. This change in n-value when the supporting electrolyte is changed from HCl to $NaClO_4$ is examined in more detail in a later section.

Equation 14 should be obeyed whether or not the electrode reactions proceed reversibly so long as the sweep rate is slow enough to insure that all of the reactant in the thin layer is consumed and the current efficiency for each reaction (after correction for any blank) is 100%.

Table XIII Determination of $\overline{m}$

Initial K_2PtCl_6 Concentration $\times 10^3$ F	Sample, volume ml	Vol. of 0.00967 F NaOH Required ml	$\overline{m}$
1.25	20	5.60	2.24
2.50	20	8.91	1.78
5.00	10	6.49	1.30
10.00	2	1.84	0.930
20.00	4	5.70	0.713

The solutions were prepared as described in the experimental section; *i.e.*, hydrolysis had essentially ceased before the titrations were carried out. The standard deviation in the experiments was about 1%.

Figure 22

The average extent of *hydrolysis* of $PtCl_6^{-2}$ solutions, $\overline{\overline{m}}$, plotted as a *function* of the initial K_2PtCl_6 *concentration.*

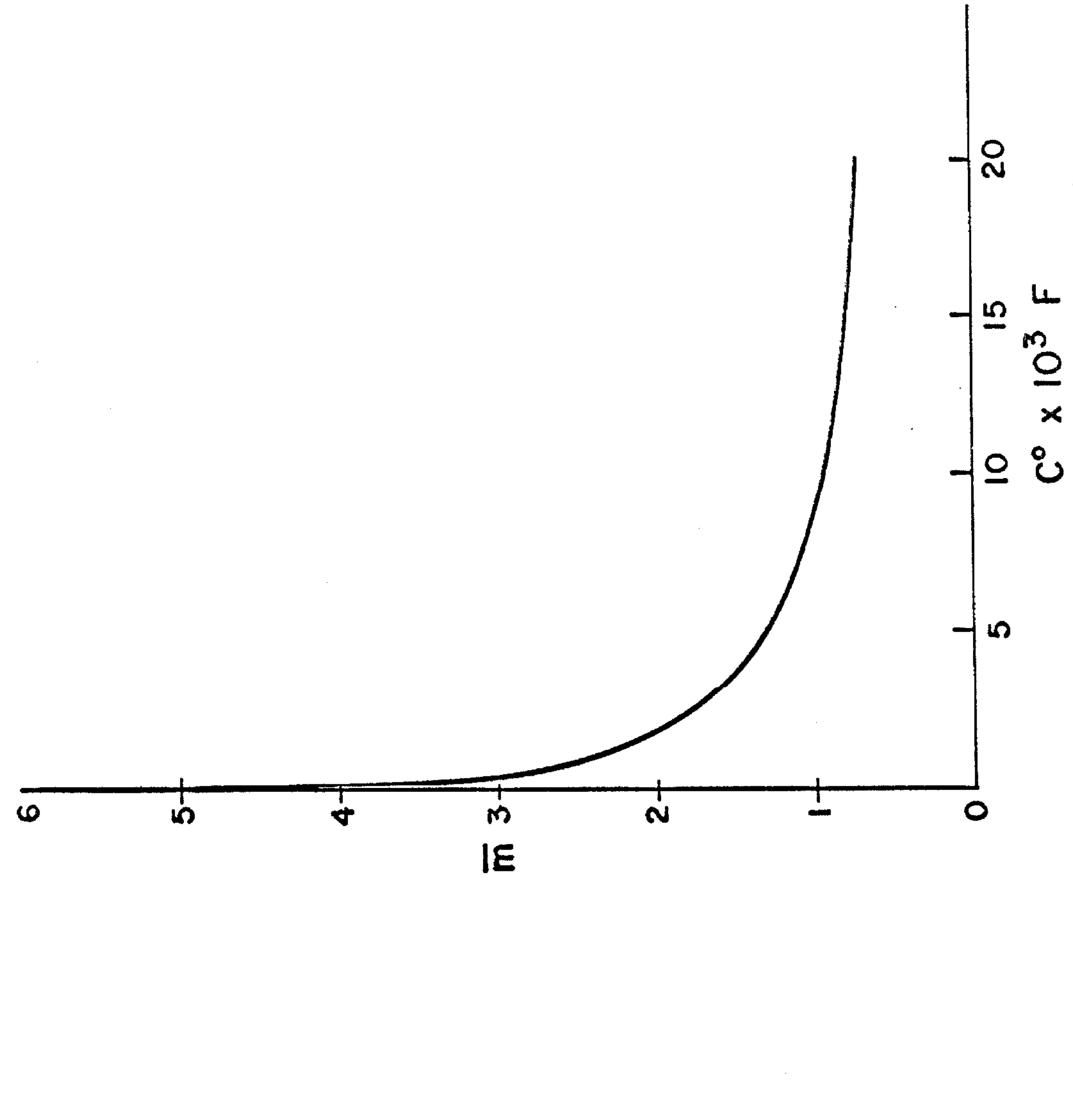
0
1
2
3
4
5
6
$\bar{m}$
5
10
15
20
$C^\circ \times 10^3$ F

Figure 23

Cathodic thin layer current-potential curves for hydrolyzed K_2PtCl_6 solutions. The thin layer volume was 1.25 microliter.

A. A hydrolyzed solution containing 20.0×10^{-3} F Pt(IV) was diluted to 16.0×10^{-3} F with 5 F $NaClO_4$. The sweep rate was 0.125 mv./second.

B. A hydrolyzed solution containing 10.0×10^{-3} F Pt(IV) was diluted to 8.0×10^{-3} F with 5 F $NaClO_4$. The sweep rate was 0.25 mv./second.

C. A hydrolyzed solution containing 5.0×10^{-3} F Pt(IV) was diluted to 4.00×10^{-3} F with 5 F $NaClO_4$. The sweep rate was 0.50 mv./second.

D. A hydrolyzed solution containing 2.50×10^{-3} F Pt(IV) was diluted to 2.00×10^{-3} F with 5 F $NaClO_4$. The sweep rate was 1.00 mv./second.

E. A hydrolyzed solution containing 1.25×10^{-3} F Pt(IV) was diluted to 1.0×10^{-3} F with 5 F $NaClO_4$. The sweep rate was 2.00 mv./second.

F. Background current.

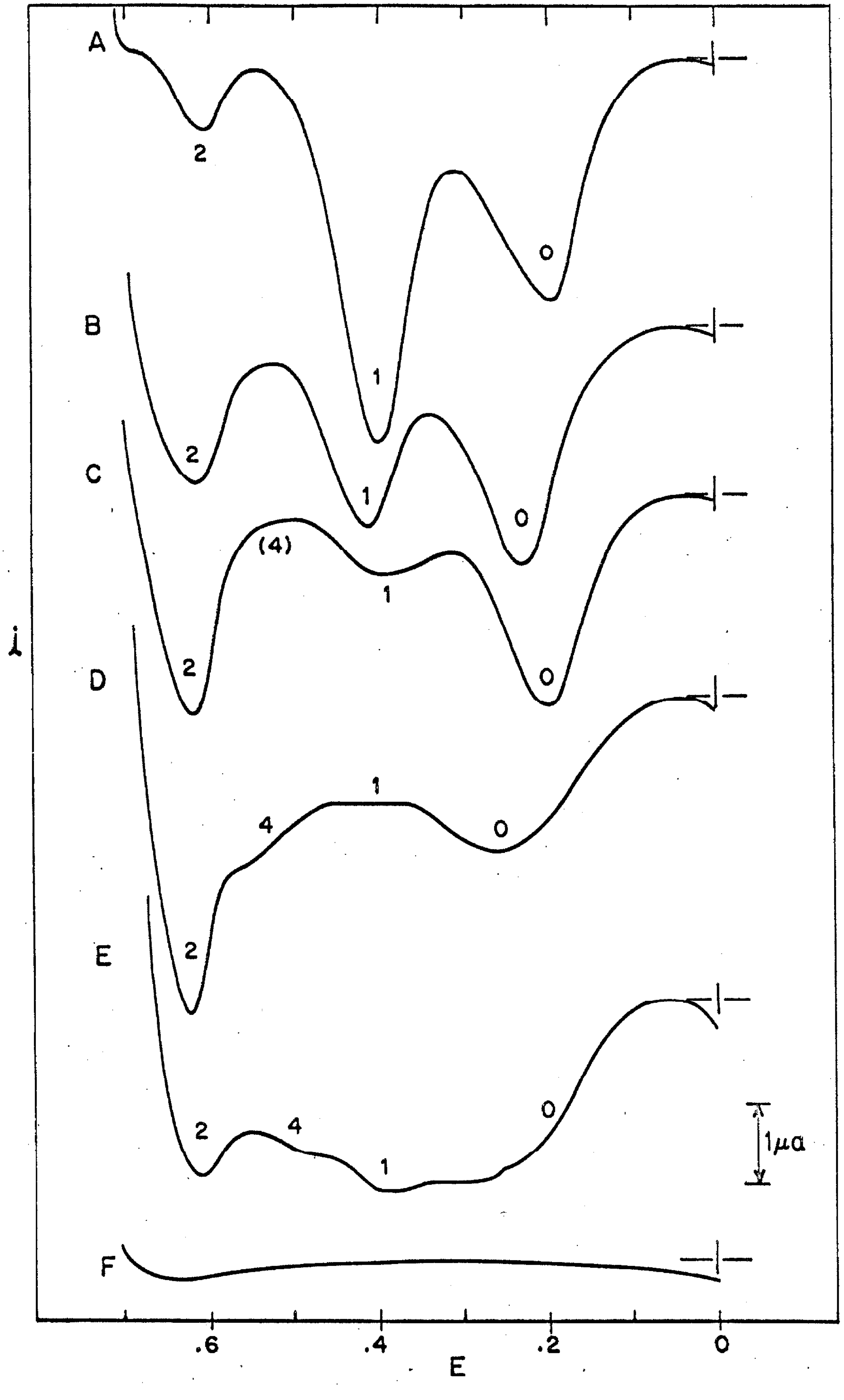
A
B
C
D
E
F
2
1
0
2
1
0
(4)
2
1
0
4
1
0
2
2
4
1
0
1μa
i
.6
.4
.2
0
E

The identity of the hydrolyzed Pt(IV) species giving rise to each of the current peaks in Figure 23 was established by comparing the ratio of the area under each peak to the total area with the value of $\overline{m}$ determined by the titration for the same solution. It follows from Equations 14 and 28 that

$$\overline{m} = \sum_{m=0}^{6} \frac{mQ_m}{Q_{Total}} \tag{29}$$

where Q_m is the area under the peak in the current-potential curve corresponding to the hydrolyzed species $Pt(OH)_mCl_{6-m}^{-2}$. The integral values of m assigned to each of the observed current peaks were chosen to give the best agreement of $\overline{m}$ calculated from Equation 29 with the measured values in Table XIII. The results of this analysis are shown in Table XIV. The agreement is quite good considering the extensive overlapping of some of the peaks. The sweep rates used in Figure 23 varied from 0.125 to 2 millivolts/sec. for the reason explained in the experimental section. At the lowest sweep rate about 90 minutes were required for the recording of the curves. This long duration of the experiment is probably responsible for the discrepancy between the total charge measured under each curve and the theoretical value calculated from Equation 14. This discrepancy was not a serious problem inasmuch as only the ratios of individual peak areas to the total area were needed for the calculation of $\overline{m}$. Thus it appears that the four peaks labeled 0, 1, 2, and 4 in Figure 23 correspond respectively to the species:

Table XIV Integration of thin layer current-potential curves (Fig. 23) obtained with hydrolyzed K_2PtCl_6 solutions

Total Pt(IV) Concentration during Hydrolysis, × 10^3 F	Total Pt(IV) Concentration After Addition of 5 F $NaClO_4$ for Thin Layer Experiment × 10^3 F	Current-time Integral, Q, under i^th^ Peak of Current-potential Curve, μc (b)					Q total from Equation 3 (a) for n = 4, μc	$\overline{m}$ Calculated from Equation 4 (c)	$\overline{m}$ Measured (from Table XIII)
		Q_0	Q_1	Q_2	Q_4	Q total			
20.00	16.00	3349	4557	813	0	8719	7712	0.71	0.71
10.00	8.00	1617	1477	1105	(0)	4199	3856	0.88	0.93
5.00	4.00	787	522	559	(243)	2111	1928	1.35	1.30
2.50	2.00	345	(330)	330	(279)	1244	964	(1.7)	1.78
(c)	-	-				-		-	-

(a) The thin layer volume was 1.25 microliter.

(b) Each Q_i was obtained from the relation: $Q_i = Q_i$ (measured) - Q_i (blank); the value of the blank was 35 microcoulombs for each peak except 4. For peak 4 the blank was taken to be approximately 0. The uncertainty in the numbers in parentheses is about ±20%; otherwise it is about ±5%.

(c) The $\overline{m}$ calculation is based on the following assignment of peaks: $\underline{0} = PtCl_6^{-2}$, $\underline{1} = Pt(OH)Cl_5^{-2}$, $\underline{2} = Pt(OH)_2Cl_4^{-2}$, $\underline{4} = Pt(OH)_4Cl_2^{-2}$.

(d) An $\overline{m}$ calculation was not attempted for more dilute solutions due to excessive overlap of individual peaks.

$PtCl_6^{-2}$, $PtOHCl_5^{-2}$, $Pt(OH)_2Cl_4^{-2}$, and $Pt(OH)_4Cl_2^{-2}$.

The reactions of these three hydroxide-containing Pt(IV) species with 1 F HCl were investigated by making each of the fully hydrolyzed solutions 1 F in HCl and recording the resulting thin layer current-potential curves. (Approximately 10 minutes elapsed between the addition of the HCl and the initiation of the potential sweep.) The results are shown in Figure 24. The fact that HCl causes peak 0 to grow at the expense of peak 1 suggests that $Pt(OH)Cl_5^{-2}$ reacts rapidly with HCl to form $PtCl_6^{-2}$. Peak 2 occurs in 1 F HCl at the same potential (+0.35 volts) as the peak resulting from the reduction of the hydroxy species obtained by oxidation of $PtCl_4^{-2}$ in 1 F HCl (Figure 21). From the relative heights of the two peaks in Figure 21 it seems likely that the oxidation of $PtCl_4^{-2}$ in 1 F HCl proceeds according to

$$PtCl_4^{-2} - 2e^- \xrightarrow{\text{1 F HCl}} \underline{\text{ca.}}\ 1/3PtCl_6^{-2} + \underline{\text{ca.}}\ 2/3Pt(OH)_2Cl_4^{-2}$$

The persistence of peaks 2 and 4 in the 1 F HCl suggests that $Pt(OH)_2Cl_4^{-2}$ and $Pt(OH)_4Cl_2^{-2}$ are more resistant to attack by chloride than is $PtOHCl_5^{-2}$. This resistance to attack by chloride is consistent with the suggestion that the hydroxide ligands have the *trans* configuration in $Pt(OH)_2Cl_4^{-2}$ and $Pt(OH)_4Cl_2^{-2}$ (34).

---

[34] F. Basolo and R. G. Pearson, in *Progress in Inorganic Chemistry*, F. A. Cotton, ed., **4**, 381, Interscience, N.Y., 1962.

Figure 24

Cathodic thin layer current-potential curves for hydrolyzed K_2PtCl_6 solutions after addition of HCl. Thin layer volume was 1.25 microliter.

A. A hydrolyzed solution containing 20.0 mF Pt(IV) was diluted to 16.0 mF with 5 F HCl. The sweep rate was 1.25 mv./second; x = 10 microampere.

B. A hydrolyzed solution containing 10.0 mF Pt(IV) was diluted to 8.0 mF with 5 F HCl. The sweep rate was 1.25 mv./second; x = 5 microampere.

C. A hydrolyzed solution containing 5.0 mF Pt(IV) was diluted to 4.0 mF with 5 F HCl. The sweep rate was 1 mv./second; x = 2 microampere.

D. A hydrolyzed solution containing 2.5 mF Pt(IV) was diluted to 2.0 mF with 5 F HCl. The sweep rate was 2 mv./second; x = 2 microampere.

E. A hydrolyzed solution containing 1.25 mF Pt(IV) was diluted to 1.0 mF with 5 F HCl. The sweep rate was 1 mv./second; x = 1 microampere.

F. Background current. 1 F HCl. The sweep rate was 2 mv./second; x = 1 microampere.

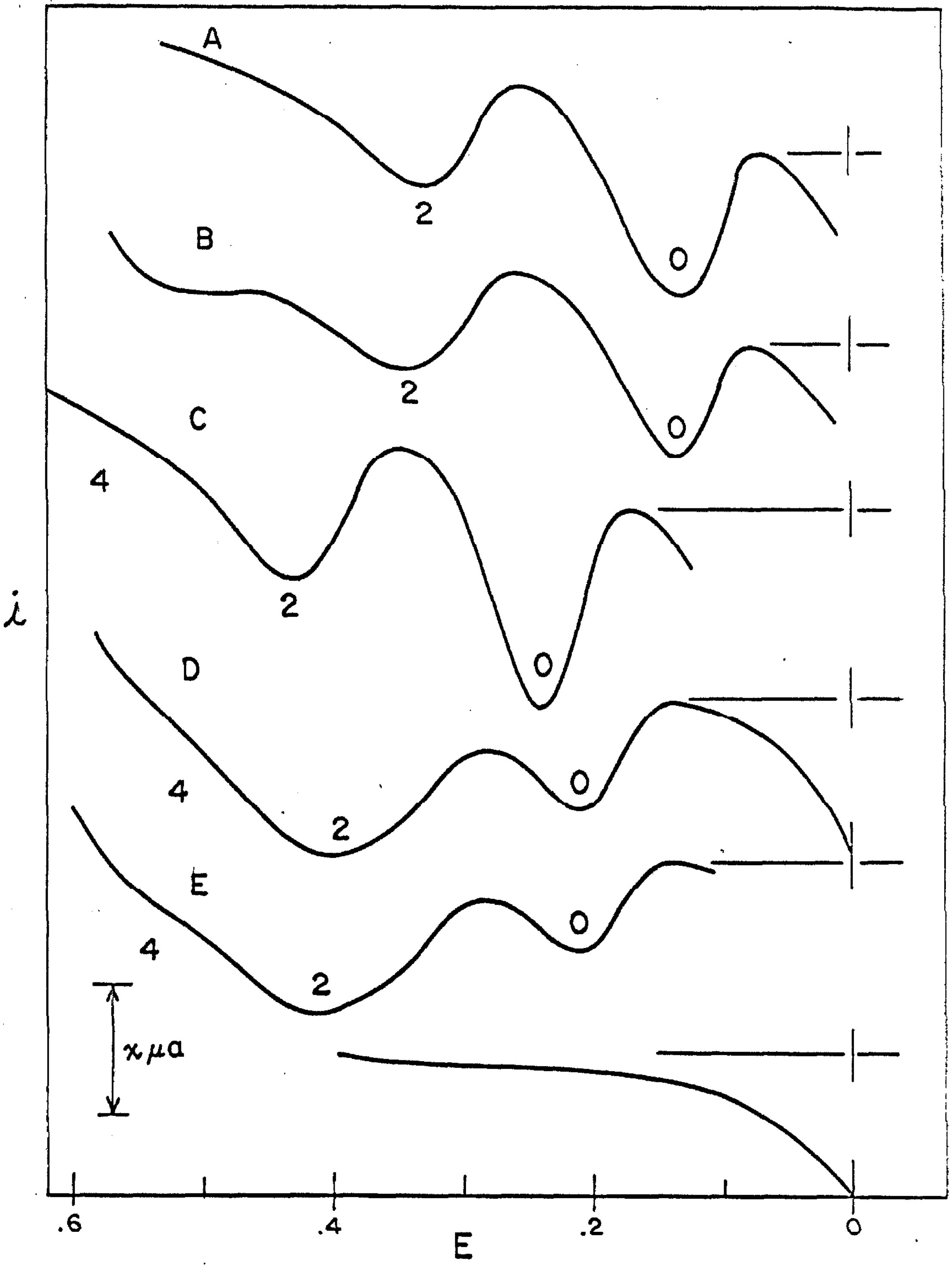
A
2
O
B
2
O
C
4
2
O
i
D
4
2
O
E
4
2
O
x μa
.6
.4
.2
0
E

(iv). Supporting Electrolyte Effects

To further define the effect of solution pH and chloride concentration on the reduction of $PtCl_6^{-2}$ and its hydrolysis products, aliquots of a 1.25 mM hydrolyzed $PtCl_6^{-2}$ solution (for which $\overline{m} = 2.20$) were made 1 F in HCl, $HClO_4$, NaCl, or $NaClO_4$ and the n-values for reduction obtained by thin layer chronocoulometry. The results appear in Table XV and indicate that in HCl, $HClO_4$ or NaCl the reduction product is Pt(II) whereas in $NaClO_4$ the reduction proceeds all the way to platinum metal. The $PtCl_4^{-2}$ experiments in Table XV reflect the large difference in the rate of reduction of $PtCl_4^{-2}$ when the electrolyte is changed from HCl, $HClO_4$, or NaCl to $NaClO_4$. The cathodic thin layer current-potential curve obtained with $PtCl_4^{-2}$ in 1 F $NaClO_4$ appears in Figure 25.

The fact that a 2 electron reduction wave is observed for $PtCl_4^{-2}$ in $NaClO_4$ but not in HCl is consistent with the fact that $PtCl_6^{-2}$ is reduced to $PtCl_4^{-2}$ in HCl but all the way to platinum metal in $NaClO_4$.

The reasons for such a strong dependence of the n-values on the composition of the supporting electrolytes are not elucidated by these experiments.

(v). $PtBr_6^{-2}$ and $PtBr_4^{-2}$

Figure 26, curve A, shows the thin layer current-potential curve obtained with a solution of $PtBr_6^{-2}$ in 1 F NaBr. As was true

Table XV. Determination of the n-values for reduction of $PtCl_4^{-2}$ and of $PtCl_6^{-2}$ and its hydrolysis products by potential step with current integration in thin layers of solution

Exp. No.	Reactant(a)	Supporting Electrolyte	Number of Trials	E_1	E_2	Q observed, μc	Q blank, μc	Q obs-Q blank, μc	$n = \frac{Q\ obs - Qblank}{FVC^0}$
1	Pt(IV)	1 F HCl	6	+0.4	0.0	207 ± 4	60 ± 3	147 ± 7	2.08 ± 0.1
2	Pt(IV)	1 F NaCl	6	+0.5	0.05	248 ± 12	91 ± 3	157 ± 15	2.2 ± 0.2
3	Pt(IV)	1 F $HClO_4$	4	+0.6	0.1	243 ± 10	80 ± 11	163 ± 22	2.3 ± 0.3
4	Pt(IV)	1 F $NaClO_4$	5	+0.6	0.0	537 ± 4	261 ± 5	276 ± 9	3.9 ± 0.1
5	Pt(II)	1 F HCl, or 1 F NaCl, or 1 F $HClO_4$	-	0.5	0.0	-	-	-	~ 0.0(b)
6	Pt(II)	1 F $NaClO_4$	4	0.4	0.05	202 ± 6	52 ± 5	150 ± 11	2.1 ± 0.2

Experimental Conditions

The thin layer volume was 0.73 microliter.

The supporting electrolyte was used as the blank solution in each experiment.

E_1 is the initial electrode potential; E_2, the potential to which it was stepped, in volts vs. S.C.E.

(a) For exp. Nos. 1-4 aliquots of a hydrolyzed 1.25 mF K_2PtCl_6 solution were diluted to 1.00 mF with the appropriate volume of supporting electrolyte and used at once. For exp. Nos. 5-6, aliquots of a fresh 1.25 mF K_2PtCl_4 solution were treated according to the same procedure.

(b) The current-potential curves and their integrals did not differ appreciably from the blank solution in these experiments.

Figure 25

Thin layer current-potential curve for reduction of 1.00 mF $PtCl_4^{-2}$ in 1 F $NaClO_4$.
The thin layer volume was 0.73 microliter and the sweep rate was 2.0 mv./second.

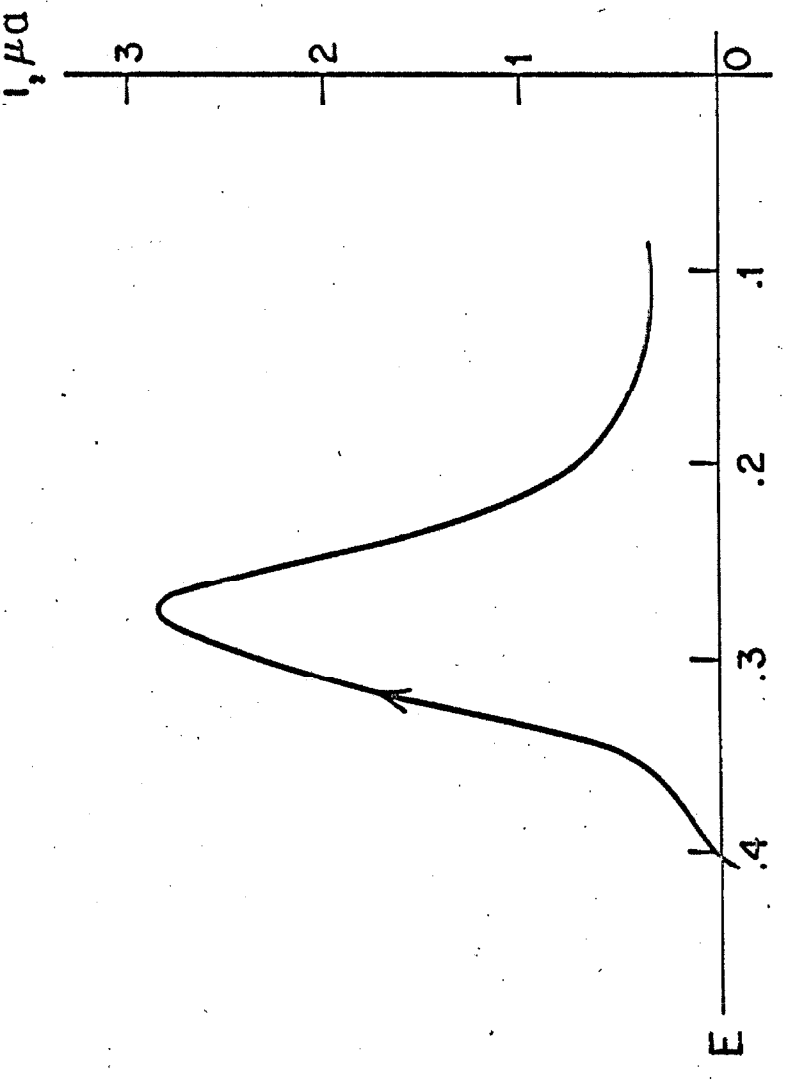
i, μa
3
2
1
0
.1
.2
.3
.4
E

Figure 26

A. Thin layer current-potential curve for reduction of 1.00 mF $PtBr_6^{-2}$ in 1 F NaBr.

B. As in A except that the direction of the potential sweep was reversed at 0.18 volt.

C. Background current in 1 F NaBr alone. The thin layer volume was 0.73 microliter and the sweep rate was 2 mv./second.

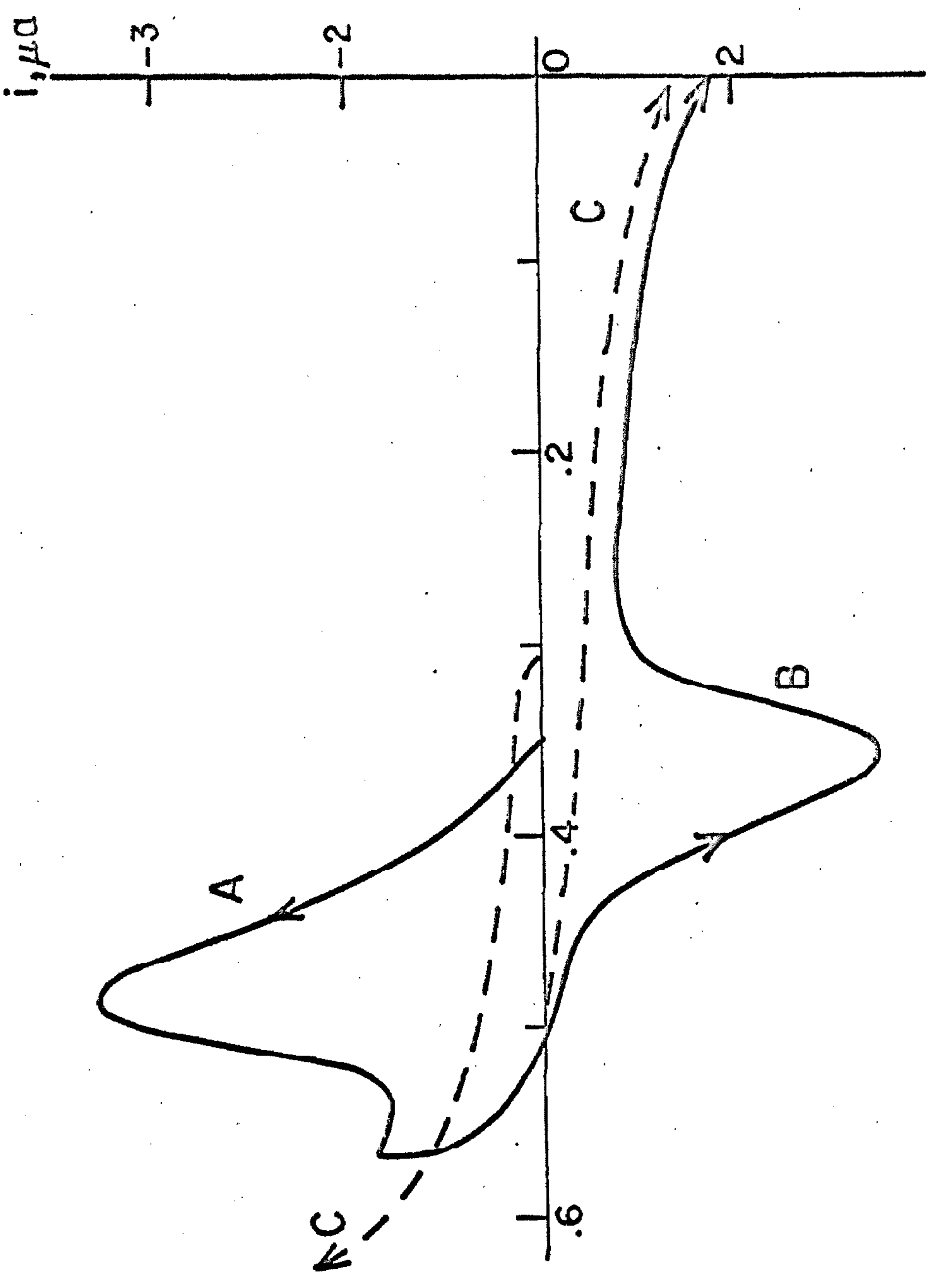
i, μa
−3
−2
0
2
.2
.4
.6
A
B
C
C

with $PtCl_6^{-2}$ no distinct second peak for the reduction of $PtBr_4^{-2}$ is present. However, it is certain that $PtBr_4^{-2}$ is formed from the reduction of $PtBr_6^{-2}$ because reversal of the potential sweep direction immediately after the $PtBr_6^{-2}$ reduction wave leads to an anodic current peak (Figure 26, curve B) which is identical with the peak obtained with a separate solution of pure $PtBr_4^{-2}$ (Figure 27, curve A).

As can be seen from Figure 27, curve B, the final product of $PtBr_4^{-2}$ oxidation is simply $PtBr_6^{-2}$. If species such as $Pt(OH)_2Br_4^{-2}$ are intermediates in the reaction they are apparently rapidly converted to $PtBr_6^{-2}$ in 1 F solutions of bromide.

(vi). Hydrolysis of $PtBr_6^{-2}$

Solutions of $PtBr_6^{-2}$ in water were hydrolyzed, aliquots of the hydrolyzed solutions were made 1 F in $NaClO_4$, and the current-potential curves in Figure 28 obtained. The results indicate that $PtBr_6^{-2}$ undergoes hydrolysis similar to that observed with $PtCl_6^{-2}$; however, $\overline{m}$ values could not be obtained by titration of the hydrolyzed solutions with NaOH, apparently because the hydrolysis products (presumably $Pt(H_2O)_mBr_{6-m}^{m-2}$) were not as acidic as the analogous chloro compounds. The current-potential curves obtained from hydrolyzed K_2PtBr_6 solutions which were made 1 F in NaBr displayed only the wave characteristic of $PtBr_6^{-2}$ reduction, indicating that bromide ion rapidly converts the products of hydrolysis back into $PtBr_6^{-2}$.

Figure 27

A. Thin layer current-potential curve for oxidation of 1.00 mF $PtBr_4^{-2}$ in 1 F NaBr.

B. As in A except that the direction of the potential scan was reversed at +0.57 volt.

C. Background current in 1 F NaBr alone. The thin layer volume was 0.73 microliter and the sweep rate was 2 mv./second.

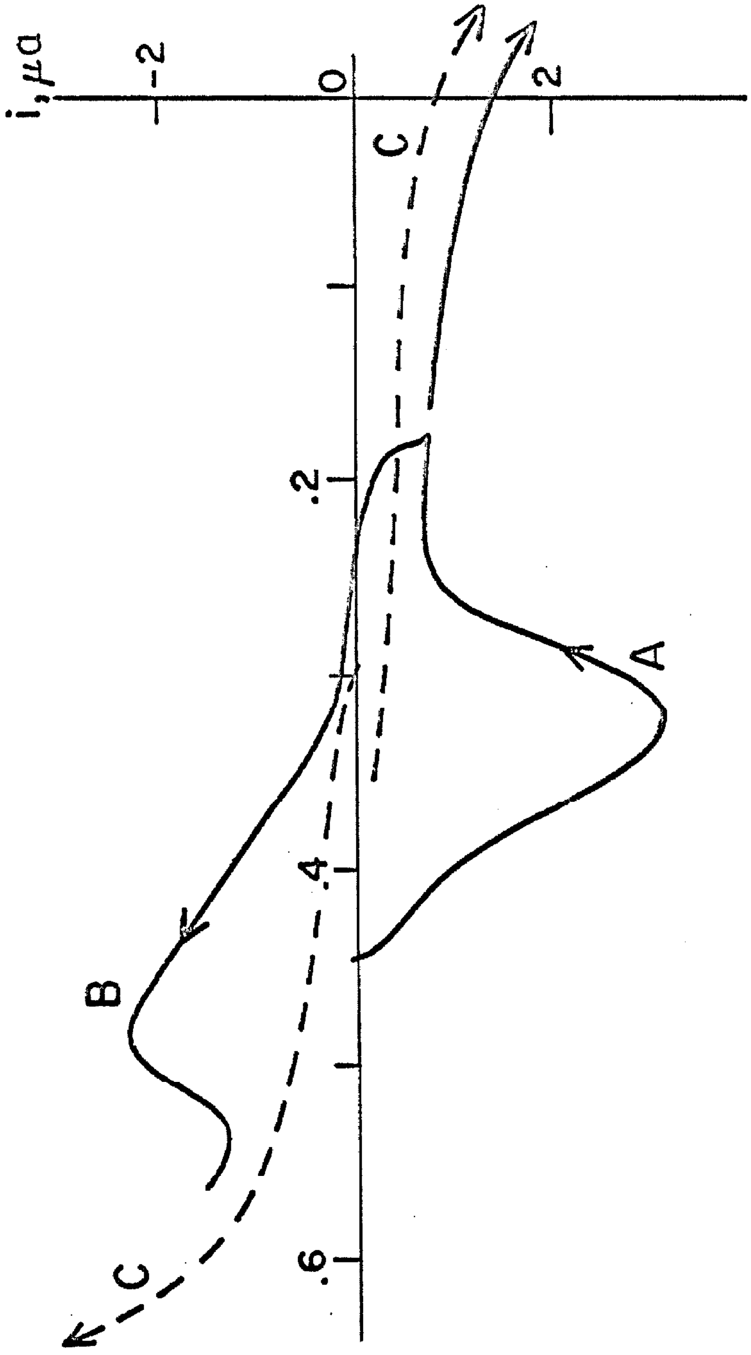
i, μa
-2
0
2
.2
.4
.6
A
B
C
C

Figure 28

Thin layer current-potential curves for reduction of $PtBr_6^{-2}$ and its hydrolysis products in 1 F $NaClO_4$.

The thin layer volume was 0.73 microliter.

A. A hydrolyzed K_2PtBr_6 solution containing 20 mF Pt(IV) was diluted to 16 mF with 5 F $NaClO_4$. The sweep rate was 1 mv./second and x = 10 microampere.

B. A hydrolyzed K_2PtBr_6 solution containing 10 mF Pt(IV) was diluted to 8 mF with 5 F $NaClO_4$. The sweep rate was 1 mv./second and x = 5 microampere.

C. A hydrolyzed K_2PtBr_6 solution containing 5 mF Pt(IV) was diluted to 4 mF with 5 F $NaClO_4$. The sweep rate was 2 mv./second and x = 5 microampere.

D. A hydrolyzed K_2PtBr_6 solution containing 2.5 mF Pt(IV) was diluted to 2.0 mF with 5 F $NaClO_4$. The sweep rate was 1.6 mv./second and x = 2 microampere.

E. A hydrolyzed K_2PtBr_6 solution containing 1.25 mF Pt(IV) was diluted to 1.0 mF with 5 F $NaClO_4$. The sweep rate was 1.6 mv./second and x = 1 microampere.

F. Background current in 1 F $NaClO_4$ alone. The sweep rate was 1.6 mv./second and x = 1 microampere.

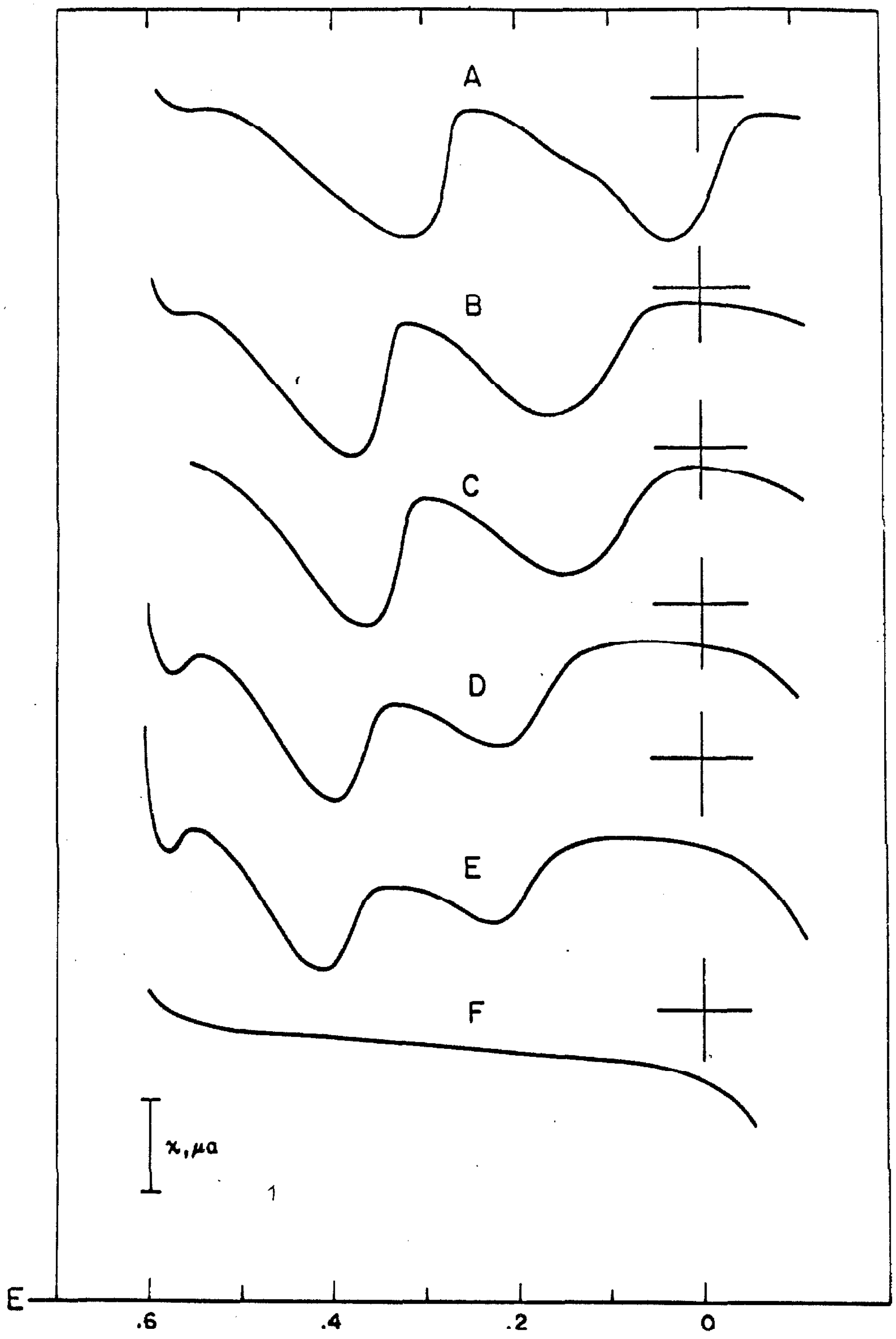
A
B
C
D
E
F
x, μa
1
E
.6
.4
.2
0

The results of thin layer chronocoulometric experiments with hydrolyzed $PtBr_6^{-2}$ and with $PtBr_4^{-2}$ solutions are summarized in Table XVI. The n-value for $PtBr_6^{-2}$ reduction is 2 only in 1 F Br^- solutions. In both 1 F $HClO_4$ and 1 F $NaClO_4$ solutions n is 4. It is interesting, if unexplained, that $PtBr_4^{-2}$ gives a 2-electron reduction wave in $HClO_4$ while $PtCl_4^{-2}$ does not.

(vii). PtI_6^{-2} and PtI_4^{-2}

Figure 29 shows the current-potential curve for reduction of PtI_6^{-2} in 0.5M NaI solution. The thin layer chronopotentiograms obtained with this solution showed two waves which occurred at the potentials anticipated from the sweep data; the number of coulombs required to reach the transition time for the first wave corresponds to an n = 2 reaction. The peak potential (+0.15 volt S.C.E.) of the first reduction peak is in good agreement with the standard potential for the PtI_6^{-2} - PtI_4^{-2} couple (E^0 = +0.148 volt S.C.E.) (35) and the first wave thus corresponds to the reaction

$$PtI_6^{-2} + 2e^- \rightarrow PtI_4^{-2} + 2I^-.$$

Figure 29 (dashed curve) also shows the result of an anodic sweep initiated immediately after cessation of the first wave.

---

[35] A. A. Grinberg, et. al., J. Phys. Chem. (USSR) 10, 661 (1937).

Table XVI. Determination of the n-values for the reduction or oxidation of $PtBr^{-2}$ and the reduction of $PtBr_6^{-2}$ and its hydrolysis products by potential step with current integration in thin layers of solution.

Exp. No.	Reactant[(a)]	Supporting Electrolyte	Number of Trials	E_1	E_2	Q observed, μc	Q blank, μc	Q obs-Q blank, μc	$n = \frac{\text{Q obs-Q blank}}{FVC^0}$
1	$PtBr_6^{-2}$	1 F NaBr	6	+0.5	0.2	174 ± 5	20 ± 1	154 ± 6	2.18 ± 0.09
2[(b)]	$PtBr_4^{-2}$	1 F NaBr	5	+0.25	0.55	-161 ± 2	-22 ± 0.4	-139 ± 2	1.97 ± 0.03
3	Pt(IV)	1 F $HClO_4$	7	+0.55	0.1	312 ± 18	64 ± 3	248 ± 21	4.4 ± 0.4
4	Pt(IV)	1 F $NaClO_4$	6	+0.6	0.0	311 ± 10	86 ± 6	225 ± 16	4.0 ± 0.3
5	Pt(II)	1 F $HClO_4$	4	+0.5	0.1	180 ± 3	62 ± 3	118 ± 6	2.09 ± 0.1
6	Pt(II)	1 F $NaClO_4$	3	+0.55	0.2	188 ± 4	72 ± 4	116 ± 8	2.05 ± 0.1

Experimental Conditions

The thin layer volume was 0.73 microliter.

The supporting electrolyte was used as the blank in each experiment.

E_1 is the initial electrode potential; E_2, the potential to which it was stepped in volts *vs.* S.C.E.

(a) The reactant concentration was 1.00 mF in exp. Nos. 1-2. In exp. Nos. 3-4 aliquots of hydrolyzed 1.00 mF $PtBr_6^{-2}$ were diluted to 0.8 mF with the appropriate volume of supporting electrolyte. In exp. Nos 5-6 aliquots of a freshly prepared 1.00 mF $PtBr_4^{-2}$ solution were diluted to 0.8 mF with the appropriate volume of supporting electrolyte.

(b) The electrode reaction is an oxidation in this experiment only.

Figure 29

Current potential curve for reduction of 1.3 mM PtI_6^{-2} in

0.5 F NaI

The sweep rate was 3.7 millivolt per second.

The thin layer volume was 1.4 liter (ℓ = 40 microns).

The broken curve shows the result of reversal of sweep direction immediately after completion of the first cathodic wave.

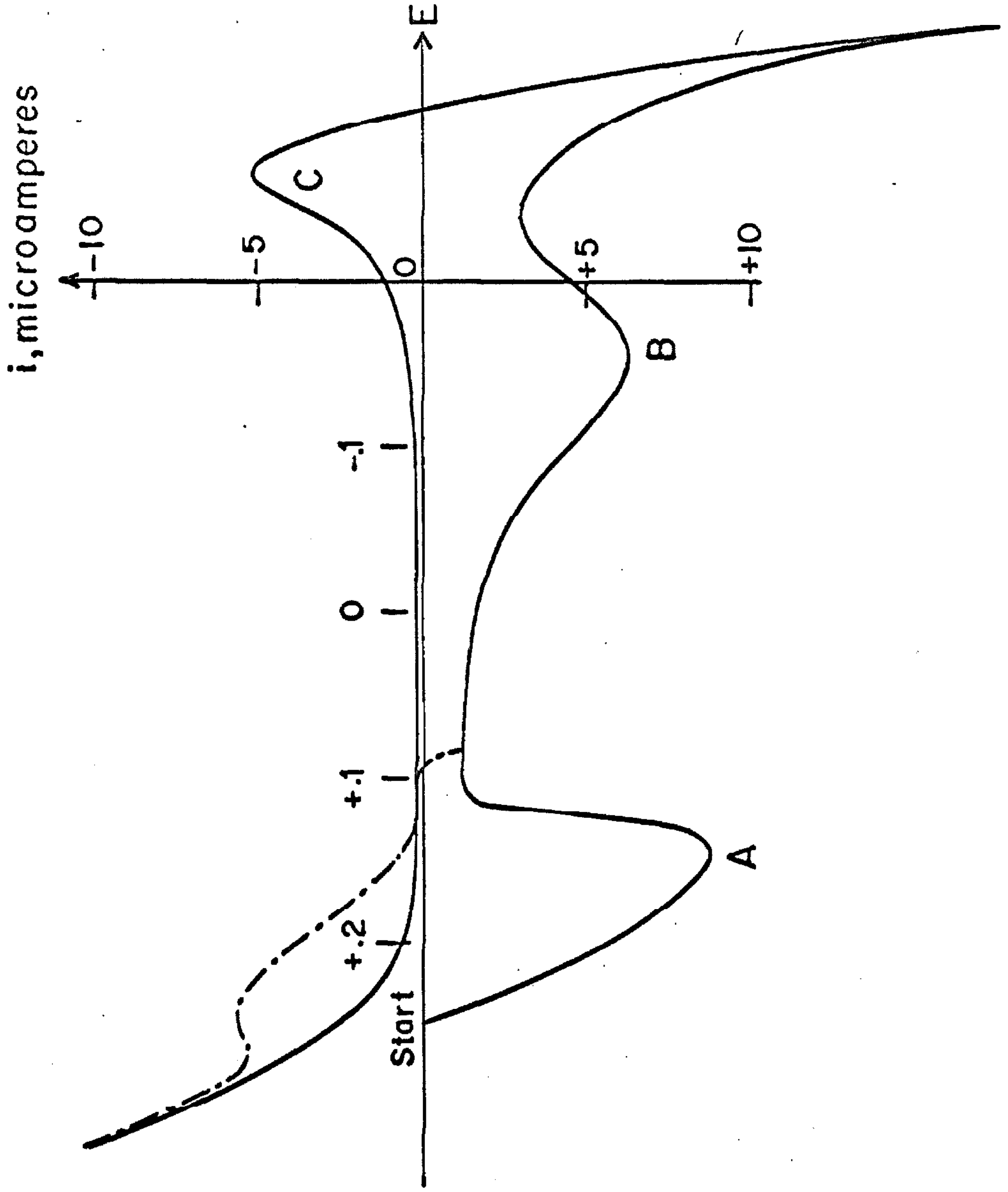
i, microamperes
−10
−5
0
+5
+10
E
C
B
A
−.1
0
+.1
+.2
Start

The anodic peak which results is due to the reaction

$$PtI_4^{-2} + 2I^- \rightarrow PtI_6^{-2} + 2e^-$$

This reaction does not take place if the PtI_6^{-2} is reduced all the way to Pt metal due to the extremely small rate of the reaction

$$Pt + 4I^- \rightarrow PtI_4^{-2} + 2e^-.$$

The peak current due to PtI_4^{-2} reduction (second peak) is somewhat smaller than that for PtI_6^{-2} (first peak), apparently because of the lesser reversibility of the electrode reaction which is

$$PtI_4^{-2} + 2e^- \rightarrow Pt + 4I^-.$$

An important point here is that slow linear sweep voltammetry in thin layers allows the second reaction to be clearly distinguished from the background current. Chronopotentiometry, even in thin layers, did not yield a wave with a distinguishable transition time.

(viii). Conclusions

The thin layer electrochemical experiments described above suggest the following conclusions:

I. $PtCl_6^{-2}$ and $PtCl_4^{-2}$

A. In 1 F HCl:

1. The oxidation of $PtCl_4^{-2}$ occurs according to

$$PtCl_4^{-2} \xrightarrow{HCl} \underline{ca.}\ 1/3Pt(OH)_2Cl_4^{-2} + \underline{ca.}\ 2/3PtCl_6^{-2} + 2e^-$$

2. The reduction of $PtCl_6^{-2}$ occurs according to

   $PtCl_6^{-2} + 2e^- \xrightarrow[\text{or } HClO_4]{HCl} PtCl_4^{-2} + 2Cl^-$

3. The reduction product of $Pt(OH)_2Cl_4^{-2}$ and $Pt(OH)_4Cl_2^{-2}$ (produced by hydrolysis of $PtCl_6^{-2}$) is $PtCl_4^{-2}$.

B. In 1 F $NaClO_4$ solutions:

1. The reduction of $PtCl_6^{-2}$ occurs according to

   $PtCl_6^{-2} + 4e^- \longrightarrow Pt + 6Cl^-$

2. The reduction of $PtCl_4^{-2}$ occurs according to $PtCl_4^{-2} + 2e^- \longrightarrow Pt + 4Cl^-$

3. The reduction of $Pt(OH)_mCl_{6-m}^{-2}$ occurs according to

   $Pt(OH)_mCl_{6-m}^{-2} + 4e^- \longrightarrow Pt + mOH^- + (6-m)Cl^-$

II. $PtBr_6^{-2}$ and $PtBr_4^{-2}$

A. In 1 F NaBr:

1. The oxidation of $PtBr_4^{-2}$ occurs according to

   $PtBr_4^{-2} \rightarrow PtBr_6^{-2} + 2e^-$

2. The reduction of $PtBr_6^{-2}$ occurs according to

   $PtBr_6^{-2} + 2e^- \longrightarrow PtBr_4^{-2} + 2e^-$

B. In 1 F $NaClO_4$ or 1 F $HClO_4$:

1. The reduction of $PtBr_6^{-2}$ occurs according to $PtBr_6^{-2} + 4e^- \longrightarrow Pt + 6Br^-$

2. The reduction of $PtBr_4^{-2}$ occurs according to

   $PtBr_4^{-2} + 2e^- \longrightarrow Pt + 4Br^-$

3. The reduction of $Pt(H_2O)_mBr_{6-m}^{m-2}$ occurs according to

   $Pt(H_2O)_mBr_{6-m}^{m-2} + 4e^- \longrightarrow Pt + (6-m)\ Br^- + mH_2O$

III. PtI_6^{-2} and PtI_4^{-2}

A. In 0.5M NaI:

1. The reduction of PtI_6^{-2} occurs according to
   $PtI_6^{-2} + 2e^- \longrightarrow PtI_4^{-2} + 2I^-$
2. The reduction of PtI_4^{-2} occurs according to
   $PtI_4^{-4} + 2e^- \longrightarrow Pt + 4I^-$
3. The oxidation of PtI_4^{-2} occurs according to
   $PtI_4^{-2} + 2I^- \longrightarrow PtI_6^{-2} + 2e^-$.